Dominant terms in the freshwater and heat budgets of the subpolar North Atlantic Ocean and Nordic Seas from 1992 to 2015

Jan-Erik Tesdal[1] and Thomas W N Haine[2]

[1]Columbia University
[2]Johns Hopkins University

November 22, 2022

Abstract

The Arctic and subarctic oceans exhibit distinct decadal variations in freshwater and heat content. We describe freshwater and heat budgets with the ECCOv4 reanalysis product and compare budget variability and mechanisms within the subpolar North Atlantic Ocean, Nordic Seas and Labrador Sea from 1992 to 2015. For all regions, changes in freshwater content are largely anti-correlated with changes in heat content. Since 1995, the subpolar North Atlantic Ocean has undergone a decade of warming and salinification followed by ongoing cooling and freshening. The recent increase in freshwater content and the reduction in heat in the subpolar North Atlantic can largely be attributed to anomalous circulation of mean salinity and temperature, respectively. Interannual variability in heat and freshwater mostly corresponds to boundary fluxes from the subtropics. Meanwhile the Nordic Seas have undergone an overall warming and salinification from the mid-1990s to 2015. Salinification is primarily driven by reduced sea ice flux through Fram Strait, while warming is due to changes in both sea surface heating and advective flux. In the last five years, Labrador Sea freshwater convergence remained unchanged, as increased inflow via the Baffin Island Current is balanced by increased outflow via the Labrador Current. Hence the observed freshening of the Arctic Ocean is expected to be an increasingly important source of future freshwater increases in the subpolar North Atlantic. This stands in contrast to variability in freshwater flux from the subtropical North Atlantic, which is associated with variability in the Atlantic Meridional Overturning Circulation.

Posted on 22 Nov 2022 — CC-BY 4.0 — https://doi.org/10.1002/essoar.10503232.1 — This a preprint and has not been peer reviewed. Data may be preliminary.

Dominant terms in the freshwater and heat budgets of the subpolar North Atlantic Ocean and Nordic Seas from 1992 to 2015

Jan-Erik Tesdal[1], Thomas W. N. Haine[2]

[1]Lamont-Doherty Earth Observatory, Columbia University, Palisades, New York, USA
[2]Earth and Planetary Sciences, The Johns Hopkins University, Baltimore, Maryland, USA

Key Points:

- An ocean state estimate identified mechanisms governing freshwater and heat content in the northern North Atlantic over 1992-2015
- Decadal variation in the subpolar North Atlantic is due to advective convergence while sea ice melt is more relevant in the Nordic Seas
- Freshwater variability is due to southern boundary transport in subpolar North Atlantic and Fram Strait sea ice export in Nordic Seas

Corresponding author: Jan-Erik Tesdal, `tesdal@ldeo.columbia.edu`

Abstract

The Arctic and subarctic oceans exhibit distinct decadal variations in freshwater and heat content. We describe freshwater and heat budgets with the ECCOv4 reanalysis product and compare budget variability and mechanisms within the subpolar North Atlantic Ocean, Nordic Seas and Labrador Sea from 1992 to 2015. For all regions, changes in freshwater content are largely anti-correlated with changes in heat content. Since 1995, the subpolar North Atlantic Ocean has undergone a decade of warming and salinification followed by ongoing cooling and freshening. The recent increase in freshwater content and the reduction in heat in the subpolar North Atlantic can largely be attributed to anomalous circulation of mean salinity and temperature, respectively. Interannual variability in heat and freshwater mostly corresponds to boundary fluxes from the subtropics. Meanwhile the Nordic Seas have undergone an overall warming and salinification from the mid-1990s to 2015. Salinification is primarily driven by reduced sea ice flux through Fram Strait, while warming is due to changes in both sea surface heating and advective flux. In the last five years, Labrador Sea freshwater convergence remained unchanged, as increased inflow via the Baffin Island Current is balanced by increased outflow via the Labrador Current. Hence the observed freshening of the Arctic Ocean is expected to be an increasingly important source of future freshwater increases in the subpolar North Atlantic. This stands in contrast to variability in freshwater flux from the subtropical North Atlantic, which is associated with variability in the Atlantic Meridional Overturning Circulation.

Plain Language Summary

We utilized an ocean model state that is optimally close to real-world observations over the period 1992 to 2015 to investigate processes behind the recent changes in freshwater and heat content of the subpolar North Atlantic and Nordic Seas. The subpolar North Atlantic has cycled between ten-year periods of becoming warmer and saltier, and then colder and fresher, while the Nordic Seas have mostly become saltier. This pattern was broken down into individual components such as atmospheric exchanges and transport processes within the ocean. Ocean circulation in the North Atlantic is key in controlling freshwater and heat content in the subpolar North Atlantic, mostly by changing the movement of water masses from the subtropical Atlantic. Conversely the overall decline in freshwater content within the Nordic Seas comes mostly from a drop in sea ice export from the Arctic Ocean. These findings help us to better understand what drives the year-to-year and longer term variation in freshwater and heat content in the northern North Atlantic. This is important because changes in freshwater and heat in the upper layers of that region can affect the global climate by influencing the amount of atmospheric heat and carbon stored in the ocean.

1 Introduction

The large-scale circulation in the subpolar North Atlantic (SPNA) Ocean plays a crucial role in the global climate (Rhein et al., 2011; Lozier et al., 2017) and influences ocean storage of atmospheric heat and carbon, specifically through deep water formation and the Atlantic Meridional Overturning Circulation (AMOC). Freshwater flux to the SPNA and Nordic Seas (NSEA) is key in understanding this process as it influences stratification and hence deep convection. Several studies showed that an increase in freshwater in the upper layers of the SPNA weakens deep convection and the AMOC (Wadley & Bigg, 2002; Vellinga et al., 2008; Jahn & Holland, 2013; Thornalley et al., 2018).

Over the last 25 years the freshwater content of the Arctic Ocean has increased substantially (Proshutinsky et al., 2009, 2015; Rabe et al., 2014). As all outflows from the Arctic Ocean lead to the SPNA and NSEA, it is expected that some of that freshwater will eventually be transported to the SPNA and NSEA regions. Furthermore, the Greenland Ice Sheet is losing mass at an accelerating rate (Rignot et al., 2008; J. Bamber et al., 2012; Trusel et al., 2018) providing additional freshwater into these regions (J. L. Bamber et al., 2018; Dukhovskoy et al., 2019). Future climate change is expected to further increase the freshwater fluxes into both the Arctic and North Atlantic, as the result of an intensification of the water cycle, loss of sea ice and glacial melting (Held & Soden, 2006; Rennermalm et al., 2007; Koenigk et al., 2007; Durack et al., 2012; Jahn & Holland, 2013; Lau et al., 2013; Nummelin et al., 2016). In the following paragraphs, past literature on freshwater variability within the SPNA and NSEA from the mid-20th century to present is summarized, in particular the notion of episodic freshening events known as "Great Salinity Anomalies". In addition, we review the principal mechanisms that have been identified for this variability, and address whether exchange through Arctic gateways or with the subtropical North Atlantic is more important.

Reliable basin-scale inferences of salinity changes from in-situ observations go as far back as the mid-20th century, starting when decadal variation in salinity or equivalent freshwater content of the SPNA and NSEA were documented by a number of observational studies (B. Dickson et al., 2002; R. Curry et al., 2003; R. Curry & Mauritzen, 2005; Boyer et al., 2007). B. Dickson et al. (2002) observed uniform freshening trends from 1960 to 1990 for multiple deep water masses within the SPNA, which was attributed mostly to surface freshening of the upper NSEA that subsequently propagated into the deep Atlantic along overflow waters across the Denmark Strait and the Faroe-Shetland Channel. Over approximately the same time period (i.e., 1950s to 1990s), R. Curry et al. (2003) confirmed decadal freshening of both upper and deep water masses in the high-latitude North Atlantic. This freshening was associated with a symmetric response to changes in evaporation minus precipitation (E-P) over the entire Atlantic basin, characterized by a shift in atmospheric flux to increased net precipitation in the high latitudes, whereas the observed increasing salinity at low latitudes was associated with increased net evaporation. Regionally specific studies also confirmed freshening trends consistent with the larger spatial focus of B. Dickson et al. (2002) and R. Curry et al. (2003). Blindheim et al. (2000) reported on freshening in the Norwegian Sea between the 1960s and late 1990s, which they attribute to wind-driven advection of Arctic waters. Reverdin et al. (2002) focused on the subpolar gyre (SPG) and reported freshening in the eastern SPG and Iceland Basin during the mid to late 1970s, with associated freshening in the Irminger Sea lagging by one year.

Besides the overall freshening trend in the northern North Atlantic during the second half of the 20th century, specific anomaly events have been described and subsequently coined "Great Salinity Anomalies" (GSAs). These are postulated to be spatially constrained patches of low-salinity water that are advected within the SPNA and NSEA (R. R. Dickson et al., 1988; Belkin et al., 1998; Häkkinen, 2002; Belkin, 2004). The first GSA to be properly documented with available observations occurred in the 1970s. R. R. Dickson et al. (1988) tracked this GSA, which penetrated to at least 500 m, from its apparent emergence north of Iceland around 1968 to its path along the counterclockwise circulation of the SPG over a time span of 14 years. A subsequent GSA emerged in the western Labrador Sea in 1982 and then advected along the predominant circulation pattern of the SPNA to reach the Barents Sea in 1989 (Belkin et al., 1998). The most recent GSA to be clearly identified as such formed in the Labrador Sea in the early 1990s and was similarly advected along the SPG circulation, reaching into the NSEA in the mid 1990s (Belkin, 2004).

From observations, R. Curry and Mauritzen (2005) quantified the freshwater content of the SPNA and NSEA and found that $19\,000 \pm 5000\,\mathrm{km}^3$ of freshwater were added to these regions between 1965 and 1995. Similarly, Boyer et al. (2007) showed the change in freshwater content in the North Atlantic by dividing the North Atlantic into six major regions. From their analysis, the SPNA and NSEA regions are the only ones that showed an increase in freshwater content, defined from 0 to 2000 meters depth and amounting to approximately $16\,000\,\mathrm{km}^3$ from 1966 to 1994. Most of that increase occurred between the late 1960s and early 1990s, including the GSA of the 1970s which has been estimated to be an addition of 10 000 km^3 (R. Curry & Mauritzen, 2005). This freshwater increase was followed by a decline of around 9500 km^3 from the mid 1990s to the end of the time series in 2006 (Boyer et al., 2007). The freshwater increase of 16 000 km^3 estimated by Boyer et al. (2007) is slightly less than but within the margin of error (14 000–24 000 km^3) of the estimate by R. Curry and Mauritzen (2005).

The overall freshening in the SPNA and NSEA has not been persistent. Especially over the eastern SPG and NSEA, the freshening that occurred between 1960 and 1990 was essentially nullified between 1990 and 2006 (Holliday et al., 2008). Similar warming and salinification in the intermediate and deep waters of the Irminger Sea and Iceland Basin over the same period were reported by Sarafanov et al. (2007). This is partly connected to the warming and salinification of Labrador Sea Water (LSW) that was reported for the period 1994 to 2005 (Avsic et al., 2006; Yashayaev, 2007). An 18-year long record of a well-sampled section between Scotland and Iceland (crossing Rockall Trough, Hatton-Rockall and Iceland Basins) reveals cooling and freshening between 1997 and 2001 followed by warming and salinification from 2001 to 2006 and a cycling back to cooler and fresher water between 2006 and 2014 (Holliday et al., 2015). After a decade long salinification (1993-2005) there has been widespread freshening in the upper water over the latest period (2004-2015) reaching from the Labrador Sea to the central and eastern North Atlantic (Tesdal et al., 2018).

The substantial decadal variability in freshwater content and salinity of the SPNA and NSEA is intriguing, and attributable to a range of mechanisms. These can be broadly categorized as either the local influence of atmospheric (E-P) freshwater flux, ice melt and continental runoff or remote influences due to changing advection of relatively saline or fresher waters, including transport of continental runoff, glacial melting, and sea-ice export from the Arctic. It can be expected that the balance between individual mechanisms depends on region, and might change for different time periods and at different time scales. One important question is whether the dominant mechanisms in particular regions (e.g., eastern SPG or Labrador Sea) are still relevant when considering the freshwater content of the entire high latitude North Atlantic (i.e., SPNA and NSEA). Similarly, mechanisms driving higher frequency variability (i.e., daily to seasonal anomalies) might not be the same as relevant mechanisms for interannual and decadal variation in freshwater content.

Negative trends in subpolar and polar salinity have been expected to reflect an intensified hydrological cycle in which precipitation increasingly exceeds evaporation (R. Curry et al., 2003; Durack et al., 2012; Vinogradova & Ponte, 2017). In the eastern SPG, changes in E-P linked to the East Atlantic Pattern were sufficient to explain observed variability in salinity in this region from the 1960s to early 2000s (Josey & Marsh, 2005). Myers et al. (2007) suggested that an increase in E-P may also have had some contribution in causing the observed freshening of the Labrador Sea over the same time period. Peterson et al. (2006) quantified Arctic and North Atlantic freshwater sources due to increased precipitation, river discharge, sea ice melting and glacial melting. They found that for the period 1965-1995, changes in E-P contributed approximately the same volume of freshwater anomaly in the North Atlantic (here defined as the cumulative change in SPNA, NSEA and deep subtropical water) as did sea ice melt, whereas glacial melting was a comparatively minor contributor. The increased freshwater volume from all sources were associated with rising surface air temperatures and atmospheric circulation patterns linked to the North Atlantic Oscillation (NAO). These results suggested that Arctic-North Atlantic exchanges play a primary role in freshwater content variability of the North Atlantic over the latter half of the 20th century. Furthermore, the NAO was identified as a key mode that explained the increases in atmospheric freshwater fluxes at high latitudes as well as the occurrences of freshwater and sea ice exports from the Arctic.

Related studies appear to confirm that in terms of remote forcing of the SPNA and NSEA freshwater variability, changes in Arctic export of sea ice and freshwater can be regarded as the main factor (Belkin et al., 1998; Belkin, 2004; Karcher et al., 2005; Koenigk et al., 2007; Lique et al., 2009). In particular the observed GSAs has been explained mostly as derived from enhanced outflows of Arctic freshwater and sea ice (Haak et al., 2003; Karcher et al., 2005; Lique et al., 2009). However, there has been no quantification of how much the anomalous freshwater export through Fram Strait or the Canadian Archipelago affected the freshwater budget (or salinity) in the North Atlantic Ocean. Variation in freshwater content on interannual and decadal timescales has also been linked to changes in North Atlantic circulation, including SPG mediated changes in advection (Hátún et al., 2005; Häkkinen et al., 2011). Focusing on freshwater anomalies for different water masses in the NSEA (using available hydrographic observations and a hindcast simulation over 1948-2009), Glessmer et al. (2014) demonstrated that the decadal variation of salinity in the NSEA is explained by Atlantic inflow with a secondary contribution from Arctic outflow (mainly through sea ice export). Thus freshwater in the NSEA is mainly influenced by variations of salt transport from the North Atlantic subtropical gyre, with Arctic freshwater inputs of secondary importance.

The upper water masses of the Atlantic inflow, the northward flow across the Greenland-Scotland ridge, are saltier and warmer relative to other NSEA water masses. If variation in the Atlantic inflow is the main factor determining freshwater content of the NSEA (and possibly the SPNA), then a corresponding decrease in heat content (i.e., cooling) should also be observed. In fact, many studies show that salinity and freshwater variability covaries with temperature and heat variability (e.g., Holliday et al., 2008; Häkkinen et al., 2011; Robson et al., 2016). On the other hand, Arctic waters are generally fresher and colder relative to North Atlantic water, such that the distinct low salinity signatures of the GSAs are often associated with anomalously low temperatures as well (Belkin et al., 1998). The co-occurrence of freshening and cooling signatures therefore can also be associated with greater Arctic export to the SPNA and NSEA. However, it is possible that freshening occurrences such as GSAs could also be derived from a decline in northward heat and salt inflow from the subtropical North Atlantic into NSEA and SPNA. Häkkinen (2002) for example suggest that the fresher surface water in the Labrador Sea during the early 1990s can also be related to a decreasing supply of salt northward through the North Atlantic Current stemming from reduced overturning circulation.

The large data gaps in the observational records and the lack of a continuous record of boundary fluxes around the SPNA and NSEA hinder exact quantification of the contribution of different mechanisms to freshwater variability in SPNA and NSEA from observations alone. However, to determine the future response of the North Atlantic to various climate scenarios, a better understanding of the drivers of freshwater variability is imperative. As the observational record is incomplete, coupled general circulation model (GCM) simulations can be used for a sufficiently precise quantification of the contribution of different mechanisms to freshwater variability in the North Atlantic. Numerical model analyses ensures closed tracer budgets that account for every source (e.g., of freshwater, heat, etc.) and attribute advective changes to each boundary of the control volume. However, ocean GCMs come with their own uncertainties (e.g., due to incomplete description of ocean processes), exemplified by the large disagreements among climate models in terms of the North Atlantic freshwater budget (Deshayes et al., 2014). By incorporating the observational record within a dynamically consistent estimate of hydrographic variability, ocean reanalysis products can provide the diagnostics to evaluate tracer (e.g., freshwater, salt, heat, etc.) budgets in the ocean while also reflecting the observed variability as closely as possible. This approach can reconcile a diverse observational record, allowing one to extract from the data a coherent description of processes taking place to understand observed variability in the ocean.

In this paper, we report on our investigation of the drivers of variability in freshwater and heat content of the SPNA and NSEA using the fourth version of the Estimating the Circulation and Climate of the Ocean consortium (ECCOv4) state estimate. Closed budgets of freshwater and heat content are derived for the SPNA and NSEA, including a separate analysis for the Labrador Sea (which is regarded part of SPNA), using the diagnostic output from release 3 of ECCOv4 which covers the period between 1992 and 2015. The ECCOv4 ocean state estimate assimilates a suite of in situ and satellite data to reproduce ocean variability in close agreement with the observed ocean state. The ECCOv4 estimate is physically consistent, with no artificial sources or sinks of ocean properties (Forget et al., 2015). This characteristic is unique among available ocean reanalysis products and makes it ideal for ocean budget analyses (Buckley et al., 2014, 2015; Thompson et al., 2016; Piecuch et al., 2017).

Piecuch et al. (2017) used ECCOv4 to describe recent decadal variability in ocean heat content in the SPNA. They identify the dominant budget term as anomalous advection through the southern boundary acting on mean temperature, attributable to changes in the horizontal gyre circulation which in turn is driven by local variation in wind stress curl. Our study extends the budget analysis of Piecuch et al. (2017), focusing on the freshwater content of both SPNA and NSEA and also comparing it to corresponding ocean heat content anomalies for the same regions. Most studies found in the literature have investigated ocean freshwater and heat budgets of the SPNA and NSEA in isolation. As noted above, it is crucial to investigate variability in temperature (i.e., heat content) and salinity (i.e., freshwater content) together since ocean and external forcing processes influence both variables, often with concomitant and covarying change. For example, the recent changes in horizontal circulation identified by Piecuch et al. (2017) should also influence freshwater content of the SPNA. Robson et al. (2016) tied a decline in temperature and salinity in the upper northern North Atlantic since 2005 to a reduction in the AMOC, which reduced both heat and salt transport to the north. Whether this is primarily due to overturning or wind-stress-driven gyre circulation will be further investigated and discussed here.

In the following Section 2, we present our methodology with a short description of the ECCOv4 state estimate and other datasets. In Section 3 we revisit freshwater content variation of SPNA and NSEA in the observation record since 1950 and show the good fit of the ECCOv4 freshwater estimate with the observational record over the common time period between 1992 and 2015. We also present a comparison of the ECCOv4 volume, freshwater and heat flux estimates across the main boundaries of the SPNA and NSEA with observational data and previous literature. In Section 4 we present freshwater and heat budgets for the SPNA, NSEA and Labrador Sea (LSEA). We identify the dominant budget terms responsible for variability in freshwater and heat content for each region, over monthly to pentad timescales. The analysis also includes an evaluation of boundary flux exchanges. Section 5 presents a discussion of our results in the context of recent findings in related studies, including the role of the AMOC and wind-driven variability in freshwater and heat content. Summary and conclusions are presented in Section 6.

2 Data and Methods

In this section we first briefly describe the ECCOv4 global ocean state estimate and within it the definition of control volumes to represent the SPNA and NSEA. We next give an overview of the observational datasets, followed by the methods for determining liquid freshwater content, including the rationale for our choice of reference salinity. The conservation laws for freshwater and heat content are then described, followed by a brief description of our time series analysis, including a regression analysis to evaluate the relevance of each budget term.

2.1 ECCOv4 ocean state estimate

SPNA and NSEA freshwater, salt and heat content variability and their respective budgets were investigated with ECCOv4 (Release 3), which provides a physically consistent ocean circulation and sea-ice state estimate covering the period 1992-2015. The relevant output data has been produced by running the Massachusetts Institute of Technology general circulation model (MITgcm) with the ECCOv4 configuration, which includes the initial condition, atmospheric state and model parameters that minimize the misfits between simulated and observed state in a least squares sense. The diagnostic outputs include monthly mean fields from January 1992 to December 2015 of all relevant terms to formulate budgets of volume, temperature (i.e., heat), salt and salinity (i.e., freshwater). In addition diagnostics include monthly snapshots (taken at the beginning and end of each month) of temperature, salinity and sea surface height. Both the mean and snapshot fields are presented in the Lat-Lon-Cap grid (i.e., LLC90) configuration, which is organized in 12 tiles with each tile including 90 by 90 grid cells (Forget et al., 2015). Horizontal grid spacing is irregular, with an average resolution of $1^{\circ}\times1^{\circ}$. The grid size in LLC90 ranges from 40-50 km at polar to subpolar latitudes to around 110 km towards the equator. Vertical spacing comprised 50 levels of thickness from 10 m at the surface to 456.5 m for the deepest layer.

The MITgcm configuration used in ECCOv4 includes the nonlinear free surface formulation allowing temporal variability in the upper water column thickness, including a modified height coordinate (Adcroft & Campin, 2004). Realistic freshwater flux boundary conditions are applied, such that the variation in sea surface elevation also includes contributions from atmospheric freshwater flux. Tracer advection is discretized spatially using the finite volume method (Marshall et al., 1997). Several subgrid processes are parameterized including diapycnal and isopycnal diffusion (Redi, 1982), vertical mixing (using the mixed layer closure scheme by Gaspar, Grégoris, & Lefevre, 1990), simple convective adjustments and along-isopycnal transport of unresolved eddies (i.e., bolus transport; Gent & Mcwilliams, 1990). The atmospheric fields (wind stress, precipitation, evaporation, etc.) from ERA-Interim reanalysis (Dee et al., 2011) and bulk formulae (Large & Yeager, 2009) are used to describe a priori atmospheric forcing. Exchanges between ocean and sea ice/snow are represented interactively, while continental runoff is represented as a climatology field (Fekete et al., 2002). Data assimilation in ECCOv4 is applied by adjusting the initial conditions, atmospheric input and ocean mixing parameters to minimize the model-data misfits. Observations that are assimilated in ECCOv4 include in situ hydrographic data from various platforms (e.g., shipboard, Argo floats, sensors attached to elephant seals), sea surface temperature, sea surface salinity, altimetry, ocean bottom pressure and sea ice concentrations from satellites. For a more detailed description of the ECCOv4 configuration we refer to Forget et al. (2015).

Changes in freshwater and heat were investigated using ECCOv4 with a closed budget analysis conserving volume, salt and heat within the SPNA and NSEA, defined as two separate spatial domains. According to the LLC90 grid, the SPNA and NSEA subdivision are designed to represent about the same domains as in R. Curry and Mauritzen (2005). However, the domains needed to be adjusted in order to define sections representing the boundaries of and between these subregions (Figure 1). The sections are defined mainly in accordance with existing observational sections, and are located where the fluxes are constrained by topographic features. The overall region of interest is bounded to the south by the section between Newfoundland and the Iberian peninsula (NI) whereas the northern boundary consists of the Davis Strait (DaS) to the west and the Fram Strait (FrS) to the east. The western boundary is mostly land mass except for the Hudson Strait (HS). The eastern side is bounded by the section across the Barents Sea Opening (BSO), the North Sea from Scotland to Norway (SN) and the English Channel (EC). The boundaries between the SPNA and NSEA are delineated by the Denmark Strait (DeS) and sections between Iceland, the Faroe Islands and Scotland (IF and FS, respectively). The

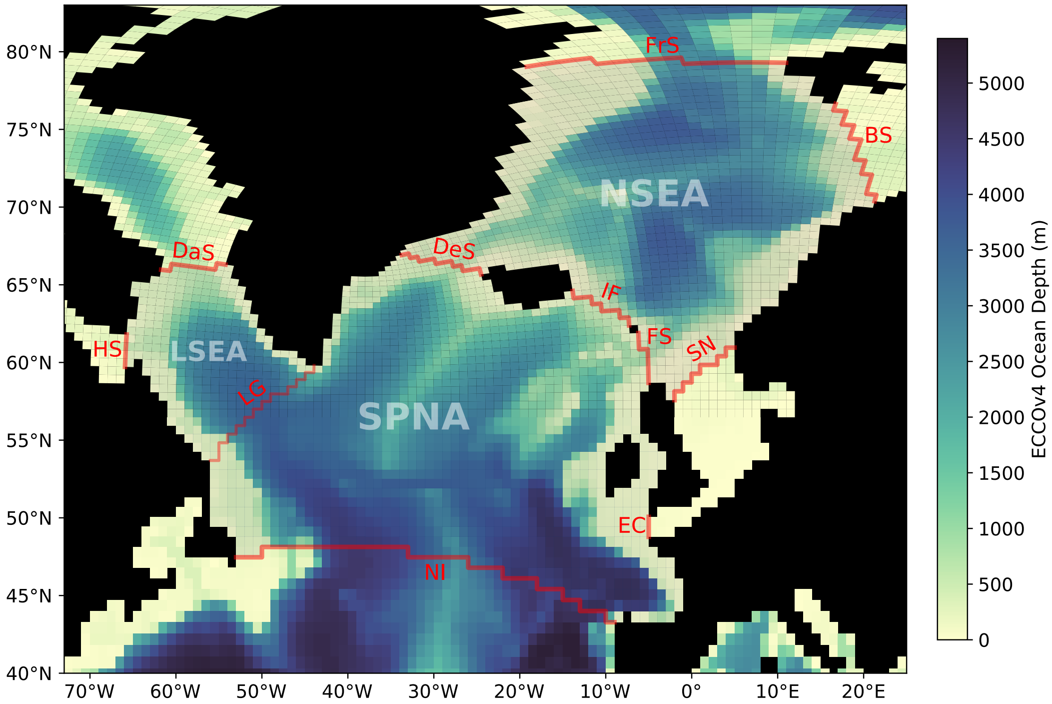

Figure 1. ECCOv4 ocean depth showing the model grid along with defined regions for budget analysis of the subpolar North Atlantic (SPNA) and Nordic Seas (NSEA). The Labrador Sea (LSEA) is separately defined as part of the SPNA. Sections across which boundary fluxes were calculated are shown as red lines: Newfoundland-Iberia (NI), Denmark Strait (DeS), Iceland-Faroe (IF), Faroe-Scotland (FS), Scotland-Norway (SN), Barents Sea Opening (BS), Fram Strait (FrS), Davis Strait (DaS), Hudson Strait (HS), Labrador-Greenland (LG) and English Channel (EC).

Labrador Sea (LSEA) is distinguished as a subregion of the SPNA and is bounded by a section between Labrador and Greenland (LG).

The design of the control volumes for SPNA and NSEA are mainly to allow for comparison with previous findings, which focused on one or the other of these regions. For example, R. Curry and Mauritzen (2005) used similar definitions for SPNA and NSEA. Glessmer et al. (2014) focused on freshwater content in the NSEA, whereas Piecuch et al. (2017) focused on heat content in the SPNA. In our opinion, it is important to study SPNA in tandem with NSEA as both regions are important to North Atlantic circulation and Arctic-Atlantic exchanges, but should also be distinguished as separate regions because they are separated by topography with exchange constrained to the Denmark Strait and Iceland-Faroe-Scotland ridges. Furthermore, defining the boundaries in alignment with key observational transects and mooring arrays allows us to assess ECCOv4 with observations in volume, freshwater and heat transport. These include the Arctic gateways Fram Strait and Davis Strait as well as the Greenland-Scotland Ridge.

2.2 Observational data

Monthly gridded salinity fields from objective analysis are obtained from the EN4 product (Good et al., 2013) for the time period 1950 to 2017. The gridded salinity fields are derived from optimal interpolation of available in situ data. The EN4 gridded fields have a horizontal resolution of 1°×1° and are vertically resolved with 42 depth levels varying in thickness from 10 m near surface (depth < 100 m) to around 300 m towards the seafloor (at 5500 m). There are a number of different sources of in situ observations in EN4. In the case of the North Atlantic Ocean, the objective analysis is based mostly on shipboard CTD casts from the World Ocean Database prior to the mid-2000s. From 2004 onwards observations are increasingly from Argo profiling floats, with additional data from the Global Temperature and Salinity Profile Programme (GTSPP). Earlier time periods are prone to large uncertainties and thus should be interpreted with caution. For the common time period (1992-2017) between ECCOv4 (Release 4) and EN4 it can be expected that the assimilated salinity profile data in ECCOv4 is about the same as that used to generate gridded salinity fields in EN4. The difference obviously is that EN4 relies on statistical data assimilation by optimal interpolation techniques to fill in observational data gaps, while ECCOv4 assimilates the observations with an ocean model to fill in observational data gaps in a dynamically consistent way.

Observational data from the RAPID/MOCHA array at 26°N were obtained from the RAPID project website (`http://www.rapid.ac.uk/rapidmoc`). The monthly time series of the NAO and AO indices were obtained from the NOAA/ESRL Physical Sciences Division website at `http://www.esrl.noaa.gov/psd/data/climateindices/list/`. Daily gridded fields of the multialtimeter absolute dynamic topography (ADT) product were downloaded from the Copernicus Marine and Environment Monitoring Service (CMEMS). The daily fields were selected for the relevant period (2004-2015) and averaged to monthly mean fields. The Subpolar Gyre Index is defined as the principal component of the second Empirical Orthogonal Function (Koul et al., 2020), but here is derived using monthly anomalies of ADT over the North Atlantic (20–70 °N , 0–80 °W).

We compare published estimates of volume, freshwater and heat transports based on observation-only datasets which are obtained from various transects (e.g., Davis Strait, Denmark Strait, Fram Strait). Mean volume transports for Davis Strait, Denmark Strait and the Iceland-Faroe-Scotland ridges are taken from Østerhus et al. (2019). Mean estimates of freshwater fluxes through Davis Strait, Fram Strait and the Barents Sea Opening have been taken from the synthesis by Haine et al. (2015), from which we used the average of their estimates for 1980-2000 and 2000-2010. Ice exports are considered through Fram Strait and Davis Strait and are taken from estimates presented in Haine et al. (2015), as they distinguished between liquid and solid (i.e., sea ice) fluxes. Estimates of heat transport through the Davis Strait, Fram Strait and Barents Sea Opening are from Beszczynska-Möller et al. (2011) and references therein. Furthermore, we include estimates of volume and heat fluxes across the Greenland-Scotland Ridge from Rossby et al. (2018). Our focus here is on net transports such that flux estimates that were only provided for particular water masses or currents are added to reflect the net exchange through each section. In cases where transport estimates are combined with corresponding uncertainties, standard error propagation is used (i.e., taking the square root of the sum of squared uncertainties as the combined uncertainty).

Mean transports in ECCOv4 were calculated for the period 1992-2015 and compared to the observed mean transports over the available time period. Since current meter data are not used to constrain ECCOv4, transport estimates serve as an independent assessment of ECCOv4. Due to the vagaries of deploying and maintaining mooring arrays, observational datasets do not cover the entire ECCOv4 period, and usually represent shorter periods where measurements have been undertaken. The time periods over which observational estimates are determined vary substantially. Because the various flux estimates represent different periods and are often derived with certain assumptions and approximations, most of them are associated with large uncertainties. See Beszczynska-Möller et al. (2011), Haine et al. (2015) and Østerhus et al. (2019) for an in-depth explanation and discussion of how these flux estimates are derived and the sources of errors due to various challenges associated with collecting observational data. A final caveat regarding the use of observational datasets to assess ECCOv4 performance is that observations do not ensure a closed system, which creates the possibility of double-counting or missing entirely some flux measures, whereas ECCOv4, by design, maintains an exact balance between boundary fluxes. Volume, freshwater and heat estimates taken from the literature are presented in Table 1 along with estimates from ECCOv4, which will be further discussed in Section 3.1.

2.3 Estimating the liquid freshwater content

The liquid freshwater content is defined here as the volume of freshwater (i.e., zero-salinity water) that needs to be added (or subtracted) to account for the deviation between salinity S from a given reference salinity S_{ref}. Thus, within a control volume V the liquid freshwater content is calculated as

$$V_{fw} = \int_V \frac{S_{ref} - S}{S_{ref}} dV \tag{1}$$

V_{fw} is presented as volume (in km^3). Since we use gridded salinity fields, the integrand of Equation (1) is evaluated for each grid cell and then summed over depth, latitude and longitude. Since analysis is focused on the full-depth budgets, summing is done from ocean bottom to surface. S_{ref} is chosen to be $35\,\mathrm{g\,kg^{-1}}$ because it roughly represents the mean salinity across the entire SPNA, considering the major inflows of relatively salty waters from the south (i.e., tropics and subtropics) and relatively fresh water sourced from the north (i.e., East Greenland and Labrador Currents). The analysis in this study emphasizes freshwater mechanisms on interannual timescales. Seasonal anomalies are determined by subtracting seasonality from monthly averages.

Recent studies have pointed to problems associated with the use of reference salinities (Tsubouchi et al., 2012; Bacon et al., 2015; Schauer & Losch, 2019) or reference temperatures (Forget & Ferreira, 2019). For example, Bacon et al. (2015) pointed out the ambiguity of choice of reference salinity and reasons that the only appropriate reference value is a boundary-mean salinity calculated for an assumed closed-volume freshwater supply. However, this mean can vary both spatially (according to geographical location of the boundary) and temporally (according to variability in salinity of water flowing through that boundary). Schauer and Losch (2019) argue that the concept of freshwater content itself is an ambiguous measure because it is based on arbitrary reference salinities. This indicates that because freshwater anomalies and trends are based on an arbitrary reference value, any estimate is not physically consistent with the true freshwater flux. Furthermore, the use of mean salinity across a section as reference salinity that was proposed by Bacon et al. (2015) also poses the problem of inconsistency among ocean basins and so can not yield truly universal estimates in freshwater fluxes. In the case of ECCOv4, closed control volumes with zero net volume flux are used such that results are physically consistent and the outcome does not depend on the choice of reference values.

Schauer and Losch (2019) propose to abandon the use of reference salinities and instead refer to salt transports. However, this does not explicitly account for atmospheric freshwater fluxes, runoff and freshwater exchanges with sea ice, as those do not affect the overall salt content of the ocean. Furthermore, boundary fluxes of salt covary with volume fluxes, such that any increase in volume flux will increase the salt flux no matter how fresh or salty that boundary flux is. Since one goal of this study is to identify the importance of Arctic freshwater exchanges through northern boundaries (e.g., Davis Strait, Fram Strait) versus exchanges through the southern boundary flux (i.e., the section across Newfoundland and the Iberian peninsula), we chose to present freshwater transport and their anomalies as a way to compare fresher (i.e., Arctic) with saltier (i.e., subtropical) source waters. Salt and salinity budgets for the SPNA and NSEA are presented in the supplementary information which allows a comparison to the freshwater variability that is presented in the main results. This shows that the freshwater budget is comparable to the salt budget and equivalent to the salinity budget within our closed volume analysis. Since most of our analysis is based on seasonal anomalies of closed-budget terms, the choice of reference salinity does not alter our results. The one exception is absolute freshwater fluxes across boundaries, which we only present in the supplementary information for illustrative purposes.

Furthermore, using freshwater content allows us to compare our estimates of gateway fluxes with previous estimates in the literature. In order to compare freshwater flux estimates with observational records we adjust Equation 1 according to the reference salinity and integration method used in each particular study. For these estimates we replaced $35\,\mathrm{g\,kg^{-1}}$ with the same S_{ref} value as stated in the corresponding study. Also, in some instances, freshwater fluxes are obtained by integrating from the isohaline depth of S_{ref} to the surface, rather than the entire water column across the section, which therefore estimates flux only for the section that is fresher than S_{ref}. This is the case for freshwater flux studies through the Fram Strait (de Steur et al., 2009) and the Denmark Strait (de Steur et al., 2017). Thus, mean freshwater flux in ECCOv4 through the Denmark and Fram Straits are estimated by integrating ECCOv4 freshwater fluxes only from the S_{ref} isohaline depth to the surface.

2.4 Budget calculations

In this section we present the budget calculations. Although we focus on freshwater content, budgets have also been evaluated for heat, volume, and salt. An equation for salinity conservation is also presented to demonstrate that it is consistent with our freshwater budget. Equations for freshwater and heat are presented here, and information for volume, salt and salinity are given in the supplementary material. The budgets are expressed as tendencies (i.e., change over time), such that the total tendency is the sum of the tendencies due to advective convergence, diffusive convergence, and forcing. We evaluate the budget terms on a grid-by-grid point basis. In terms of the freshwater budget, we present tendencies of each budget term in milli-Sverdrup (mSv, 10^3 m^3 s^{-1}). The freshwater tendency is volume-integrated in a manner similar to the equation for freshwater content (Equation 1). Essentially, the time derivative is applied to the volume-integrated freshwater content to yield the total freshwater tendency as a balance of advective and diffusive convergence and a forcing term:

$$\frac{\partial V_{fw}}{\partial t} + \nabla \cdot \mathcal{F}_{\mathbf{adv}} = -\nabla \cdot \mathcal{F}_{\mathbf{diff}}{}^{fw} + \mathcal{F}^{fw}_{\mathrm{forc}} \tag{2}$$

The forcing term ($\mathcal{F}^{fw}_{\mathrm{forc}}$) is the sum of atmospheric freshwater input at the sea surface (i.e., E-P), sea ice melt and terrestrial runoff. Advective fluxes of freshwater are calculated offline using salinity and velocity fields:

$$\mathcal{F}_{\mathbf{adv}} = \iint_A \mathbf{u}_{res} \cdot \left(\frac{S_{ref} - S}{S_{ref}}\right) dA \tag{3}$$

$\mathcal{F}_{adv}$ is evaluated at each grid point. S is interpolated to the grid cell faces where the velocity vector $\mathbf{u}_{res}$ is defined. $\mathbf{u}_{res}$ is the residual mean velocity field, which contains both the resolved (Eulerian), as well as the Gent-McWilliams bolus velocity (i.e., the parameterization of unresolved eddy effects). Diffusive freshwater fluxes ($\mathcal{F}_{\mathbf{diff}}{}^{fw}$) are not provided as a separate diagnostics in ECCOv4, such that $\nabla \cdot \mathcal{F}_{\mathbf{diff}}{}^{fw}$ is inferred from the difference of the total tendency minus advective convergence ($\nabla \cdot \mathcal{F}_{\mathbf{adv}}$) and $\mathcal{F}^{fw}_{\mathrm{forc}}$. On the other hand, diffusive fluxes of salt are provided in ECCOv4. In the supplementary information we present budgets for both salt and salinity for the SPNA and NSEA in which diffusive convergence is resolved. Diffusive convergence of salt is shown to be identical to salinity and matches the inferred diffusive convergence of freshwater that is presented in the main text.

In terms of the heat budget, we simply evaluate the budget in terms of temperature tendency (with units $^{\circ}\mathrm{C\,s^{-1}}$) and then convert it to heat content by multiplying tendencies with the specific heat capacity, seawater density and volume of each grid cell. These can then be summed over the region of interest (e.g., SPNA, NSEA, LSEA). Thus, the heat budget presented here is a balance of temperature tendencies (i.e., change over time) for each budget term. The total tendency is a sum of the tendencies due to advective convergence, diffusive convergence, and forcing:

$$\frac{\partial \theta}{\partial t} + \nabla \cdot (\theta \mathbf{u}_{res}) = -\nabla \cdot \mathcal{F}_{\mathbf{diff}}{}^{\theta} + \mathcal{F}^{\theta}_{\mathrm{forc}} \tag{4}$$

Here, the forcing term for heat ($\mathcal{F}^{\theta}_{\mathrm{forc}}$) is essentially the downward heat flux from the atmosphere (with minor input from geothermal heating).

Following the derivation from previous studies (e.g., Doney et al., 2007; Buckley et al., 2015; Piecuch et al., 2017) we also present a temporal decomposition of the advective convergence into linearized budget terms. Anomalies in advective convergence of freshwater and heat can be partially due to variability in velocity (i.e, anomalies in velocity acting on the mean), variability in salinity / temperature (i.e., anomalies in the tracer advected by the mean velocity field), and due to the covariability of salinity / temperature and velocity anomalies. As noted above, the advection of freshwater is derived offline. This is also the case for the linearized budget terms, which are derived from monthly-averaged velocity and tracer (i.e, temperature or salinity) fields. The derivation of these terms entails some residual due to neglecting sub-monthly covariation and variability in the scaling factor related to the non-linear free surface formulation in ECCOv4. Our analysis confirms that the residual term is very small in all instances, especially integrated over the large area of SPNA, NSEA and LSEA, and therefore do not prevent closing of the budgets to a sufficient degree of accuracy that accounts for virtually all variability. Thus, the residual terms are omitted in the presentation of the budgets in the main text, but are included in the supplementary information.

2.5 Time series and correlation analysis

Most of our analysis is presented as time series of tendencies. To derive the time series of each budget term, the gridded fields were summed over each ocean region presented in Figure 1. Thus, for each region (SPNA, NSEA, LSEA) we have a monthly time series of each budget term as presented in Equation (2) for freshwater and Equation (4) for heat. Monthly time series of volume, freshwater and heat flux are also derived for each boundary presented in Figure 1 by integrating the advective fluxes over the cross sectional area of each boundary. We also calculate the freshwater flux due to sea ice transport across the Fram and Davis Straits, converting sea ice volume to freshwater volume by the same approach as presented in Haine et al. (2015). Besides the tendencies and flux terms, which represents the change per unit of time, we also integrate temporally to derive time series of freshwater and heat content, which can be compared to observational estimates (derived directly from salinity and temperature data). Furthermore, temporal aggregation of tendencies and fluxes was done on the monthly time series by summing them over annual and pentad intervals to describe freshwater and heat changes at those time scales.

To analyze how relevant each budget term is in driving changes in freshwater and heat content at a given time scale, we consider the correlation between the total tendency (i.e., left-hand side in Equations (2) and (4)) and each individual budget term (i.e., terms on the right-hand side in Equations (2) and (4)). In light of the conservation of freshwater and heat in ECCOv4, the total tendency term on the left-hand side of each equation (denoted here in general as y) is the sum of the corresponding budget terms on the right-hand side of each equation. Thus for any particular budget term x, we can calculate the covariance ratio as

$$r_x = \frac{\sigma^2_{x\,y}}{\sigma^2_{y\,y}} \tag{5}$$

where $\sigma^2_{x\,y}$ is the covariance between x and y and $\sigma^2_{y\,y}$ is the variance of y.

In any particular budget, the covariance ratios describe the contributions of each budget term to the total tendency. Because the budgets in ECCOv4 are closed and thus the total tendency is the exact sum of all the budget terms, the sum of the covariance ratios should equal 1.0. The covariance ratio for a given term can therefore be regarded as the contribution of that term to the variability of the freshwater/heat content for a given ocean region and time scale, assuming that there is no significant covariation between budget terms, which we show to be the case. A covariance ratio between 0 and 1 implies a positive contribution (and correlation) to the total tendency, and a covariance ratio between -1 and 0 implies a negative contribution (and an inverse correlation) to the total tendency.

3 Results

In this section we first present a comparison of liquid freshwater content for the SPNA and NSEA between the observation-based EN4 and ECCOv4. Transport estimates through key sections from observational studies and from ECCOv4 are also compared. We next describe the freshwater and heat budgets for the SPNA and NSEA and from them identify the dominant mechanisms driving variability in freshwater and heat content anomalies. The most important boundary fluxes impacting the anomalies are identified as well. Finally, we present a separate budget analysis of freshwater and heat content in the Labrador Sea, with a focus of the recent changes in boundary fluxes.

3.1 Comparison to observations

Estimates of liquid freshwater content (LFWC) in the subpolar North Atlantic (SPNA) and the Nordic Seas (NSEA) were derived from the EN4 salinity fields, using Equation (1) for monthly time series and the method of R. Curry and Mauritzen (2005) for pentad averages (Figure 2). Monthly estimates employed a reference salinity of $35.0\,\mathrm{g\,kg^{-1}}$, while pentad averages were derived using the climatological annual cycle over 1950-1959 (i.e., ranging from 34.89 in September to 35.1 in April) as a reference. All time series represent full-depth estimates, integrated over the entire water column and defined in the same spatial domain as presented in R. Curry and Mauritzen (2005) (see black outlines in Figure 3a). Equation (1) and the method of R. Curry and Mauritzen (2005) yield similar results even though the choice of reference salinity is different (i.e., $35\,\mathrm{g\,kg^{-1}}$ versus 1950-1959 baseline averages). With the methodology of R. Curry and Mauritzen (2005), pentad averages of EN4 salinity fields are consistent with their published time series, which were based on HydroBase2 (Figure 2a, b; red lines). The bias seen in the SPNA might be explained by the different type of observation data used (i.e., EN4 versus HydroBase2), with HydroBase2 systematically fresher relative to EN4 in the SPNA. There is no clear bias in the NSEA between EN4 and HydroBase2 derived time series.

There has been clear decadal variability in the LFWC of the SPNA and the NSEA over the last 60 to 70 years. As described by R. Curry and Mauritzen (2005), LFWC in these regions increased between the late 1960s to mid-1990s. However, the estimated increase in the SPNA is lower with the updated observations from EN4, suggesting the to-

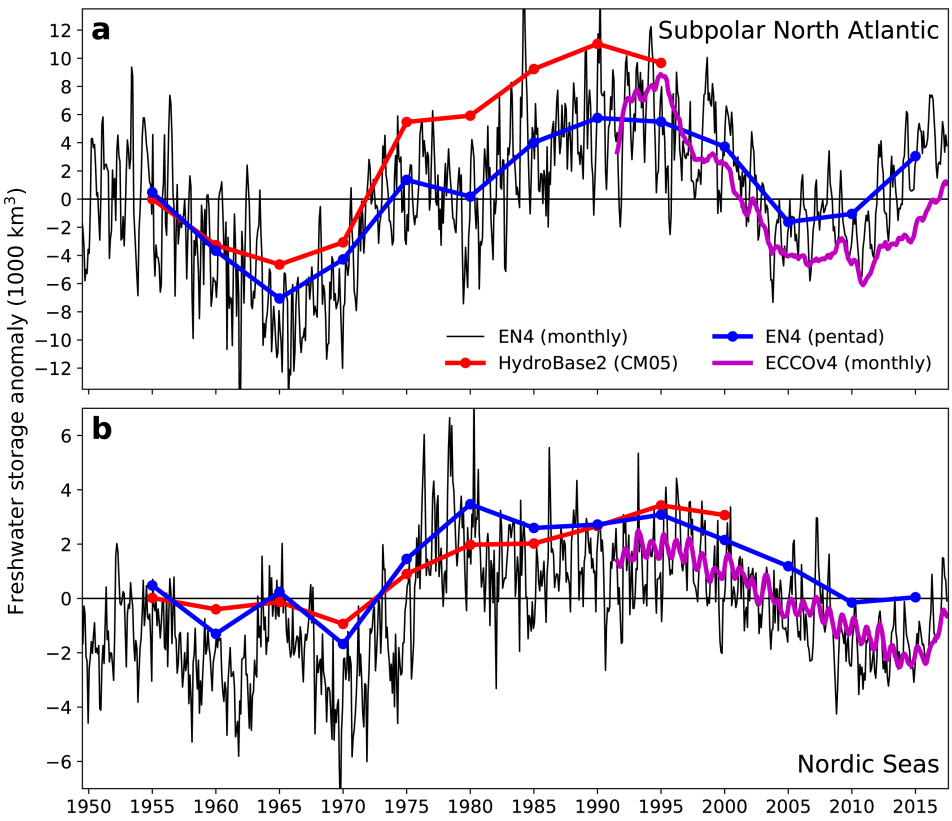

Figure 2. Freshwater variability in the (a) subpolar North Atlantic and (b) Nordic Seas. The thick solid lines represent pentadal means from EN4 (blue) and HydroBase2 (red, taken from R. Curry & Mauritzen, 2005). The pentad time series are anomalies to their 1950-1955 mean. Black lines represent the monthly anomaly from EN4 and the purple line from ECCOv4, both relative to a reference salinity of $35\,\mathrm{g\,kg^{-1}}$. Note that the scale of the y axis for (a) the subpolar North Atlantic is about twice that of (b) the Nordic Seas.

tal accumulation to be around half of the original estimates. The overall change from the minimum in 1965 to the maximum in 1990 is approximately $13\,000\,\mathrm{km^3}$ using EN4, as compared to $16\,000\,\mathrm{km^3}$ estimated with HydroBase2. Since approximately the end of the R. Curry and Mauritzen (2005) study period, by using the latest observational data from EN4, a decline in freshwater content is evident in both the SPNA and NSEA. In 2005, LFWC in the SPNA is approximately the same as observed in the 1950s. Beginning in 2010, a renewed freshening in the SPNA is evident. In general, the LFWC variability in NSEA follows that of the SPNA with a delay of 3 to 5 years. The rise in LFWC seen in the SPNA in the late 1960s is followed by a rise in the NSEA in the early 70s, though the magnitude of the rise in the NSEA is only a fraction of the rise in the SPNA. The same temporal lag between SPNA and NSEA can be seen in the recent freshening, which occurred over the last 10 years in the SPNA but can be observed only after 2015 in the NSEA.

Monthly freshwater anomalies for the period 1992 to 2017 were also derived with the ECCOv4 reanalysis product. Here we used the regular gridded salinity fields of Release 4, as it extends the time coverage to 2017, and converted to liquid freshwater content using Equation (1) with a reference salinity of $35\,\mathrm{g\,kg^{-1}}$. The long term change in freshwater content in ECCOv4 is mostly consistent with the EN4 observations, despite minor discrepancies. For example, there is a clear seasonal cycle evident in EN4, while seasonality is only somewhat discernible in ECCOv4 (mostly for the NSEA). In the SPNA, the freshening of the recent 7 years does not manifest as clearly in the ECCOv4 reanalysis compared to EN4. While the declining trend over 1998-2005 in ECCOv4 ($-1110\,\mathrm{km^3\,yr^{-1}}$) is very close to EN4 ($-1190\,\mathrm{km^3\,yr^{-1}}$), the positive trends over 2010-2017 are reduced in ECCO ($770\,\mathrm{km^3\,yr^{-1}}$) compared to EN4 ($1140\,\mathrm{km^3\,yr^{-1}}$). Furthermore, we observe a slight bias towards a saltier SPNA for most of the time period in ECCOv4.

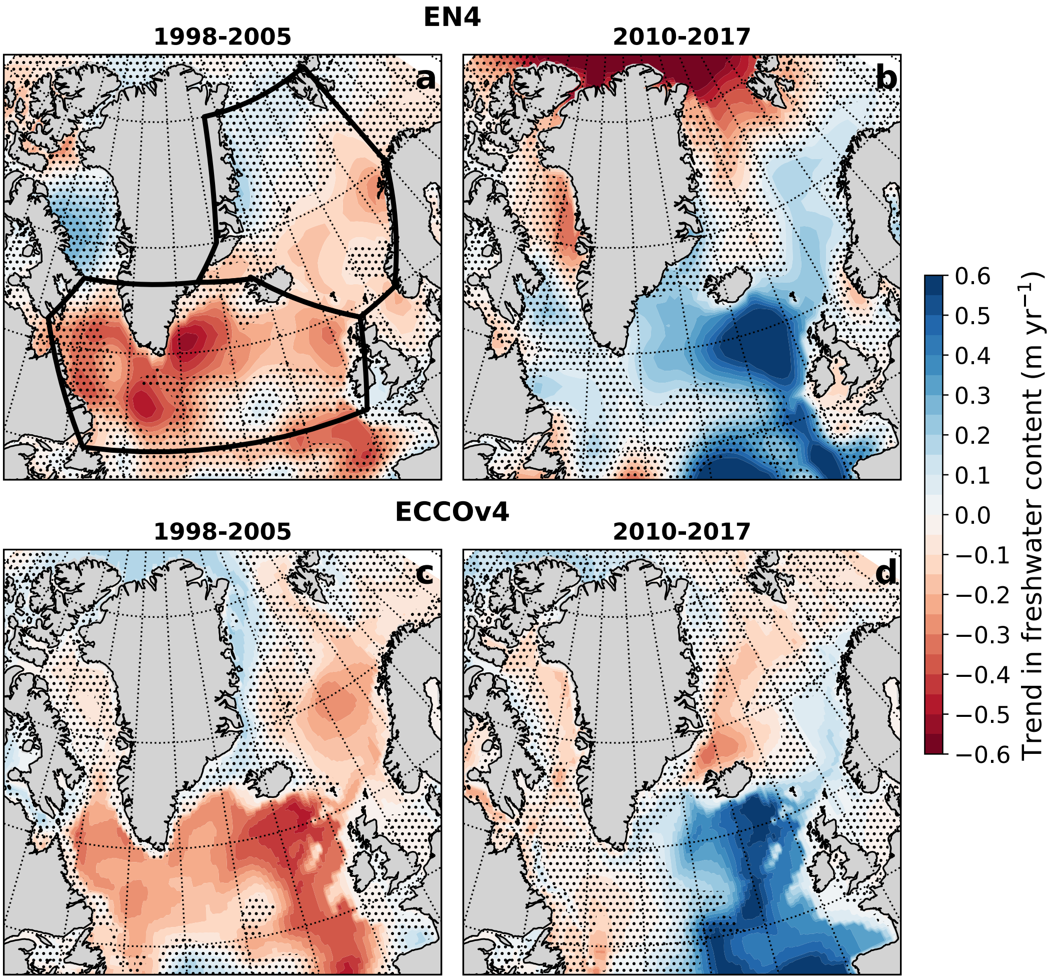

Figure 3. Spatial distribution of linear trends in freshwater content for the periods 1998-2005 and 2010-2017 as seen in (a,b) EN4 and (c,d) ECCOv4. The stippling indicates regions where the linear trend is not significant (i.e., a trend of zero is within the 95% confidence interval). Black outlines denote the SPNA and NSEA regions over which the freshwater content time series in Figure 2 are derived.

The overall consistency between EN4 and ECCOv4 is also apparent in the spatial pattern of LFWC trends over the periods 1998-2005 and 2010-2017 (Figure 3). There are second order differences between EN4 and ECCOv4 which mostly only apply to areas where trends are not significant. EN4 and ECCOv4 both show a decline during 1998-2005 over most of the SPNA and Norwegian Sea (i.e., the eastern half of the NSEA). However, the salinification is focused in the eastern SPG in EN4, while in ECCOv4 the strongest trends are further east. This difference could likely be due to spatial sampling bias in

EN4. Over 2010-2017, LFWC is increasing over most of the SPNA and eastern NSEA. EN4 shows weak positive trends in the western SPG which is not seen in ECCOv4. This suggests a missing freshening source in ECCOv4 (e.g., enhanced Greenland Ice Sheet melting over recent years). However, most of the positive trends that one sees with EN4 over the Labrador Sea and western SPG are not significant.

Volume, freshwater and heat fluxes across selected straits and transects, from which there are sufficient observations reported in the literature, were compared to mean fluxes found in ECCOv4 (Table 1). Here, positive terms indicate northward/eastward fluxes, while negative terms indicate southward/westward fluxes. The confidence intervals for ECCOv4 values are defined as ± 2 standard deviations and reflect the temporal variability of the monthly fluxes. These are not the same as the confidence intervals presented for the observations, which also include instrument error and uncertainties related to spatial and temporal limitations of mooring design (see Section 2.2). In general, mean volume transports in ECCOv4 are in good agreement with observations. The ECCOv4 estimates nearly all fall within the error ranges of the observational estimates. The southward volume flux through Denmark Strait is only slightly greater in ECCOv4 compared to what observations suggest. On the other hand, in case of the northward volume flux through the Faroe-Scotland ridge, ECCOv4 suggests a mean transport about twice as large compared to observations.

Greater disagreement is seen in the freshwater and heat fluxes. The ECCOv4 freshwater flux through Davis Strait is within the error ranges of observations. Also, the relatively small (essentially zero) net freshwater flux through the Barents Sea Opening (BSO) in ECCOv4 is within the error ranges of observations. More importantly, heat fluxes through BSO in ECCOv4 matches very well with observations. In the case of Davis Strait heat fluxes (into the Arctic Ocean), the ECCOv4 estimate is considerably smaller (8 TW) compared to what observations suggest (20 ± 9 TW). In the case of Fram Strait and Denmark Strait, both the freshwater and heat fluxes are smaller in ECCOv4 compared to observations. This could suggest an insufficient resolution of the East Greenland Current, which is important for freshwater flux in the Fram Strait and Denmark Strait (de Steur et al., 2017, 2018). Similarly, limited resolution of warm currents such as the West Spitsbergen Current (relevant to Fram Strait heat flux) and the North Iceland Irminger Current (relevant to Denmark Strait heat flux) in ECCOv4 could be the reason for the underestimations in ECCOv4 heat fluxes through these straits. To our knowledge, no observational estimates of freshwater flux through the Iceland-Faroe-Scotland ridges have been reported in the literature. We see a slight underestimation in ECCOv4 heat flux across the Iceland-Faroe section and a slight overestimation across the Faroe-Scotland section. Again, we point out that even though there is some disagreement between ECCOv4 and observations, observational estimates are often based on shorter time frames and include various uncertainties due to incomplete spatial and seasonal coverage of measurements. In ECCOv4, the fluxes represent complete temporal means (from the 1992 to 2015) throughout the whole section and include all seasons.

Sea ice flux through Fram Strait has a mean of -49.4 ± 59.4 mSv in ECCOv4 which is somewhat smaller compared to observations of -67 ± 14 mSv (Haine et al., 2015). Sea ice flux through Davis Strait is much smaller with a mean of -13.8 ± 30.8 mSv in ECCOv4, which is consistent with the observational estimate of -5 mSv between 1980-2000 and -10 mSv between 2000-2010 (Haine et al., 2015).

Other sections that are included in the ECCOv4 budgets are assumed to have insignificant influence on the freshwater and heat budgets. However, observational records of these sections are limited and associated with large uncertainties. For example, the volume transport across Hudson Strait into the Labrador Sea has been assumed to be irrelevant ($\sim$0.1 Sv) by a previous synthesis study (Haine et al., 2015), which is consistent with the mean of 0.03 Sv determined in ECCOv4. However, (Straneo & Saucier, 2008) observed a transport of 1–1.1 Sv for 2004-2005. Similarly, observed freshwater fluxes through

Table 1. Mean fluxes of volume, freshwater and heat through selected sections along the boundaries of the SPNA and NSEA. Observational estimates are presented together with the mean 1992-2015 fluxes in ECCOv4. Positive values represent a net northward/eastward flux and negative values a net southward/westward flux. All fluxes are depth-integrated over the entire water column unless otherwise noted. Freshwater fluxes in ECCOv4 are calculated in the same way as in the observational studies (see table notes). In cases where there is no observational estimate, a reference salinity of 35.0 g kg^{-1} is used. The confidence intervals for the ECCOv4 estimates are presented as ±2 standard deviations.

Section Name	Volume flux (Sv)		Freshwater flux (mSv)		Heat flux (TW)	
	Observation	ECCOv4	Observation	ECCOv4	Observation	ECCOv4
Davis Strait (DaS)	-1.7±0.2[1]	-1.6±0.6	-97±11[2]	-87±31[a]	20±9[3]	8±10
Fram Strait (FrS)	-0.8±1.5[4] -2.0±2.7[5]	-2.9±2.0	-88±22[2] -65±1[6]	-49±26[b]	36±6[7]	11±13
Denmark Strait (DeS)	-4.3±0.7[1]	-5.4±2.6	-65±11[8]	-41±42[c]	21.8±0.2[9]	5±31
Iceland-Faroe (IF)	3.4±0.6[1] 4.46±0.7[9]	3.6±1.8	–	-21±15	141±22[9]	114±60
Faroe-Scotland (FS)	1.0±0.6[1]	2.2±3.9	–	-28±22	101±15[9]	128±107
Barents Sea Opening (BSO)	3.2[10]	3.3±2.1	-2.85±2.85[2]	-1.5±3.4[c]	73[9]	79±47

[1] Østerhus et al. (2019); [2] Haine et al. (2015); [3] B. Curry et al. (2011);
[4] Marnela et al. (2016); [5] Schauer, Ursula and Beszczynska-Möller, Agnieszka and Walczowski, Waldemar and Fahrbach, Eberhard and Piechura, Jan and Hansen, Edmond (2008);
[6] de Steur et al. (2009); [7] Schauer and Beszczynska-Möller (2009); [8] de Steur et al. (2017);
[9] Rossby et al. (2018); [10] Smedsrud et al. (2010); [a] $S_{ref} = 34.8$ and integrated from sill depth (640 m) according to B. Curry et al. (2014); [b] $S_{ref} = 34.9$ and integrated from isohaline depth according to de Steur et al. (2009); [c] $S_{ref} = 34.8$ and integrated from isohaline depth according to de Steur et al. (2017) and Haine et al. (2015).

Hudson Strait are not very constrained, with estimates of 38 mSv (Haine et al., 2015) and 78–88 mSv (using reference salinity of 34.8 for 2004-2005 being reported (Straneo & Saucier, 2008). The present study finds a mean freshwater flux across Hudson Strait into the Labrador Sea in ECCOv4 of 29 mSv (using a reference salinity of 34.8). Volume flux through the English Channel is negligible, with a mean of 0.06 Sv in ECCOv4. This is consistent with the 0.1 Sv flux determined from observations (Prandle, 1993).

3.2 Budgets for the subpolar North Atlantic and Nordic Seas

We present both the liquid freshwater content (LFWC) and ocean heat content (OHC) derived from ECCOv4 salinity and temperature, respectively. LFWC was calculated as the zero-salinity water volume necessary to account for deviations from a reference salinity of 35 g kg^{-1} (see section 2.3). OHC was calculated by multiplying the temperature tendencies by the specific heat capacity and density of seawater. As with the freshwater calculation, heat content estimates rely on a reference temperature, which is here set to 0℃. Freshwater and heat content are calculated for each grid point and then integrated over full depth for the SPNA and the NSEA. The spatial domain given by the ECCOv4 grid design (Figure 1) results in LFWC variability that is almost identical to variability determined by the domain design of R. Curry and Mauritzen (2005) (Figure S1a,b). Though slightly discernable in the NSEA, overall very little seasonality in LFWC is observed. On the other hand, clear seasonality is evident in the heat content anomaly time series in both the SPNA and the NSEA (Figure S1c,d). By focusing on interannual variability while disregarding seasonality, a clear anti-correlation between LFWC and OHC anomalies is revealed. Whereas there is a decline in LFWC since the mid-1990s to the mid-2000s, there is a clear increase in OHC over the same time period in the SPNA. Similarly, the recent increase in LFWC since 2010 occurs alongside a decline in OHC in the SPNA. The same anti-correlation is evident in the NSEA especially when comparing the long-term trends between LFWC and OHC.

3.2.1 Balance of forcing, advection and diffusion

In the most basic form the freshwater and heat budgets in a region can be described as a balance between forcing terms and transport (i.e., advection and diffusion) terms. These are presented here as fluxes showing the change in freshwater and heat content over time. The total tendency of freshwater content for both the SPNA and the NSEA is a balance between forcing and advection (Figure 4a,c). The forcing over the SPNA contributes to freshening, while advection mostly counteracts freshening, as those fluxes are predominantly negative. The interannual variability in total freshwater flux in the SPNA is predominantly due to the advective flux (Figure 4a). In the case of NSEA, on the other hand, advection is not the obvious driver in freshwater variability, and the forcing term dominates (Figure 4c). The heat tendency in both the SPNA and the NSEA is dominated by forcing (i.e., seasonal warming and cooling at the sea surface), while advection represents a positive heat input for both regions. The diffusion term, being a relatively constant negative flux, represents a minor contribution to salinification over the whole time period (Figure 4a,c). Convergence of diffusive heat fluxes are negligible in both the SPNA and the NSEA (Figure 4b,d).

Budgets of volume, salt and salinity are presented in the supplementary materials (Figure S2). Comparison of salinity (Figure S2c,f) with freshwater budgets (Figure 4a,c) for SPNA and NSEA, respectively, confirms that they are equivalent, as freshwater tendencies are the inverse of the respective salinity tendencies. Our calculation of diffusive freshwater fluxes is similar to diffusive salinity fluxes (Figure S3), which suggests that the residual terms in the freshwater budgets are negligible. Furthermore, the spatial distribution of mean tendencies for freshwater (Figure S4) and salinity (Figure S5) over 1998-2005 and 2010-2015 again shows that our estimates of freshwater tendencies closely match the inverse of salinity tendencies.

Comparing the major terms for freshwater and heat fluxes reveals a clear difference in seasonality between forcing and advection (Figure 4). The climatological annual cycles of the flux terms (Figure 5) illustrate that seasonality is mostly seen in the forcing terms for both the SPNA and NSEA. A distinct seasonality in freshwater flux is driven by forcing and to a lesser degree by advection (Figure 5a,c). In both SPNA and NSEA the freshening (i.e., positive tendency) is partly driven by less negative advective convergence in the late summer (July to September). Conversely, forcing alone drives the seasonality of the total heat tendency in both the SPNA and the NSEA, with advection representing a warming contribution with very little seasonality (Figure 5b,d).

Removing the seasonal cycle from the budget terms emphasizes which terms drive seasonal anomalies in freshwater and heat content. Seasonal anomalies in SPNA fresh-

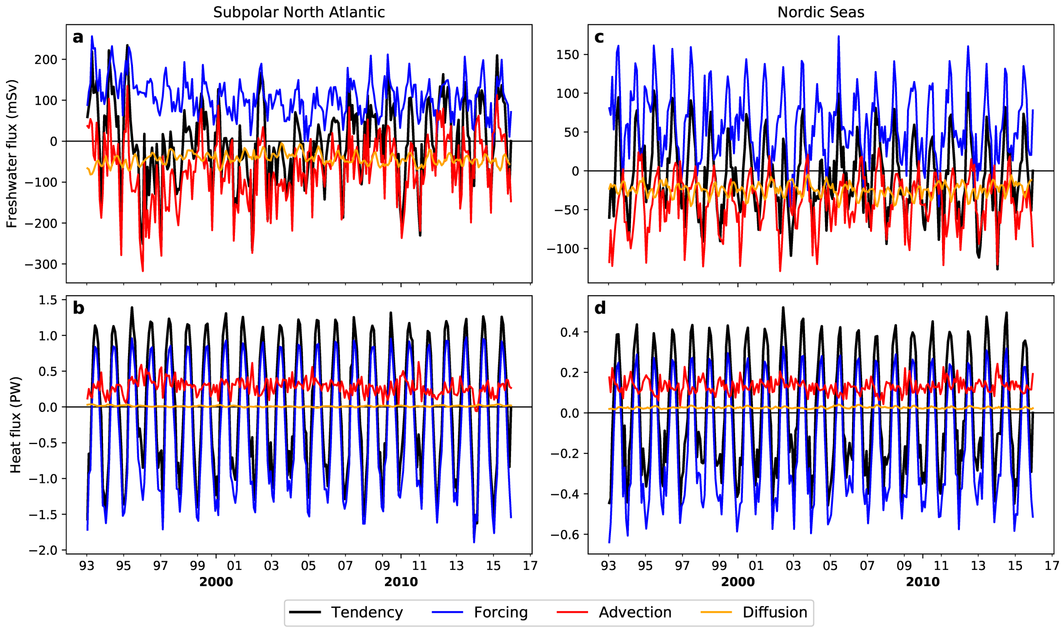

Figure 4. Monthly time series of tendencies/fluxes for freshwater (a,c) and heat (b,d) from ECCOv4 for the subpolar North Atlantic (a,b) and Nordic Seas (c,d), including separate components for surface forcing, advection, and diffusion. Freshwater tendencies/fluxes are derived with Equation (2) and heat tendencies/fluxes are derived with Equation (4). Note the different y scales for the subpolar North Atlantic (a,b) and Nordic Seas (c,d).

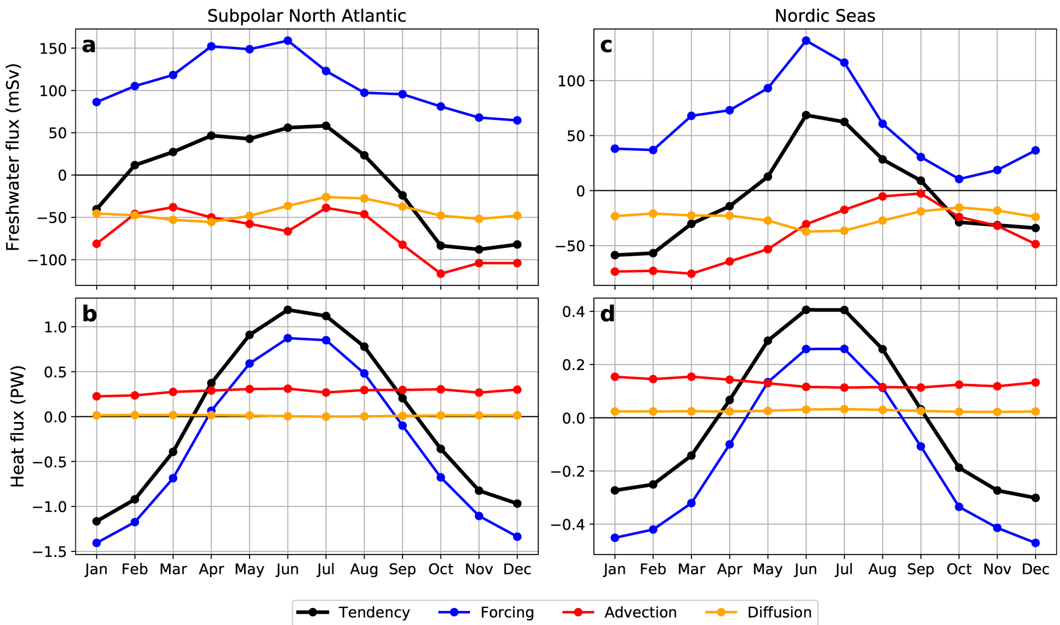

Figure 5. Mean seasonal cycle of ECCOv4 freshwater (a,c) and heat (b,d) tendencies for the subpolar North Atlantic (a,b) and Nordic Seas (c,d), including separate components for surface forcing, advection, and diffusion. Note the different y scales for the subpolar North Atlantic (a,b) and Nordic Seas (c,d).

water fluxes are clearly driven by advective convergence, with forcing and diffusion playing only a minor role (Figure 6a). This is also illustrated in the covariance ratio (Equation (5)) that quantifies the contribution of each term to the total tendency anomaly (Table 2). The high frequency (i.e., monthly) covariance ratio from advection is 0.88 (versus 0.16 for forcing). For the annual time scale the covariance ratio for advection is 0.87 (versus 0.24 for forcing), and for the pentad it is 1.25 for advection (versus -0.05 for forcing). The situation is a little different in the case of heat fluxes in the SPNA. Here, both forcing and advection seem to affect the monthly variability in heat flux anomaly (Figure 6b). Advection shifts from 0.41 at monthly frequency to 0.98 for the pentad, while forcing shifts from 0.59 for monthly frequency to 0.06 for the pentad (Table 2). The dominance of advection in driving low frequency (e.g., pentad) heat variability is not obvious in the monthly time series (Figure 6b). Whereas variability in freshwater flux anomalies seems to be determined solely by advection at the monthly timescale, forcing is still relevant for monthly (and presumably sub-monthly) heat anomaly variation.

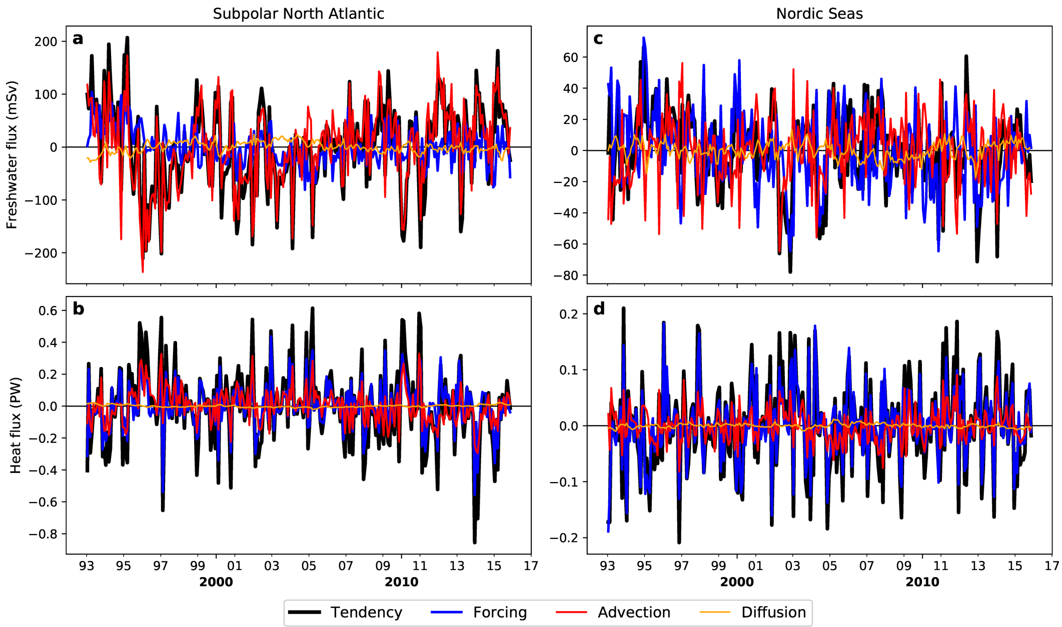

Figure 6. Monthly time series of seasonal anomalies in ECCOv4 freshwater and heat fluxes for the subpolar North Atlantic (a,b) and Nordic Seas (c,d), including separate components for surface forcing, advection, and diffusion. Note the different y scales for the subpolar North Atlantic (a,b) and Nordic Seas (c,d).

The freshwater flux variability in the case of the NSEA does not show an obvious dominant role of advection. The monthly variability of the total flux anomaly mostly follows the variability in forcing (Figure 6c), and this seems to be the case for heat flux as well (Figure 6d). The freshwater flux contributions as determined from covariance ratios shows that forcing and advection are approximately the same when considering variability at monthly (i.e., 0.58 and 0.44 for forcing and advection, respectively) to annual (i.e., 0.58 and 0.46 for forcing and advection, respectively) resolution (Table 2). However, the balance is clearly dominated by forcing on pentad time scale (i.e., forcing correlation = 1.08). For heat flux, forcing remains important across the different time scales from monthly to pentad, however, the importance of advection increases as the time scale increases. Where the advection contribution is only 0.26 at the monthly time scale, it increases to 0.67 at the pentad time scale (Table 2).

Table 2. Covariance ratios for forcing, advection and diffusion for heat and freshwater variability in the SPNA and NSEA. Covariance ratios are evaluated for each budget term on monthly, annual and pentad scales. Significant contributions are indicated by bold numbers.

	Freshwater						Heat					
	SPNA			NSEA			SPNA			NSEA		
	monthly	annual	pentad	monthly	annual	pentad	monthly	annual	pentad	monthly	annual	pentad
Forcing	0.16	0.24	−0.05	**0.58**	**0.58**	**1.08**	**0.59**	**0.46**	0.06	**0.74**	**0.66**	**0.46**
Advection	**0.88**	**0.87**	**1.26**	0.44	0.46	0.23	0.41	**0.57**	**0.98**	0.26	0.34	**0.67**
Diffusion	−0.04	−0.11	−0.21	−0.01	−0.04	−0.30	−0.01	−0.03	−0.04	0.00	−0.01	−0.13

Another way to emphasize variability over longer time scales is to time-integrate each flux term and compare these with the time-integrated total tendency, representing freshwater and heat content anomalies (Figure 7; see Figure S6a,b for integrated salinity fluxes in SPNA and NSEA). Time-integration makes obvious that advection is the dominant driver in the overall variability in freshwater content in the SPNA (Figure 7a). Both the decline from the mid-90s to mid-2000s and the recent freshwater increase since 2010 has been driven by changes in advective flux convergence. Over the same time period, forcing and diffusion play only a minor role, and it is evident that they partially compensate each other. The dominance of advective convergence in decadal variability is also clear for heat content in the SPNA (Figure 7b).

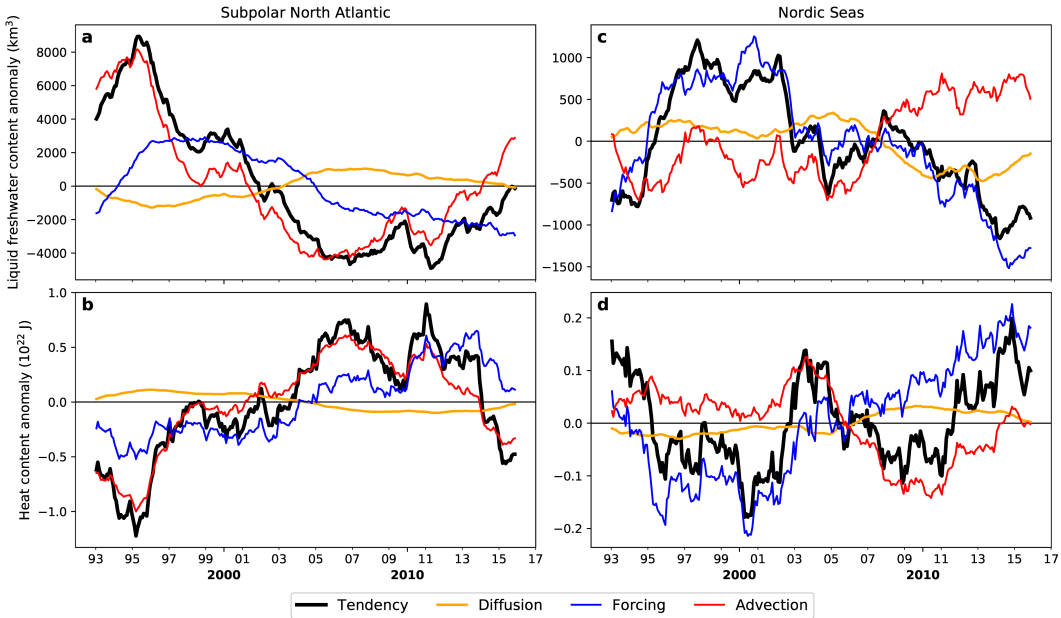

Figure 7. Integrated monthly time series of ECCOv4 freshwater and heat content anomalies of the subpolar North Atlantic (a,b) and Nordic Seas (c,d), including separate components for surface forcing, advection, and diffusion. Note the different y scales for the subpolar North Atlantic (a,b) and Nordic Seas (c,d).

Similar to the variation in freshwater and heat content, the anomaly time series of the different components that regulate freshwater and heat content (i.e., forcing, advection and diffusion) are clearly anti-correlated. Freshwater variability in the SPNA due to forcing alone suggests a long term decline since the mid-1990s, while heat content variability due to forcing alone suggests a long term increase over the same time period. However, these trends are dwarfed by the decadal variability due to changes in the advective flux, such that both freshwater/heat content in the SPNA follow the ~10 year decline/rise between 1995 to 2005 and overall increase/decline thereafter due to advective flux changes. There is some higher frequency variability in the heat content due to forcing that is not seen in the freshwater content, however this is only a second-order variability compared to the long term change due to advection.

In contrast to the SPNA, changes in advective flux convergence are not the sole driver of interannual anomalies in the NSEA (Figure 7c, d). Here, changes in freshwater content are predominantly driven by the forcing term (Figure 7c). This is surprising, given the clear covariation in LFWC between SPNA and NSEA (Figure 2 and 3). However, the increase in the early 1990s, and the overall decline that occurs since then, is clearly due to the variation in the forcing term, while advective flux convergence only plays a secondary role in freshwater content changes in the NSEA. The picture is slightly different in the NSEA heat budget, in that forcing is the dominant term that drives the overall variation heat content in the 1990s, but the variability becomes more affected by advection in the early 2000s. While heat content variability due to forcing is increasing from 2003 to 2011, the total tendency is actually declining over this period, driven by variability in advective flux convergence. This shift is likely due to the magnitude of change in advection being greater, and therefore counteracting, the change in forcing during that time period. After 2011, the increase in the total heat content tendency is reflected by increases in both the forcing and advective flux terms. The diffusion term is a negligible factor for the balance of the integrated flux terms for LFWC as well as heat budgets in both the SPNA and NSEA.

3.2.2 Temporal decomposition of the advection term

The dominance of advective fluxes in the SPNA prompts further analysis of how advection changes over the time period under consideration. Greater detail can be gained by temporally decomposing freshwater and heat advection (Piecuch et al., 2017), which separates the total change in advective convergence into changes due to anomalies in the circulation, changes due to anomalies in the scalar field (i.e., salinity or temperature), or changes due to the covariation of both (Figure 8). In both the SPNA and the NSEA, the change in advective convergence is largely due to the anomalous circulation that advects the mean. This holds for both freshwater (Figure 8a, c), salinity (Figure S7a, b) and heat (i.e., temperature; Figure 8b, d) where the anomalies in those fields play a minor role. In all cases, the advection of anomalies demonstrates a compensating role that counteracts variability due to anomalous advection of the mean. The nonlinear term due to the covariation of both anomalies in circulation and the property field is negligible in all cases. As noted previously (Section 2.4), derivation of the anomaly budget needs to account for a residual term. Figure 8b and d confirms that the residual terms are negligible in the case of heat advection. The residual term for freshwater content is contained within the diffusive flux, but we see that in the case of salinity it is essentially zero (Figure S7).

3.2.3 Flux across the subpolar North Atlantic and Nordic Seas boundaries

We refer to supplementary Figure S8 for monthly fluxes of freshwater and heat across the different boundaries into the SPNA and NSEA. These are defined as positive when adding freshwater or heat to the region, such that their sum equals the total convergence of advection (red lines in Figure 4). The advective convergence of freshwater in the SPNA is a balance between a dominant southern salinification across the Newfoundland-Iberia boundary and freshening through the Davis and Denmark Straits (Figure S8a). There are smaller freshening fluxes from the Hudson Strait and the Iceland-Faroe-Scotland sections, while changes in freshwater due to English Channel transport is essentially zero relative to the other transport terms. On the other hand, the advective convergence of heat in the SPNA is primarily a result of heat flux through the southern boundary, minus those of the Iceland-Faroe-Scotland sections and with negligible heat fluxes through the other sections (Figure S8b).

In the case of the NSEA, advective convergence of freshwater is a balance between freshwater input from the Fram Strait and salinification through Denmark Strait. Of transport through the Iceland-Faroe-Scotland sections, salinification through Faroe-Scotland is slightly more prevalent (Figure S8c). Fluxes through the Barents Sea Opening (BSO) and the section between Scotland and Norway (i.e., exchanges to and from the North Sea) are much smaller by comparison. The BSO flux mostly represents the flux of saltier Atlantic water into the Arctic, while most freshwater outflow from the Arctic goes through

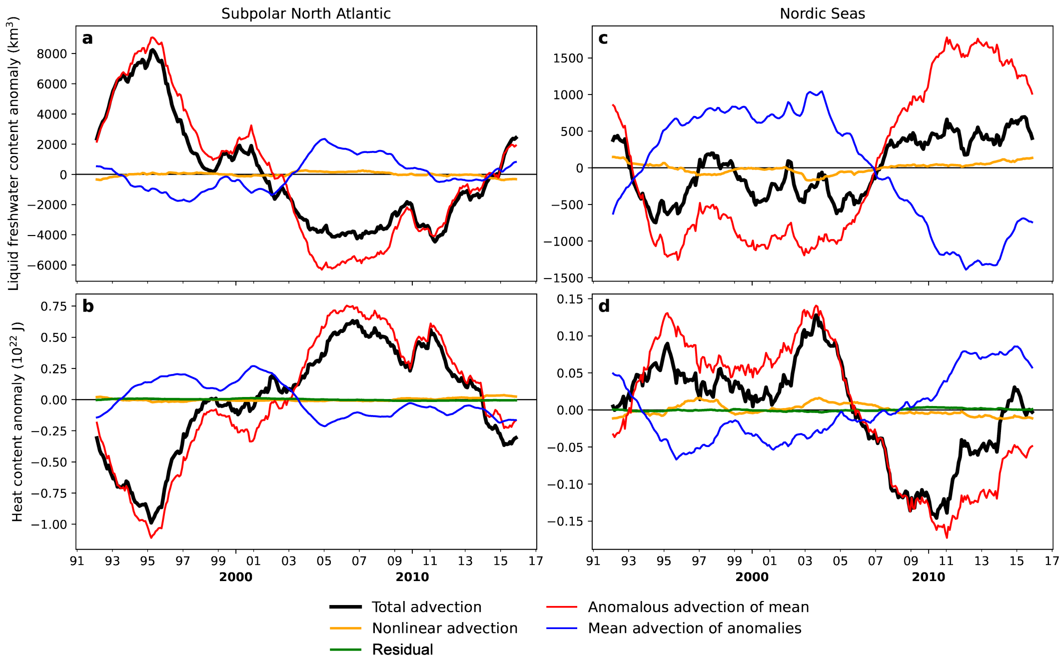

Figure 8. Decomposition of advection into contributions from anomalous advection of the mean, mean advection of anomalies and nonlinear advection into the subpolar North Atlantic (a,b) and Nordic Seas (c,d) for freshwater (a,c) and heat content (b,d). Note the different y scales for the subpolar North Atlantic (a,b) and Nordic Seas (c,d).

Fram Strait. Again, for the NSEA the balance is different for heat compared to freshwater (Figure S8d). Here, the input through Iceland-Faroe and Faroe-Scotland constitutes the main flux of heat to the NSEA, with the BSO representing the greatest outflow of heat. The fluxes through Fram Strait and Denmark Strait represent minor negative fluxes, while exchanges to the North Sea through the Scotland-Norway section can be either positive or negative but represent a negligible flux of heat for the entire NSEA. Overall, advective variations across the Greenland-Scotland ridge are dominant, but because forcing is also significant in the NSEA these results are less significant to the respective total tendency.

Figure S9 shows the corresponding monthly anomaly fluxes through each section. Clear covariation is evident between the anomaly flux through the southern boundary and the total advective convergence for freshwater (Figure S9a) and heat content (Figure S9b) in the SPNA. Other boundaries represent minor or negligible contributions to heat and freshwater anomalies in the SPNA. Comparing the covariance ratios for each term at each boundary with the total advective convergence in the SPNA shows that the variability in the southern boundary flux is still the dominant term at longer time scales. For the pentad time scale the covariance ratio for the Newfoundland-Iberia section is 0.69 for freshwater and 0.75 for heat (Table 3). Both Iceland-Faroe and Faroe-Scotland throughflows are small contributions (i.e., 0.14 and 0.11, respectively) of the pentad variation in freshwater, and similarly for pentad variation in heat fluxes (i.e., 0.16 and 0.12, respectively).

The anomaly fluxes were also integrated with respect to time and normalized to a zero mean (Figure S10). In order to improve readability we only present the major net fluxes in Figure 9, where fluxes through the Denmark Strait and the Iceland-Faroe-Scotland ridges are added together and presented as Greenland-Scotland. In the SPNA the vari-

Table 3. Covariance ratios for freshwater and heat fluxes through each boundary of the SPNA. The boundaries are shown in Figure 1. Covariance ratios are evaluated for each boundary flux on monthly, annual and pentad scales. Significant contributions are indicated by bold numbers.

	Freshwater			Heat		
	monthly	annual	pentad	monthly	annual	pentad
Newfoundland Iberia	**0.76**	**0.80**	**0.69**	**0.78**	**0.80**	**0.75**
Denmark Strait	0.12	0.09	−0.01	−0.03	−0.01	−0.02
Iceland Faroe	0.00	0.04	0.14	0.05	0.03	0.16
Faroe Scotland	0.07	0.07	0.11	0.16	0.17	0.12
Davis Strait	0.04	0.02	0.10	−0.01	−0.02	−0.02
Hudson Strait	0.01	−0.01	−0.02	0.00	0.00	0.00
English Channel	0.00	0.00	0.00	0.04	0.03	0.01

ability of both freshwater and heat content is almost entirely driven by the flux through the southern boundary (i.e., the section across Newfoundland-Iberia). The time-integrated boundary fluxes into the SPNA shows that the total anomaly variation of advective convergences are driven by changes in the southern boundary (Figure 9a,b). Over the ECCOv4 time period, it is the decline of freshwater flux (equivalent to increased salt flux from the south) that is responsible for the freshwater content decline from 1995 to 2005, as is the subsequent increase in freshwater (equivalent to a decrease in salt flux from the south). None of the other boundary flux variations makes a noticeable contribution to the overall shift in freshwater content, although in the past few years Davis Strait outflow has made some contribution to the convergence of freshwater in the SPNA. The variation in the southern boundary freshwater flux is mirrored by the variation in the southern boundary heat flux. The fact that this variation stems from circulation anomalies (Figure 8), suggests that it is mainly the change in the circulation at the southern boundary that simultaneously affects both the freshwater and heat content in the SPNA.

In the case of NSEA, several sections appear to contribute to the variation in advective convergences of freshwater, and it is less clear which boundary dominates (Figure 9c and Figure S10c). Both variability in the northern boundaries (Fram Strait and BSO) and the southern throughflow across the Greenland-Scotland ridge are important. For monthly freshwater anomalies, Denmark Strait anomalies appear to be the dominant variation as seen from a covariance ratio of 0.56 for the monthly scale (Table 4). Smaller contributions in monthly variability are through Faroe-Scotland boundary (0.18) and the Fram Strait (0.19). The Denmark Strait still contributes around half (0.54) at the annual scale, with approximately one quarter of the contribution from the Fram Strait (0.28). The contribution at larger time scales (i.e., pentad or longer) shifts to Fram Strait and BSO (Table 4 and Figure S10c). Other boundary fluxes counteract the variation in Fram Strait and BSO (as seen by the negative covariance ratios in Table 4). It should be noted that none of the liquid freshwater boundary fluxes are significantly correlated with freshwater content variability, because the NSEA freshwater budget is mostly controlled by the forcing term.

Throughflow across the Greenland-Scotland ridge is the dominant driver for monthly, annual and pentad variations in heat advection in the NSEA (Figure 9d). This is mostly the sum of the throughflows across the Iceland-Faroe-Scotland sections with a minor secondary role of the BSO throughflow, which determines the interannual variation in advective convergence of heat within the NSEA. Fluxes through the Denmark Strait, Fram Strait and Scotland-Norway boundaries are negligible for heat advection in the NSEA (Table 4 and Figure S10d).

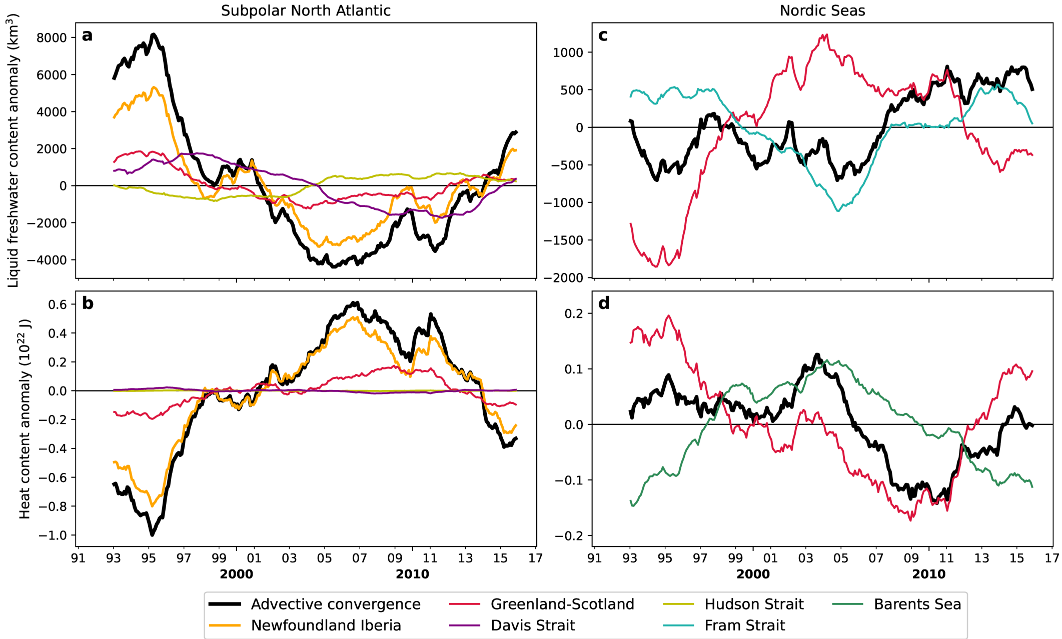

Figure 9. Integrated time series showing the contribution of major boundary fluxes into the subpolar North Atlantic (a,b) and Nordic Seas (c,d) for freshwater (a,c) and heat content (b, d). Note different anomaly scales for SPNA and NSEA.

Table 4. Covariance ratios for freshwater and heat fluxes through each boundary of the NSEA. The boundaries are shown in Figure 1. Covariance ratios are evaluated for each boundary flux on monthly, annual and pentad scales. Significant contributions are indicated by bold numbers.

	Freshwater			Heat		
	monthly	annual	pentad	monthly	annual	pentad
Denmark Strait	**0.56**	**0.54**	−0.32	−0.12	0.01	−0.08
Iceland Faroe	0.05	0.01	−0.43	**0.41**	**0.42**	**0.76**
Faroe Scotland	0.18	0.17	**−0.61**	**0.56**	**0.46**	0.24
Scotland Norway	−0.03	−0.05	−0.17	0.06	0.04	−0.06
Fram Strait	0.19	0.28	**1.65**	0.00	−0.07	0.00
Barents Sea	0.05	0.06	**0.88**	0.08	0.13	0.14

The absolute freshwater and heat fluxes across the sections as shown in Figure S8 are sensitive to the choice of reference salinity (i.e., $35\,\mathrm{g\,kg^{-1}}$) and reference temperature (i.e., 0°C). However the anomalies shown in Figure 9 (as well as Figures S9-S10) are robust for different choices of references. As noted in Section 2.3, closed control volumes with zero net volume flux ensure that the results are physically consistent and robust for the choice of other reference values commonly used in previous studies.

3.2.4 Decomposition of the forcing term

The forcing term for freshwater constitutes the addition of freshwater at the sea surface through atmospheric (precipitation minus evaporation), sea ice and land (i.e., runoff) sources. The interannual variability in the total forcing term in the SPNA is mostly determined by the air-sea freshwater flux (Figure 10a-c). The freshwater flux due to precipitation minus evaporation (E-P) yields mostly positive anomalies in the 1990s and predominantly negative anomalies in the 2000s. The variability in air-sea freshwater flux is due to changes in precipitation (Figure S11). There is a strong seasonal signal in the sea ice component, but it is only a minor factor in the interannual variability of the total forcing term. Freshwater contributions from both air-sea exchange and sea ice declines over most of the ECCOv4 time period (Figure 10c). In the case of the SPNA, the decline in the forcing term is driven by a decline in precipitation (Figure S11a). Freshwater fluxes from runoff are prescribed as a climatology with no interannual variation, and represent a negligible fraction of total variability due to forcing. The additional contributions of freshwater due to the Greenland ice sheet and its accelerating mass loss was not accounted for here. This additional source of freshwater has not had a significant impact to date (Böning et al., 2016; Rhein et al., 2018), but the potential error due to its omission will be discussed in Section 4.

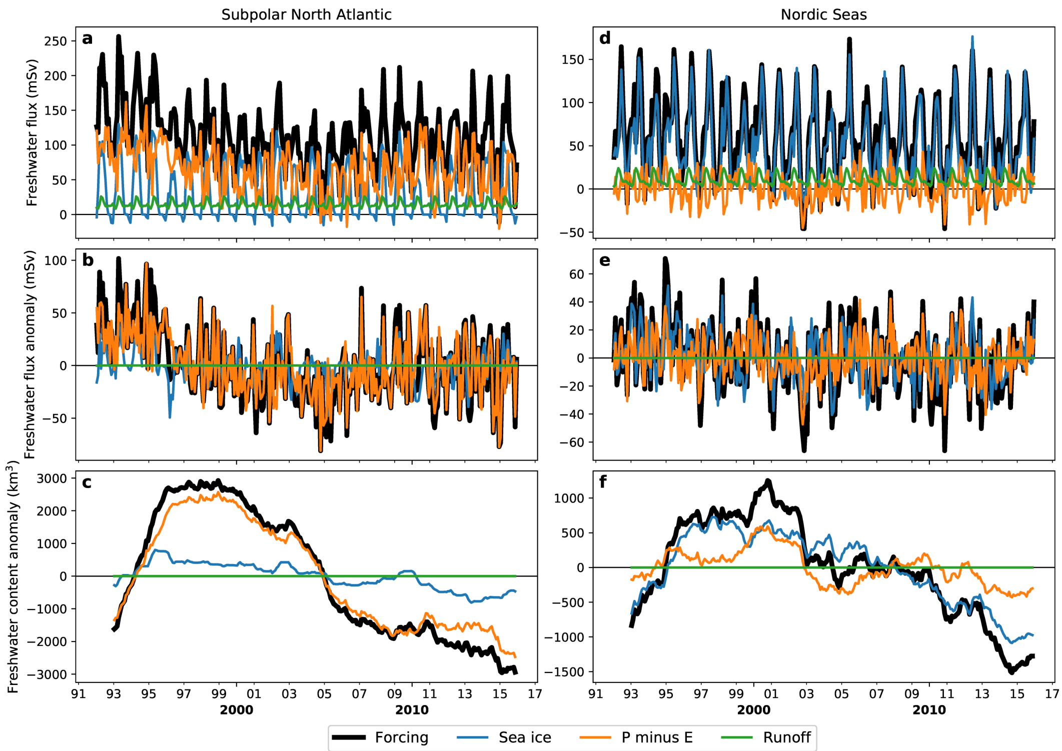

Figure 10. Decomposition of ECCOv4 freshwater forcing at the sea surface of the subpolar North Atlantic (a-c) and Nordic Seas (d-f). (a,d) Monthly time series of freshwater fluxes; (b,e) seasonal freshwater anomalies; (c,f) integrated time series. Time series are shown for total tendency (black), and contributions due to sea ice (blue), atmospheric exchange (orange) and runoff (green). Note the different y scales for the subpolar North Atlantic (a,b) and Nordic Seas (c,d).

The contributions of freshwater forcing terms differ in the NSEA, where sea ice constitutes a much bigger proportion of forcing. This is apparent especially in the seasonality, which is mainly driven by sea ice (Figure 10d). The anomaly time series do show a secondary contribution by atmospheric fluxes (largely driven by variability in precipitation; Figure S11b), but the overall increase in freshwater forcing in the 1990s and the decline since 2003 are primarily driven by changes in sea ice freshwater fluxes. Given that it is mostly the forcing term that drives interannual changes in the freshwater content of the NSEA (Figure 7c), it can be further stated that the overall change in LFWC in the NSEA is mainly due to changes in sea ice.

Comparison between freshwater flux due to sea ice in the NSEA and Arctic sea ice export through the Fram Strait (Figure 11) shows a strong correlation ($r = 0.87$ for annual means). This demonstrates that the sea ice component of freshwater flux within NSEA is mostly sourced from the Arctic sea ice export through Fram Strait. As the anomaly freshwater flux due to sea ice is the major driver in the NSEA freshwater budget (Figure 10d-f), consequently we can infer that the overall decline in NSEA freshwater content since 1995 (Figure 2b) is largely due to a decline in the sea ice export through Fram Strait. Whereas liquid freshwater fluxes clearly vary with volume fluxes, this is not the case for the Fram Strait sea ice flux (see Figure S12). In general sea ice flux was highest in the mid 90s (occurring with the most recent GSA), with an equivalent freshwater flux of 73 mSv to the south. Sea ice flux in the NSEA subsequently declined to around 40–50 mSv after that time. Sea ice export through the Davis Strait is much smaller than through the Fram Strait (Figure S13), at approximately 10–20 mSv or about half of export from the lower end of Fram Strait (i.e., approximately 40 mSv). There is no decline in export observed from the mid-90s as observed in the Fram Strait. In fact, the last few years saw one of the larger sea ice exports though Davis Strait (reaching around 18 mSv). Therefore, the freshwater budget outside of the Arctic is only affected by sea ice export through Fram Strait.

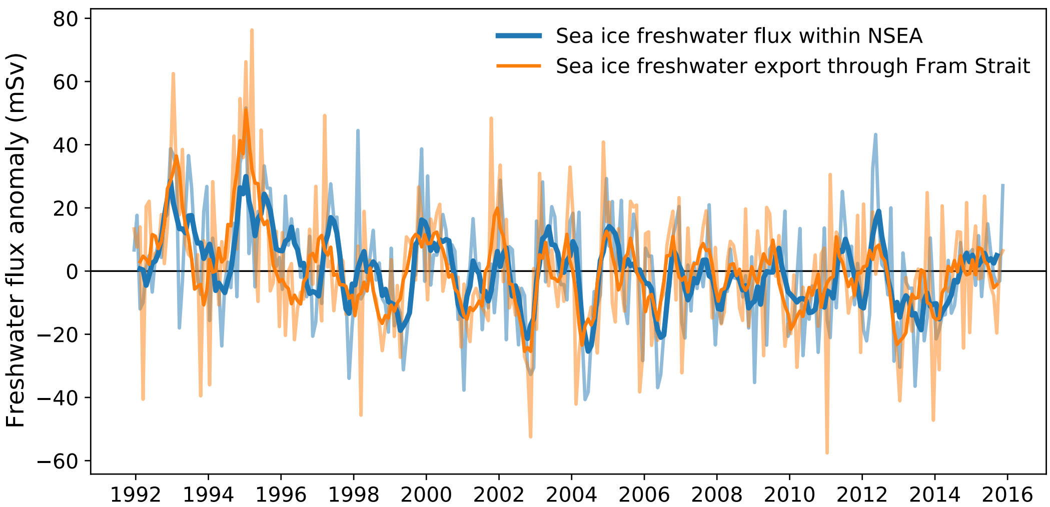

Figure 11. Monthly anomalies in ECCOv4 freshwater tendency due to sea ice within the NSEA (blue) along with anomalies in ECCOv4 sea ice freshwater flux through the Fram Strait into the NSEA (orange). The monthly anomalies are shown as thin lines, and the 5-month running means are shown as thick lines.

3.3 Budgets for the Labrador Sea

The Labrador Sea is included within the budget analysis of the SPNA. The interest here is whether variation in freshwater content in the Labrador Sea is directly connected to the rest of the SPNA or is more affected by Arctic outflow through the Davis and Hudson Straits. The freshwater content of the Labrador Sea shows variations similar to the SPNA over the last 20 years, notably in the decline between the mid-1990s and the mid-2000s (Figure 12a). However, unlike the SPNA there is no steady increase since the mid-2000s, but rather regular fluctuations with a period of 4 to 6 years. The variability in Labrador Sea LFWC is characterized by a sharp drop in the mid-90s followed by a further decline over the early 2000s and a minimum reached in 2006, approaching a local maximum around 2008, declining to another minimum in 2011 and then an intermediate rise in 2012, with freshwater being relatively unchanged since that time. Similar to variation in the SPNA, this interannual variability is largely caused by changes in advection.

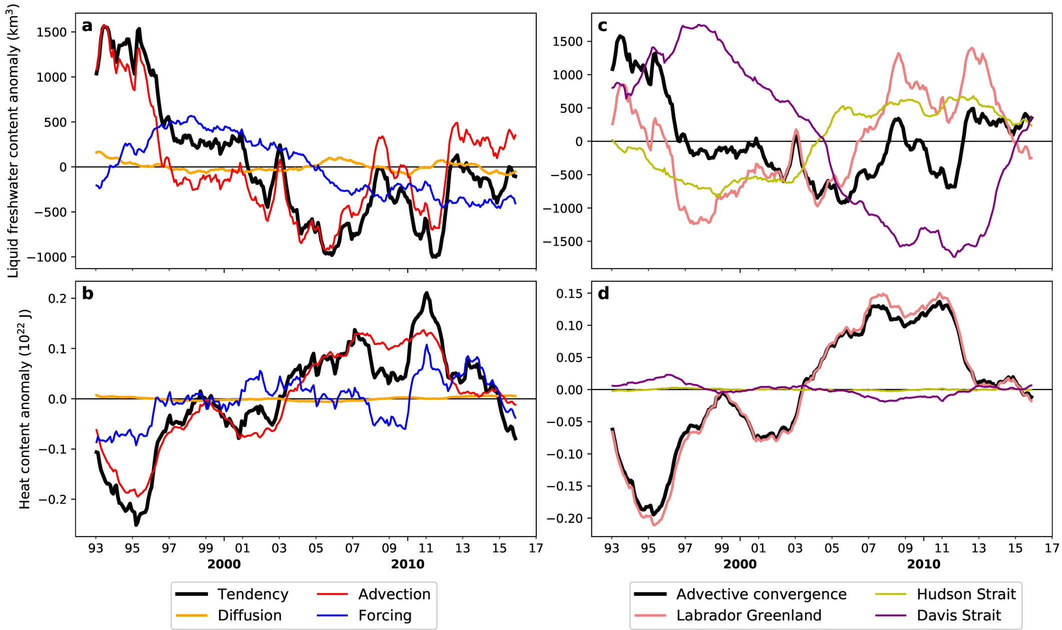

Figure 12. Integrated anomaly time series of ECCOv4 freshwater and heat content of the Labrador Sea, including separate components for surface forcing, advection, and diffusion (a,b) and also showing the contribution of each boundary flux (c,d) into the Labrador Sea for both freshwater (a,c) and heat content (b,d).

In accordance to the large role of advective convergence it is not surprising to observe the LFWC of the Labrador Sea follow variations similar to those of OHC (Figure 12a,b). As seen in the SPNA, changes in heat content are overall the inverse of freshwater content. The decline in freshwater in the late 1990s and 2000s is accompanied by an overall increase in the heat content, although there is a clear decline in heat content starting in 2011 that is not reflected by a corresponding increase in freshwater. Advection across the Labrador-Greenland boundary is largely responsible for heat variability in the Labrador Sea, but the anomalous forcing component of heat introduces an interannual variability that is a larger factor than the anomalous forcing variability of the freshwater budget (Figure 12a,b; Table 5). For example, some of the recent decline in Labrador Sea heat content can be attributed to a decline in forcing, particularly in the last two years of the state estimate (2014-2015). As in the case of SPNA and NSEA, diffusion has negligible impact on the freshwater and heat budgets of the Labrador Sea (Figure 12a,b).

The advective convergence of heat and freshwater are in an overall sense reflective of each other. However, there are some positive anomalies in the advective convergence of freshwater that are not seen in the case of heat, for example in 2003, between 2007 and 2010 and between 2012 and 2014. As for boundary fluxes for the Labrador Sea, freshwater convergence is largely determined by the exchange across the Labrador-Greenland section, though variability due to fluxes through the Davis Strait and the Hudson Strait are not negligible (Figure 12c; Table 6). On the other hand, heat flux into the Labrador

Table 5. Covariance ratios for forcing, advection and diffusion for heat and freshwater variability in the Labrador Sea. Covariance ratios are evaluated for each budget term on monthly, annual and pentad scales. Significant contributions are indicated by bold numbers.

	Freshwater			Heat		
	monthly	annual	pentad	monthly	annual	pentad
Forcing	0.09	0.07	−0.06	**0.71**	**0.48**	0.14
Advection	**0.93**	**1.00**	**1.10**	**0.29**	**0.53**	**0.90**
Diffusion	−0.02	−0.07	−0.04	−0.00	−0.01	−0.05

Sea is entirely determined by exchanges through the Labrador-Greenland section (Figure 12d; Table 6).

Table 6. Covariance ratios for freshwater and heat fluxes through each boundary of the Labrador Sea. The boundaries are shown in Figure 1. Covariance ratios are evaluated for each boundary flux on monthly, annual and pentad scales. Significant contributions are indicated by bold numbers.

	Freshwater			Heat		
	monthly	annual	pentad	monthly	annual	pentad
Labrador Greenland	**0.94**	**1.22**	**0.84**	**1.02**	**1.11**	**1.07**
Davis Strait	0.05	−0.17	0.17	−0.03	−0.13	−0.10
Hudson Strait	0.01	−0.06	0.01	0.00	−0.00	−0.00

In the Labrador Sea, changes in freshwater flux convergence do not always co-occur with changes in heat flux convergence. Unlike in the SPNA, the freshwater and heat content in the Labrador Sea does not seem to be affected by anomalies in circulation (which would bring concomitant changes in both freshwater and heat convergence). The observed anomalies in freshwater advection (namely the peaks in 2003, 2009 and 2013) are due to variability in Labrador-Greenland throughflow (Figure 12c). However, there are no such anomalies in the Labrador-Greenland throughflow of heat (Figure 12d). There is a decline in the freshwater flux into the Labrador Sea through the Labrador-Greenland section after 2013. At the same time heat flux into the Labrador Sea remained relatively unchanged. Over the last three or so years of the state estimate (2013-2015) we see that there is a balance between a reduction in freshwater flux through the Labrador-Greenland section and an increase in freshwater flux through the Davis Strait, such that advective freshwater convergence remained relatively unchanged. This is interesting, as it suggests increased freshwater input from the Arctic Ocean in the last three years after a 15-year long decline (1998-2012). Currently, exchanges to the south east (through the Labrador-Greenland section) balance this freshwater flux through the Davis Strait.

It is worthwhile to further investigate whether the decline of freshwater flux through the Labrador-Greenland section is due to increased outflow of freshwater (Labrador Current), increased inflow of saltier water (Irminger Current) or decrease in freshwater inflow (West Greenland Current). Depth-integrated freshwater fluxes across the vertical section between Labrador and Greenland show a mean negative flux (i.e., out of the LSEA) in the Labrador Current, and a smaller freshwater input close to Greenland over the 1992-2015 period (Figure 13a). The anomalies over the last three years (2013-2015) show that the outflow along the Labrador Current increased in recent years while the freshwater input closer to Greenland declined (Figure 13b). Thus, the recent increased freshwater fluxes though Davis Strait have been compensated by increased outflow via the Labrador Current and with a partly reduced freshwater input along the West Greenland Current. Note further that fluxes over the 1992-2015 period (Figure 13a) do not indicate a major input of saltier water into the LSEA via the Irminger Current, as overall the freshwater flux towards the Greenland side is positive. Thus the anomalies in the LSEA are due to enhanced Labrador Current outflow and reduced freshwater inflow along the Greenland coast. The freshwater outflow over the deeper basin, such as the export of Labrador Sea Water (LSW) does not affect the net freshwater exchange.

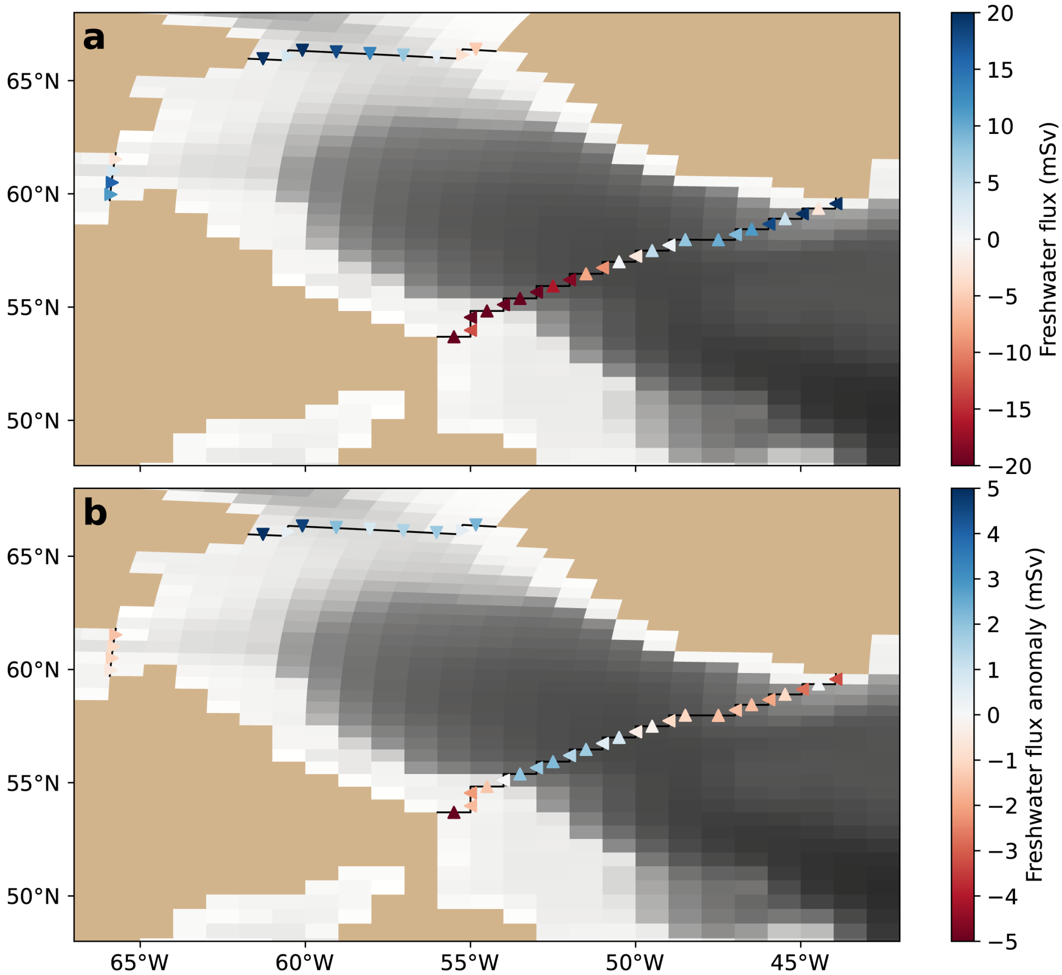

Figure 13. (a) Depth-integrated ECCOv4 freshwater flux across the three boundaries of the Labrador Sea (Davis Strait, Hudson Strait and Labrador-Greenland section) averaged over 1992-2015. (b) Depth-integrated anomaly in ECCOv4 freshwater flux across the three boundaries of the Labrador Sea (Davis Strait, Hudson Strait and Labrador-Greenland section) averaged over 2013-2015. Positive fluxes are directed into the Labrador Sea and are indicated by individual markers at each grid point. Basemap color indicates ECCOv4 bathymetry.

As was done for the SPNA and NSEA, temporal decomposition of the freshwater and heat advection terms separates their individual components to show that in the LSEA advective convergence is mostly due to the mean advection of anomalies (Figure 14), which is different from what was seen in the SPNA and NSEA. Thus, changes in freshwater and heat content are driven by anomalies being advected into and out of the LSEA. For the 2013-2015 period, this indicates that fresher water is exiting the Davis Strait into the LSEA and that fresher water is exiting the LSEA through the Labrador Current, while negative anomalies (i.e. saltier water than is usual) are entering the LSEA off the Greenland coast.

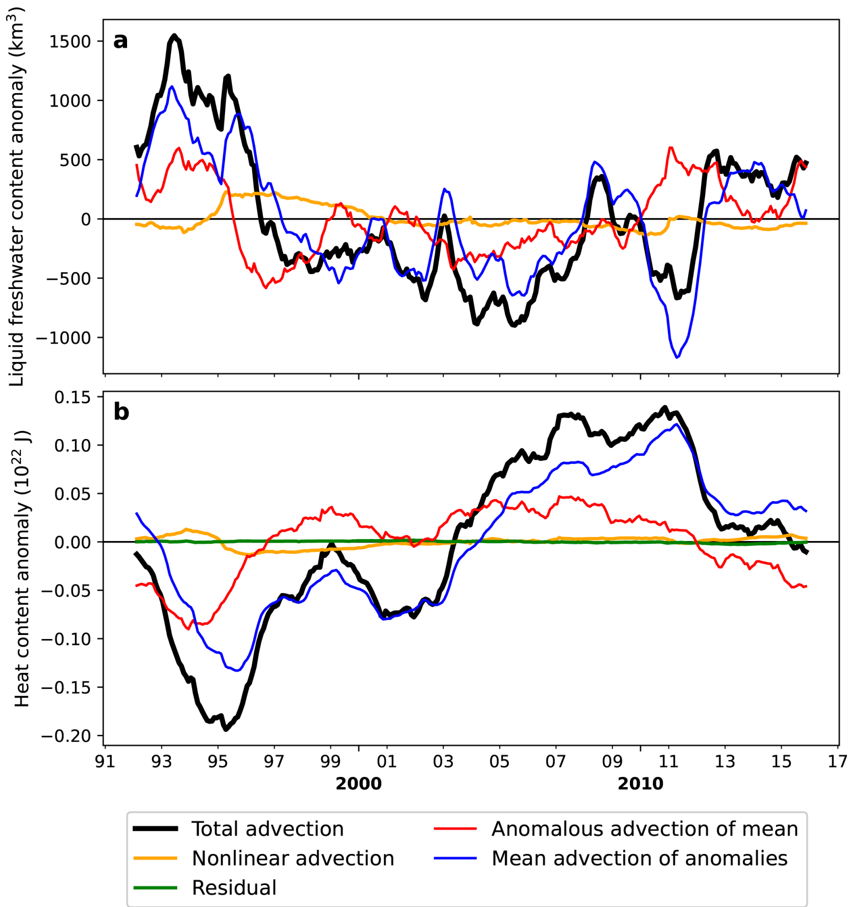

Figure 14. Decomposition of total advection into contributions from anomalous advection of the mean, mean advection of anomalies and nonlinear advection into the LSEA for (a) freshwater and (b) heat content. A residual term is also included in the heat content decomposition (panle b).

In the context of freshwater flux across the northern boundaries, it is important to distinguish exchanges across the Davis Strait into the LSEA from exchanges across the Fram Strait into the NSEA. Sea ice flux through the Davis Strait is relatively small compared to the Fram Strait. On the other hand, the liquid freshwater flux through Davis Strait is comparable with Fram Strait, according to observational estimates, and almost twice as large as Fram Strait according to ECCOv4 (Table 1). Thus, the total freshwater flux (sea ice + liquid) is about the same between Fram Strait and Davis Strait ($\sim$100 mSv). It is also interesting to note that over the last five years, the outflow of liquid freshwater through Davis Strait has been increasing ($\sim$20 mSv) while it declined in the Fram Strait ($\sim$10 mSv) (Figure S14), yet these changes had no effect in the freshwater convergence in the SPNA, NSEA or LSEA. As we do not present a budget for the Arctic Ocean, we cannot quantify whether or not the changing outflow is significant to the Arctic freshwater budget. We expect that the recent change in outflow through either the Davis Strait or Fram Strait is very small compared to the total variability in Arctic Ocean freshwater, and that the increased outflow through the Davis Strait has been partially compensated by a reduced outflow through the Fram Strait.

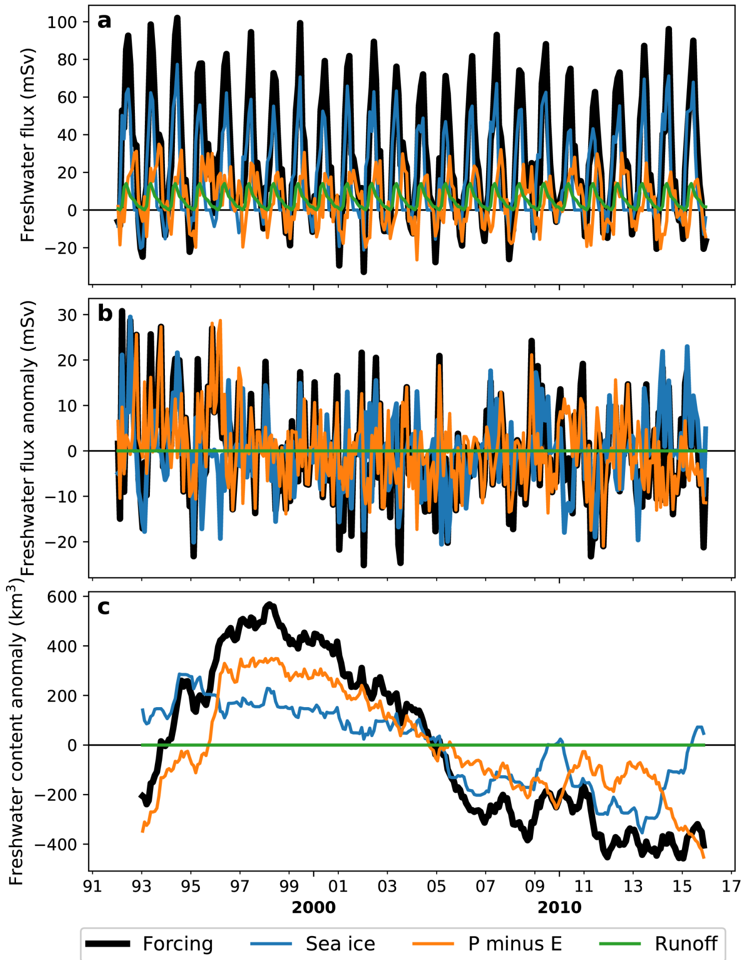

Figure 15. Decomposition of ECCOv4 freshwater forcing at the sea surface of the LSEA showing (a) monthly time series (b) seasonal anomalies, and (c) integrated time series of freshwater fluxes due to sea ice (blue), atmospheric exchange (orange) and runoff (green). Total forcing is shown in black.

The forcing term is not a major factor in the freshwater budget of the Labrador Sea. However it is still of interest to determine which component controls most of the variation in freshwater forcing. The strongest seasonal signal is due to sea ice, with a smaller signal coming from the atmospheric freshwater flux (Figure 15a). Both components are mostly positive and represent a contribution to freshwater content. During the winter months (i.e., December-March) there are minor negative fluxes which can be attributed to sea ice growth and lower precipitation rates (compared to evaporation). As is the case in the SPNA and NSEA, runoff is a very small source of freshwater, with no interannual variability. The seasonal anomalies of sea ice and atmospheric sources are comparable, and both affect the interannual variability of freshwater forcing in the Labrador Sea (Figure 15b). When the anomalies are integrated, negative anomalies dominate (Figure 15c) and therefore forcing, which is a freshening term, becomes weaker from the late 1990s to present. This is mostly due to a decline in atmospheric freshwater fluxes (driven by a decline in precipitation as in the SPNA and NSEA), but also because of reduced freshwater from sea ice melting, which is generally declining when viewed over the entire period. It is only in the last 3 years that there are substantial positive freshwater anomalies from sea ice, and these are compensated by negative anomalies in atmospheric freshwater fluxes.

4 Discussion

The present study extends previous work (e.g., R. Curry & Mauritzen, 2005; Boyer et al., 2007; Buckley et al., 2014, 2015; Piecuch et al., 2017) to describe freshwater and heat variability in the subpolar North Atlantic (SPNA) and Nordic Seas (NSEA). Variability is described using detailed budget analyses with an established ocean reanalysis product, which allows for accounting of all sources and sinks of freshwater and heat. We distinguish the SPNA and NSEA as two separate domains of the northern North Atlantic. Furthermore, we present budgets for the Labrador Sea (LSEA) as a subdomain of the SPNA. Within these domains we report a clear anticorrelation in freshwater and heat content variability and establish differences in the balance of mechanisms between the budgets for the SPNA, NSEA and LSEA. As we have shown, the relevance of different budget terms varies among freshwater and heat, among regions, and depends on which time scale is considered (monthly, annual, decadal).

4.1 Role of overturning, gyre circulation and its relationship to wind

Considering the study region as a whole (i.e., the SPNA and NSEA), and that the volume of the SPNA is almost four times larger than the NSEA, it is evident that circulation anomalies at the southern boundary (i.e., Newfoundland-Iberia) dominate variation in freshwater and heat over the entire study region. In this section, underlying mechanisms of these circulation anomalies are further investigated and thus the focus here is on the SPNA budgets. We documented an overall heating and subsequent cooling of the SPNA (accompanied by corresponding salinification and freshening) during the study period 1992-2015. This is consistent with Robson et al. (2016), who showed that decadal variations in temperature and salinity are linked to changes in the Atlantic Meridional Ocean Circulation (AMOC). Assuming this link to be the case, the major factor in our budgets appears to be an internal feedback involving the strengthening (weakening) of the AMOC which leads to increased (decreased) northward heat transport as well as increased (decreased) salt transport into the SPNA and LSEA. These changes in heat and salt transport create negative (positive) density anomalies that lead to reduced (enhanced) deep convection, which in turn will weaken (strengthen) the AMOC after a lag of around five years (Robson et al., 2016; Jackson et al., 2016; Haine, 2016). Note that in this feedback mechanism, density anomalies are principally driven by heat anomalies. The assumption of AMOC being the underlying mechanism for heat (and freshwater) content changes in the SPNA is also compatible with the hypothesized role of AMOC in explaining Atlantic Meridional Variability (R. Zhang et al., 2019). Furthermore, recent cooling and freshening in the eastern SPNA has been directly linked to trends in the observational RAPID array data at 26°N (Bryden et al., 2020).

ECCOv4 well reproduces the observed variability in the overturning circulation and heat fluxes at 26°N (Figure S15). Therefore the findings based on RAPID observations (Bryden et al., 2020) are applicable to our analysis. However, the variation in AMOC as the key factor in decadal changes in SPNA heat content has been questioned by Piecuch et al. (2017). In accordance with our study, they identified anomalous circulation of the mean temperature field as the dominant driver of heat changes, but they attribute it to changes in horizontal gyre circulation driven by changes in wind stress. They found that larger/smaller wind stress curl at the southern boundary of the SPNA (which they defined as 46°N) leads to reduced/enhanced northward transport into the SPNA. Whether the decadal variability in SPNA is due to low frequency internal ocean variability or mainly forced by variations in winds is out of scope for this study. However, we provide here some points regarding potential future research to clarify the source(s) of freshwater and heat variability in the SPNA.

Higher frequency (monthly to interannual) variability in freshwater and heat convergence in the SPNA is related to variability in the NAO and AO (Figure S16). The freshwater tendencies due to changes in advection derived from ECCOv4 show significant positive correlation with both NAO and AO ($r = 0.36$, 0.48, respectively), while the heat tendencies show significant negative correlation ($r = -0.43$, -0.56, respectively). The SPNA freshwater and heat advection convergence also show correlation with the Subpolar Gyre Index (SPGI; Figure S17) which is associated with the strength and size of the North Atlantic SPG (Häkkinen & Rhines, 2004; updated by Hátún & Chafik, 2018; Koul et al., 2020). The SPGI is correlated positively with freshwater convergence ($r = 0.54$) and negatively with heat convergence ($r = -0.44$). This indicates a relationship, such that advective heat and salt input are reduced when the SPG is stronger and more expanded (and vice versa). In turn the strength of the AMOC as well as the SPG has been associated with the NAO and wind stress curl over the North Atlantic (Bersch, 2002; Bersch et al., 2007; R. G. Curry & McCartney, 2001). The AMOC variability at 26°N has been linked to variability in wind (Zhao & Johns, 2014) but long term (decadal) fluctuations are believed to be buoyancy driven (Biastoch et al., 2008). All these relationships appear to be reproduced in ECCOv4. While the NAO/AO correlates with advective freshwater and heat convergences in the SPNA on short time scales, it does not match the long term trends seen in the SPNA (Figure S16), while variability in SPGI and convective depth in the Labrador Sea (Figure S17a) matches these longer term trends better. Thus, we expect that AMOC variations on decadal time scales are more or less unrelated to the NAO or the AO, which are only relevant on interannual and intraseasonal time scales.

What remains difficult to reconcile with the AMOC-weakening explanation is the decadal relationship to wind (Piecuch et al., 2017). It is likely that both wind and buoyancy forcing are important to the decadal variability. The apparent correlation between wind and buoyancy forcing, however, makes it difficult to tease out the distinct influences of one or the other. It is likely necessary to look beyond correlation/covariance analyses in order to quantify the contribution between these underlying causal mechanisms of change in the North Atlantic circulation. Furthermore, the relative importance of the AMOC (i.e., overturning) and horizontal gyre circulation might depend on the exact method in decomposing meridional heat flux in the North Atlantic. For example, it has been shown that different methods of calculating northward heat transport into the SPNA (e.g., averaging along buoyancy coordinates versus depth coordinates), yields different results in terms of the relevance of overturning versus horizontal gyre circulation (S. Jones, personal communication, 2020).

Besides the possibility that the correlation is coincidental rather than causal, one can reconcile the conundrum of the decadal relationship between wind and buoyancy forcings by hypothesizing that buoyancy anomalies are key in preconditioning the SPG and LSEA and that anomalies in wind stress are only important in the initiation of deep convection. During the weakening phase of the AMOC (since approximately 2005), the SPG and LSEA become preconditioned towards a less buoyant state (i.e., cooler and fresher), which is principally driven by negative heat anomalies (Robson et al., 2016). As the SPNA cooled and freshened over this period, there were winters of anomalously positive NAO conditions (i.e., 2007-2008, 2012). However, this did not lead to enhanced winter convection over consecutive years. Only in recent years (starting 2015) were the buoyancy anomalies in the SPG and LSEA negative enough such that the occurrence of a persistently positive NAO forcing (since 2014) ultimately reinvigorated deep convection in the LSEA (Yashayaev & Loder, 2016, 2017). These NAO+ conditions were associated with anomalously cold winters and strong winds and thus large negative (i.e., outward) heat flux at the ocean surface (Grist et al., 2016).

The NAO-driven change in winter convection established a dense column of LSW, leading to an intensified SPG, and it is expected to affect the AMOC following a lag of 5 years (Jackson et al., 2016; Robson et al., 2016). As it depends on the severity of the winter, reinvigorating deep convection is an intermittent and unpredictable process. It depends on atmospheric variability and thus is dictated by nonlinearity, associated with a threshold that must be exceeded to initiate deep convection. If this was indeed the mechanism, one might still expect a correlation between wind and AMOC, LSW density and surface buoyancy anomaly in the SPG, but it would be wrong to conclude that the wind is causally driving freshwater and heat anomaly in the SPNA. The depth of convection and LSW formation has been particularly strong since the winter of 2015 (Yashayaev & Loder, 2016, 2017). Since the intensification of deep convection in the Labrador Sea is followed by strengthening in AMOC, a reversal in the recent cooling and freshening of the SPNA might be expected in the next few years.

4.2 Arctic-North Atlantic exchanges

Historical studies (e.g., R. Curry & Mauritzen, 2005; Peterson et al., 2006) argue that the increased atmospheric freshwater, melting Arctic sea ice, and river discharge mainly explain the freshening in the whole North Atlantic basin over the latter half of 20th century. This is different from our findings over the recent two decades which suggest that for the North Atlantic subpolar basin, it is advective convergence dominated by flux variability across the southern boundary that explains trends in freshwater content. Furthermore, observations have not shown a significant increase in freshwater flux out of the Arctic in recent times (Haine et al., 2015). Together this suggests that increases in Arctic liquid freshwater content during the last 25 years have remained within the Arctic. It is expected that eventually freshwater transport into the SPNA will be substantially increased. Thus, the potential for further freshening from the northern gateways of the SPNA and NSEA exist. The question is the time scale on which this will occur. An abrupt release of freshwater will likely have very different consequences to SPNA circulation compared to a more gradual release.

In terms of possible abrupt freshwater release in the future, previous studies have linked large scale freshening events (i.e., Great Salinity Anomalies) in the SPNA to distinct releases in Arctic freshwater. The ECCOv4 output in this study does not provide a link between the observed recent freshening of the SPNA and Arctic outflow, so it cannot provide a template for understanding the mechanisms that drove previous GSAs or future occurrences of such events. Given the mechanisms of the past two decades, it is interesting to consider the possibility that mechanisms behind GSAs might be part of the decadal variability in the AMOC, besides enhanced Arctic freshwater fluxes. However, we also acknowledge that Arctic freshwater flux likely contributed to substantial freshening over NSEA and SPNA in general as that over the latter half of the 20th century, the surface layers of the Arctic became saltier, even in the presence of increased freshwater contributions. This would suggest that there had been substantial export of that freshwater from the Arctic Basin through the Fram and Davis Straits into the North Atlantic during the freshening events of the 20th century, and that this will likely occur in the future. All the GSAs occurred in decades prior to the ECCOv4 period, for which there are insufficient observations and constraints to extend ECCOv4. An extension of a physically consistent assimilation would be desirable in order to quantify the contribution of GSAs to observed changes in North Atlantic freshwater content versus other processes that might occur parallel to such events. This would confirm that over the latter half of the 20th century it was indeed Arctic freshwater flux into the SPNA and NSEA basin that dominated the observed freshening during GSA events.

In terms of a gradual increase in Arctic freshwater fluxes, this study observed changes in the recent years. We have observed a positive trend in freshwater flux through the Davis Strait starting in 2013. On the other hand, there is a negative trend in freshwater flux through the Fram Strait between 2006 and 2015. These changes are currently small compared to other budget terms. In the SPNA, the increased freshwater flux through Davis Strait is secondary to the more prominent freshening due to changes at the southern boundary. In the Labrador Sea, freshwater input through the Davis Strait is compensated by salinification due to exchanges across the section from Labrador to Greenland. The increases in Fram Strait freshwater flux during 2005-2014 are a substantial factor in the advective convergence term, but that term is minor compared to the forcing term in the NSEA freshwater budget.

While the forcing budget term has minor influence on decadal variability in the freshwater and heat content of the SPNA, this is not the case in the NSEA, where the forcing term is the main driver of freshwater variability and contributes substantially to heat variability (Figure 7). A decrease in freshwater in the NSEA suggests a reduction in sea ice melting. This would mean that the growth of sea ice is more prevalent in NSEA and/or that sea ice melting is reduced. Given the simultaneous warming with the salinification in the NSEA (Figure 7d), the former seems unlikely. The strong correlation with sea ice flux through Fram Strait suggests that this is driving the anomaly freshwater flux within the NSEA. It is surprising that changes in sea ice flux through the Fram Strait are only detected in the NSEA, even though one reasonably expects the EGC to transport sea ice out of the NSEA and into the SPNA (and LSEA), where freshwater input from melting sea ice also occurs. In fact, this mechanism has been suggested as the cause of some of the GSA events (R. R. Dickson et al., 1988; Belkin et al., 1998; Belkin, 2004). It remains to be seen, then, how the anticipated future release of Arctic freshwater through the Fram Strait will affect the NSEA versus the SPNA.

The decline in sea ice export from the Arctic, occurring over the last two decades or so, is likely a result of the decline in the Arctic sea ice formation (Comiso et al., 2008; Parkinson & Comiso, 2013). Thus, there is a direct link between Arctic and NSEA freshwater content, but somewhat counterintuitively: even though there has been a recent increase in Arctic Ocean freshwater content (Proshutinsky et al., 2009, 2015; Rabe et al., 2014), the NSEA has been salinifying because of declining sea ice discharge through the Fram Strait. Furthermore, this sea ice decline has not been compensated by increased liquid freshwater flux, as most of the accumulated freshwater within the Arctic has yet to manifest as increased freshwater flux out of the Arctic via the Fram Strait (Haine et al., 2015). Even though sea ice freshwater fluxes are the main influence on interannual variability of NSEA freshwater content, this signal does not seem to be transported further south to the SPNA. Therefore, given their differing variability and their unique underlying mechanisms, it is important to distinguish variability between the SPNA and the NSEA when studying Arctic-North Atlantic exchanges.

There is also unique variability in the freshwater content observed in the Labrador Sea (LSEA) compared to the rest of the SPNA. The LSEA is a distinct basin, connected to the Arctic Outflow through the Davis and Hudson Straits, and it has been shown to be a site of meltwater convergence (Luo et al., 2016). Thus besides being a key region for deep convection, there are notable differences in the mechanisms of freshwater and heat content variability that make the LSEA an area of special focus. Advection is still the main driver in the LSEA, but there is greater influence from transport through the Davis Strait. For the most part, there is no direct connection between Arctic freshwater fluxes and the freshwater content of the LSEA and the SPNA.

While there is no substantial contribution from anomalies (of both freshwater and heat) being advected by the mean circulation in SPNA or NSEA (Figure 8), mean advection of anomalies is contributing to most variability in freshwater and heat in the LSEA (Figure 14). To date, increases in Davis Strait freshwater export appear to be balanced by increased outflow via the Labrador Current and a decline in freshwater input on the northeastern side (e.g., via the WGC). Anomalies exported through the Davis Strait might not remain in the Labrador Sea and instead be exported via the Labrador Current. Thus, the mean circulation is essentially advecting any anomalies through the LSEA. This will be important to study further given the potential for future increases in Arctic export. However, studies have also shown that most of the meltwater from Greenland Ice Sheet melting in east Greenland is transported via the East Greenland Current to the LSEA after entering via the WGC (Luo et al., 2016; Castelao et al., 2019). This suggests a potential shift towards freshening, if freshwater flux from Greenland ice sheet is included.

4.3 Influence of recent enhancement in Greenland ice sheet melting

There are several processes absent in ECCOv4 that might be important in reproducing observed changes in the ocean. One such process is the representation of boundary current circulation and shelf break circulation around the periphery of the North Atlantic. Another is a more realistic representation of Greenland ice sheet melting and the associated discharge around Greenland, which is likely a substantial factor for North Atlantic freshwater content. As can be seen in Figures 10 and 15, runoff is included as a climatological mean based only on observations of river runoff. Dukhovskoy et al. (2019) suggested that Greenland ice sheet and land ice melting, as compiled by J. Bamber et al. (2012); J. L. Bamber et al. (2018), is a potentially important source contributing to the recent freshening observed in the SPNA. Other studies, however, show that the freshwater source from Greenland ice sheet melting is relatively small, for example as quantified in Haine et al. (2015) or simulated in Böning et al. (2016). Also, submarine meltwater from the Greenland ice sheet has not yet been detected in the Labrador Sea (Rhein et al., 2018).

With the current representation of runoff, the ECCO forcing term is negligible in driving interannual variability in the SPNA. Because ECCOv4 does not include a realistic representation of ice sheet melting and land ice runoff for the recent time period, some freshening likely is attributed to other processes, such as air-sea flux, during the assimilation of observations. Thus, the missing sources of runoff from Greenland ice sheet melting might be compensated by adjusted input fields of E-P. Our analysis has shown that E-P is not significantly contributing to freshening in any of the study regions (Figures 10 and 15). However, we need to consider whether the addition of Greenland ice sheet melting is substantial enough to change the overall finding that the dominant driver in the SPNA is advection. It is possible to compare the freshwater fluxes within the ECCOv4 forcing term in Figures 10 and 15 with the latest published estimates to put the contribution of Greenland ice sheet melting in perspective. Dukhovskoy et al. (2019) state that there has been an anomaly of $5000\,\mathrm{km}^3$ since the 1990s. As can be seen in Figure 10c, $5000\,\mathrm{km}^3$ is roughly the total change due to the combined freshwater forcing in ECCO over the SPNA. This would counteract the Greenland melt, and because advection, not forcing, is the dominant driver of the decadal changes, it can be expected that the missing source of runoff from Greenland melt would not change the outcome of our results.

Greenland melt is surely important when focusing on the upper SPNA. Since its magnitude is seasonally varying (i.e., with greatest magnitudes in summer and fall) there are important implications for stratification and ecosystem processes (Oliver et al., 2018). For the total freshwater content of the SPNA and Labrador Sea, it can be assumed that melting plays only a secondary role to advective convergence (in particular the dominant influence of advective input from the south). Freshwater due to enhanced ice sheet melting will compensate for some of the decadal trends due to the variation in input through the southern boundary, but it is not expected that it will change the overall balance. This requires further analysis, however, especially to quantify how much of the meltwater remains in the SPNA, because it will ultimately determine the long term/decadal variation in freshwater content due to Greenland meltwater. Certainly a more realistic representation of ice sheet melting in ECCO needs to be implemented, one that employs temporally and spatially resolved observations of freshwater runoff along the Greenland coast instead of climatological estimates.

5 Conclusions

We have presented a comprehensive analysis of freshwater content variability in the northern North Atlantic and compared it to variability in heat content using the ECCOv4 ocean state estimate. ECCOv4 provides closed tracer budgets (i.e., no unidentified sources of salt or heat) and detailed diagnostics of the simulation, thereby allowing the contribution of specific mechanisms to the budgets to be identified. We showed that the ECCOv4 is in good agreement with freshwater content changes in the SPNA and NSEA given by EN4 observational-based data and with mean fluxes across the boundaries found in the literature.

In the SPNA, variability in advective convergence is the main driver for both freshwater and heat content variability. While air/sea forcing is more important at higher (i.e., monthly) frequencies, advection dominates at lower (i.e., interannual to decadal) frequencies. In the NSEA forcing is most important for freshwater variability and on average contributes to about half of the heat variability (though heat advection becomes more important at longer time scales). Diffusion plays an insignificant role in freshwater and heat fluxes for both regions. Mechanisms are distinct between SPNA and NSEA and therefore those two regions should be considered separately.

We observe a clear anticorrelation between freshwater and heat content in the SPNA, NSEA and LSEA regions. This anticorrelation between freshwater and heat has been also noted by Boyer et al. (2007), and this makes sense given that both are driven by the changes in circulation. Surprisingly, the anticorrelation between freshwater and heat in the NSEA is not due to a common driver of change, but appears to be coincidental, as we see that the decline in freshwater content is in the sea ice component of the forcing term, while heat is affected by the sea surface heat fluxes as well as advection.

The freshening and cooling of the SPNA over the recent decade is due to a reduction in salt and heat flux through the southern boundary and not an increased fresher water entering from the Arctic. In the SPNA, changes in the AMOC strength appear to be the main driver, with a possible contribution from horizontal circulation. Although a correlation with wind exists, freshening and cooling are likely not driven directly by changes in wind. As Arctic freshening has been shown to be principally anthropogenic, that is not currently the case in the SPNA. Arctic-North Atlantic exchanges will likely play an important role in the future of global climate as it can be expected that accumulated Arctic freshwater will eventually outflow through major gateways into the SPNA. Thus, it can be anticipated that the anomalies between the Arctic and the North Atlantic will eventually be linked. It is intriguing to note that there is evidence of Arctic freshwater outflow through Davis Strait, which is consistent with recent modeling work that shows a proportionally greater increase in freshwater outflow through Davis Strait during a scenario of freshwater release from the Arctic Ocean (J. Zhang et al., 2020). However, according to ECCOv4, the recent increased Arctic freshwater outflow through the Davis Strait into the Labrador Sea is balanced by greater freshwater outflow from the Labrador Sea via the Labrador Current, suggesting that freshwater will not accumulate in the Labrador Sea and therefore will not be likely to affect deep convection sites. Our regional budget analysis shows that increased freshwater flow from the Arctic has only minor effects on the budgets and so do not dominate salinity changes in these regions.

Although the advective transport changes from the subtropical North Atlantic dominate, this does not exclude increased Arctic outflow in recent years. It indicates that at present Arctic outflows are small in comparison to advective convergence through exchanges with the subtropical basin. Thus, at the moment Arctic-North Atlantic exchanges are minor processes, with the exception of a connection due to the decline in sea ice export through the Fram Strait. This connection however is only relevant in the NSEA, and is too small to account for the decline in the SPNA freshwater content from 1995 to 2005. Similarly, we suggest that land ice and glacial melting are likely not a substantial part of recent freshwater input into the SPNA. Dukhovskoy et al. (2019) illustrate that land-based freshwater sources do not account for all the observed freshening and speculate that increased Arctic outflow could explain the rest of the freshening. Our analysis points to the need to consider changes in circulation related to the AMOC and NAC to fully capture the freshening signal in the SPNA.

Acknowledgments

JET acknowledges funding from NASA's Goddard Space Flight Center award NNX15AN27H. TWNH was supported by NASA under grant 80NSSC20K0823. The authors wish to thank Ali Siddiqui for helpful comments and suggestions on the manuscript. Discussions with Joaquim Goes, Ryan Abernathey and Spencer Jones were helpful. This work was made possible through the generosity of the Estimating the Circulation and Climate of the Ocean (ECCO) Consortium in providing the ECCOv4 products. Standard output and documentation for ECCOv4 can be obtained at `https://ecco-group.org/products.htm`. We reproduced the ECCOv4r3 ocean state estimate with a custom set of diagnostics which are available as a dataset on Pangeo (`http://catalog.pangeo.io/ocean/ECCOv4r3`) or can be requested from the corresponding author. HadOBS EN4 salinity fields were obtained from the Met Office (`http://hadobs.metoffice.com/en4`). Data from the RAPID AMOC monitoring project are funded by the Natural Environment Research Council and are freely available from `http://www.rapid.ac.uk/rapidmoc`. Monthly time series of NAO and AO were obtained from the NOAA/ESRL Physical Sciences Division website (`https://www.esrl.noaa.gov/psd/data/climateindices/list/`). The SSALTO/Duacs multi-altimeter product of absolute dynamic topography was downloaded from the Copernicus Marine and Environment Monitoring Service (CMEMS, `https://marine.copernicus.eu`).

References

Adcroft, A., & Campin, J.-M. (2004). Rescaled height coordinates for accurate representation of free-surface flows in ocean circulation models. *Ocean Modelling*, *7*(3), 269–284. doi: 10.1016/j.ocemod.2003.09.003

Avsic, T., Karstensen, J., Send, U., & Fischer, J. (2006). Interannual variability of newly formed Labrador Sea Water from 1994 to 2005. *Geophysical Research Letters*, *33*(21). Retrieved from `https://agupubs.onlinelibrary.wiley.com/doi/abs/10.1029/2006GL026913` doi: 10.1029/2006GL026913

Bacon, S., Aksenov, Y., Fawcett, S., & Madec, G. (2015). Arctic mass, freshwater and heat fluxes: methods and modelled seasonal variability. *Philosophical Transactions of the Royal Society A: Mathematical, Physical and Engineering Sciences*, *373*(2052), 20140169. doi: 10.1098/rsta.2014.0169

Bamber, J., van den Broeke, M., Ettema, J., Lenaerts, J., & Rignot, E. (2012). Recent large increases in freshwater fluxes from Greenland into the North Atlantic. *Geophysical Research Letters*, *39*(19). doi: 10.1029/2012GL052552

Bamber, J. L., Tedstone, A. J., King, M. D., Howat, I. M., Enderlin, E. M., van den Broeke, M. R., & Noel, B. (2018). Land Ice Freshwater Budget of the Arctic and North Atlantic Oceans: 1. Data, Methods, and Results. *Journal of Geophysical Research: Oceans*, *123*(3), 1827–1837. doi: 10.1002/2017JC013605

Belkin, I. M. (2004). Propagation of the "Great Salinity Anomaly" of the 1990s around the northern North Atlantic. *Geophysical Research Letters*, *31*(8), L08306. doi: 10.1029/2003GL019334

Belkin, I. M., Levitus, S., Antonov, J., & Malmberg, S.-A. (1998). "Great Salinity Anomalies" in the North Atlantic. *Progress in Oceanography*, *41*(1), 1–68. doi: 10.1016/S0079-6611(98)00015-9

Bersch, M. (2002). North Atlantic Oscillation-induced changes of the upper layer circulation in the northern North Atlantic Ocean. *Journal of Geophysical Research*, *107*(C10), 1–11. doi: 10.1029/2001JC000901

Bersch, M., Yashayaev, I., & Koltermann, K. P. (2007). Recent changes of the thermohaline circulation in the subpolar North Atlantic. *Ocean Dynamics*, *57*(3), 223–235. doi: 10.1007/s10236-007-0104-7

Beszczynska-Möller, A., Woodgate, R. A., Lee, C. M., Melling, H., & Karcher, M. (2011). A Synthesis of Exchanges Through the Main Oceanic Gateways to the Arctic Ocean. *Oceanography*, *24*(3), 82–99. doi: 10.5670/oceanog.2011.59

Biastoch, A., Böning, C. W., Getzlaff, J., Molines, J.-M., & Madec, G. (2008). Causes of Interannual–Decadal Variability in the Meridional Overturning Circulation of the Midlatitude North Atlantic Ocean. *Journal of Climate*, *21*(24), 6599–6615. doi: 10.1175/2008JCLI2404.1

Blindheim, J., Borovkov, V., Hansen, B., Malmberg, S.-A., Turrell, W., & Østerhus, S. (2000). Upper layer cooling and freshening in the Norwegian Sea in relation to atmospheric forcing. *Deep Sea Research Part I: Oceanographic Research Papers*, *47*(4), 655–680. doi: 10.1016/S0967-0637(99)00070-9

Böning, C. W., Behrens, E., Biastoch, A., Getzlaff, K., & Bamber, J. L. (2016). Emerging impact of Greenland meltwater on deepwater formation in the North Atlantic Ocean. *Nature Geoscience*, *9*(7), 523–527. doi: 10.1038/ngeo2740

Boyer, T., Levitus, S., Antonov, J., Locarnini, R., Mishonov, A., Garcia, H., & Josey, S. A. (2007). Changes in freshwater content in the North Atlantic Ocean 1955–2006. *Geophysical Research Letters*, *34*(16). doi: 10.1029/2007GL030126

Bryden, H. L., Johns, W. E., King, B. A., McCarthy, G., McDonagh, E. L., Moat, B. I., & Smeed, D. A. (2020). Reduction in Ocean Heat Transport at 26°N since 2008 Cools the Eastern Subpolar Gyre of the North Atlantic Ocean. *Journal of Climate*, *33*(5), 1677–1689. doi: 10.1175/JCLI-D-19-0323.1

Buckley, M. W., Ponte, R. M., Forget, G., & Heimbach, P. (2014). Low-Frequency SST and Upper-Ocean Heat Content Variability in the North Atlantic. *Journal of Climate*, *27*(13), 4996–5018. doi: 10.1175/JCLI-D-13-00316.1

Buckley, M. W., Ponte, R. M., Forget, G., & Heimbach, P. (2015). Determining the Origins of Advective Heat Transport Convergence Variability in the North Atlantic. *Journal of Climate*, *28*(10), 3943–3956. doi: 10.1175/JCLI-D-14-00579.1

Castelao, R. M., Luo, H., Oliver, H., Rennermalm, A. K., Tedesco, M., Bracco, A., ... Medeiros, P. M. (2019). Controls on the Transport of Meltwater From the Southern Greenland Ice Sheet in the Labrador Sea. *Journal of Geophysical Research: Oceans*, *44*(12), 6278–10. doi: 10.1029/2019JC015159

Comiso, J. C., Parkinson, C. L., Gersten, R., & Stock, L. (2008). Accelerated decline in the Arctic sea ice cover. *Geophysical Research Letters*, *35*(1). doi: 10.1029/2007GL031972

Curry, B., Lee, C. M., & Petrie, B. (2011). Volume, Freshwater, and Heat Fluxes through Davis Strait, 2004–05. *Journal of Physical Oceanography*, *41*(3), 429–436. Retrieved from `https://doi.org/10.1175/2010JPO4536.1` doi: 10.1175/2010JPO4536.1

Curry, B., Lee, C. M., Petrie, B., Moritz, R. E., & Kwok, R. (2014). Multiyear volume, liquid freshwater, and sea ice transports through Davis Strait, 2004-10. *Journal of Physical Oceanography*, *44*(4), 1244–1266. doi: 10.1175/JPO-D-13-0177.1

Curry, R., Dickson, B., & Yashayaev, I. (2003). A change in the freshwater balance of the Atlantic Ocean over the past four decades. *Nature*, *426*(6968), 826–829.

doi: 10.1038/nature02206

Curry, R., & Mauritzen, C. (2005). Dilution of the northern North Atlantic Ocean in recent decades. *Science*, *308*(5729), 1772–1774. doi: 10.1126/science.1109477

Curry, R. G., & McCartney, M. S. (2001). Ocean gyre circulation changes associated with the North Atlantic Oscillation. *Journal of Physical Oceanography*, *31*(12), 3374–3400.

Dee, D. P., Uppala, S. M., Simmons, A. J., Berrisford, P., Poli, P., Kobayashi, S., ... Vitart, F. (2011). The ERA-Interim reanalysis: configuration and performance of the data assimilation system. *Quarterly Journal of the Royal Meteorological Society*, *137*(656), 553–597. doi: 10.1002/qj.828

Deshayes, J., Curry, R., & Msadek, R. (2014). CMIP5 Model Intercomparison of Freshwater Budget and Circulation in the North Atlantic. *Journal of Climate*, *27*(9), 3298–3317. doi: 10.1175/JCLI-D-12-00700.1

de Steur, L., Hansen, E., Gerdes, R., Karcher, M., Fahrbach, E., & Holfort, J. (2009). Freshwater fluxes in the East Greenland Current: A decade of observations. *Geophysical Research Letters*, *36*(23). doi: 10.1029/2009GL041278

de Steur, L., Peralta Ferriz, C., & Pavlova, O. (2018). Freshwater export in the East Greenland Current freshens the North Atlantic. *Geophysical Research Letters*, *45*(24), 13,359-13,366. doi: 10.1029/2018GL080207

de Steur, L., Pickart, R. S., Macrander, A., Våge, K., Harden, B., Jónsson, S., ... Valdimarsson, H. (2017). Liquid freshwater transport estimates from the East Greenland Current based on continuous measurements north of Denmark Strait. *Journal of Geophysical Research: Oceans*, *122*(1), 93–109. doi: 10.1002/2016JC012106

Dickson, B., Yashayaev, I., Meincke, J., Turrell, B., Dye, S. R., & Holfort, J. (2002). Rapid freshening of the deep North Atlantic Ocean over the past four decades. *Nature*, *416*(6883), 832–837.

Dickson, R. R., Meincke, J., Malmberg, S.-A., & Lee, A. J. (1988). The "great salinity anomaly" in the Northern North Atlantic 1968–1982. *Progress in Oceanography*, *20*(2), 103–151. doi: 10.1016/0079-6611(88)90049-3

Doney, S. C., Yeager, S., Danabasoglu, G., Large, W. G., & McWilliams, J. C. (2007). Mechanisms Governing Interannual Variability of Upper-Ocean Temperature in a Global Ocean Hindcast Simulation. *Journal of Physical Oceanography*, *37*(7), 1918–1938. doi: 10.1175/JPO3089.1

Dukhovskoy, D. S., Yashayaev, I., Proshutinsky, A., Bamber, J. L., Bashmachnikov, I. L., Chassignet, E. P., ... Tedstone, A. J. (2019). Role of Greenland Freshwater Anomaly in the Recent Freshening of the Subpolar North Atlantic. *Journal of Geophysical Research: Oceans*, *124*(5), 3333–3360. doi: 10.1029/2018JC014686

Durack, P. J., Wijffels, S. E., & Matear, R. J. (2012). Ocean salinities reveal strong global water cycle intensification during 1950 to 2000. *Science*, *336*(6080), 455–458. doi: 10.1126/science.1212222

Fekete, B. M., Vörösmarty, C. J., & Grabs, W. (2002). High-resolution fields of global runoff combining observed river discharge and simulated water balances. *Global Biogeochemical Cycles*, *16*(3), 15-1-15-10. doi: 10.1029/1999GB001254

Forget, G., Campin, J.-M., Heimbach, P., Hill, C. N., Ponte, R. M., & Wunsch, C. (2015). ECCO version 4: an integrated framework for non-linear inverse modeling and global ocean state estimation. *Geoscientific Model Development*, *8*(10), 3071–3104. doi: 10.5194/gmd-8-3071-2015

Forget, G., & Ferreira, D. (2019). Global ocean heat transport dominated by heat export from the tropical Pacific. *Nature Geoscience*, *12*(5), 1–6. doi: 10.1038/s41561-019-0333-7

Gaspar, P., Grégoris, Y., & Lefevre, J.-M. (1990). A simple eddy kinetic energy model for simulations of the oceanic vertical mixing: Tests at station Papa and long-term upper ocean study site. *Journal of Geophysical Research: Oceans*,

95(C9), 16179–16193. doi: 10.1029/JC095iC09p16179
Gent, P. R., & Mcwilliams, J. C. (1990). Isopycnal Mixing in Ocean Circulation Models. *Journal of Physical Oceanography*, *20*(1), 150–155. doi: 10.1175/1520-0485(1990)020⟨0150:IMIOCM⟩2.0.CO;2
Glessmer, M. S., Eldevik, T., Våge, K., Nilsen, J. E. Ø., & Behrens, E. (2014). Atlantic origin of observed and modelled freshwater anomalies in the Nordic Seas. *Nature Geoscience*, *7*(11), 801–805. doi: 10.1038/ngeo2259
Good, S. A., Martin, M. J., & Rayner, N. A. (2013). EN4: Quality controlled ocean temperature and salinity profiles and monthly objective analyses with uncertainty estimates. *Journal of Geophysical Research: Oceans*, *118*(12), 6704–6716. doi: 10.1002/2013JC009067
Grist, J. P., Josey, S. A., Jacobs, Z. L., Marsh, R., Sinha, B., & Sebille, E. (2016). Extreme air–sea interaction over the North Atlantic subpolar gyre during the winter of 2013–2014 and its sub-surface legacy. *Climate Dynamics*, *46*(11), 4027–4045. doi: 10.1007/s00382-015-2819-3
Haak, H., Jungclaus, J., Mikolajewicz, U., & Latif, M. (2003). Formation and propagation of great salinity anomalies. *Geophysical Research Letters*, *30*(9). doi: 10.1029/2003GL017065
Haine, T. W. N. (2016). Vagaries of Atlantic overturning. *Nature Geoscience*, *9*(7), 479–480. doi: 10.1038/ngeo2748
Haine, T. W. N., Curry, B., Gerdes, R., Hansen, E., Karcher, M., Lee, C., ... Woodgate, R. (2015). Arctic freshwater export: Status, mechanisms, and prospects. *Global and Planetary Change*, *125*(C), 13–35. doi: j.gloplacha.2014.11.013
Häkkinen, S. (2002). Freshening of the Labrador Sea surface waters in the 1990s: Another great salinity anomaly? *Geophysical Research Letters*, *29*(24), 85-1–85-4. doi: 10.1029/2002GL015243
Häkkinen, S., & Rhines, P. B. (2004). Decline of Subpolar North Atlantic Circulation During the 1990s. *Science*, *304*(5670), 555–559. doi: 10.1126/science.1094917
Häkkinen, S., Rhines, P. B., & Worthen, D. L. (2011). Warm and saline events embedded in the meridional circulation of the northern North Atlantic. *Journal of Geophysical Research: Oceans*, *116*(C3). doi: 10.1029/2010JC006275
Hátún, H., & Chafik, L. (2018). On the Recent Ambiguity of the North Atlantic Subpolar Gyre Index. *Journal of Geophysical Research: Oceans*, *123*(8), 5072–5076. doi: 10.1029/2018JC014101
Hátún, H., Sandø, A. B., Drange, H., Hansen, B., & Valdimarsson, H. (2005). Influence of the Atlantic Subpolar Gyre on the Thermohaline Circulation. *Science*, *309*(5742), 1841–1844. doi: 10.1126/science.1114777
Held, I. M., & Soden, B. J. (2006). Robust responses of the hydrological cycle to global warming. *Journal of Climate*, *19*(21), 5686–5699. doi: 10.1175/JCLI3990.1
Holliday, N. P., Cunningham, S. A., Johnson, C., Gary, S. F., Griffiths, C., Read, J. F., & Sherwin, T. (2015). Multidecadal variability of potential temperature, salinity, and transport in the eastern subpolar North Atlantic. *Journal of Geophysical Research: Oceans*, *120*(9), 5945–5967. doi: 10.1002/2015JC010762
Holliday, N. P., Hughes, S. L., Bacon, S., Beszczynska-Möller, A., Hansen, B., Lavín, A., ... Walczowski, W. (2008). Reversal of the 1960s to 1990s freshening trend in the northeast North Atlantic and Nordic Seas. *Geophysical Research Letters*, *35*(3). doi: 10.1029/2007GL032675
Jackson, L. C., Peterson, K. A., Roberts, C. D., & Wood, R. A. (2016). Recent slowing of Atlantic overturning circulation as a recovery from earlier strengthening. *Nature Geoscience*, *9*(7), 518–522. doi: 10.1038/ngeo2715
Jahn, A., & Holland, M. M. (2013). Implications of Arctic sea ice changes for North Atlantic deep convection and the meridional overturning circulation in

CCSM4-CMIP5 simulations. *Geophysical Research Letters*, *40*(6), 1206-1211. doi: 10.1002/grl.50183

Josey, S. A., & Marsh, R. (2005). Surface freshwater flux variability and recent freshening of the North Atlantic in the eastern subpolar gyre. *Journal of Geophysical Research: Oceans*, *110*(C5). doi: 10.1029/2004JC002521

Karcher, M., Gerdes, R., Kauker, F., Köberle, C., & Yashayaev, I. (2005). Arctic Ocean change heralds North Atlantic freshening. *Geophysical Research Letters*, *32*(21). doi: 10.1029/2005GL023861

Koenigk, T., Mikolajewicz, U., Haak, H., & Jungclaus, J. (2007). Arctic freshwater export in the 20th and 21st centuries. *Journal of Geophysical Research: Biogeosciences*, *112*(G4). doi: 10.1029/2006JG000274

Koul, V., Tesdal, J.-E., Bersch, M., Hátún, H., Brune, S., Borchert, L., ... Baehr, J. (2020). Unraveling the choice of the north Atlantic subpolar gyre index. *Scientific Reports*, *10*(1), 1005–12. doi: 10.1038/s41598-020-57790-5

Large, W. G., & Yeager, S. G. (2009). The global climatology of an interannually varying air–sea flux data set. *Climate Dynamics*, *33*(2), 341–364. doi: 10.1007/s00382-008-0441-3

Lau, W. K. M., Wu, H. T., & Kim, K. M. (2013). A canonical response of precipitation characteristics to global warming from CMIP5 models. *Geophysical Research Letters*, *40*(12), 3163–3169. doi: 10.1002/grl.50420

Lique, C., Treguier, A. M., Scheinert, M., & Penduff, T. (2009). A model-based study of ice and freshwater transport variability along both sides of Greenland. *Climate Dynamics*, *33*(5), 685–705. doi: 10.1007/s00382-008-0510-7

Lozier, M., Bacon, S., Bower, A. S., Cunningham, S. A., Femke de Jong, M., de Steur, L., ... Zika, J. D. (2017). Overturning in the Subpolar North Atlantic Program: A New International Ocean Observing System. *Bulletin of the American Meteorological Society*, *98*(4), 737–752. doi: 10.1175/BAMS-D-16-0057.1

Luo, H., Castelao, R. M., Rennermalm, A. K., Tedesco, M., Bracco, A., Yager, P. L., & Mote, T. L. (2016). Oceanic transport of surface meltwater from the southern Greenland ice sheet. *Nature Geoscience*, *9*(7), 528–532. doi: 10.1038/ngeo2708

Marnela, M., Rudels, B., Goszczko, I., Beszczynska-Möller, A., & Schauer, U. (2016). Fram Strait and Greenland Sea transports, water masses, and water mass transformations 1999–2010 (and beyond). *Journal of Geophysical Research: Oceans*, *121*(4), 2314–2346. doi: 10.1002/2015JC011312

Marshall, J., Adcroft, A., Hill, C., Perelman, L., & Heisey, C. (1997). A finite-volume, incompressible Navier Stokes model for studies of the ocean on parallel computers. *Journal of Geophysical Research: Oceans*, *102*(C3), 5753–5766. doi: 10.1029/96JC02775

Myers, P. G., Josey, S. A., Wheler, B., & Kulan, N. (2007). Interdecadal variability in Labrador Sea precipitation minus evaporation and salinity. *Progress in Oceanography*, *73*(3), 341–357. doi: 10.1016/j.pocean.2006.06.003

Nummelin, A., Ilicak, M., Li, C., & Smedsrud, L. H. (2016). Consequences of future increased Arctic runoff on Arctic Ocean stratification, circulation, and sea ice cover. *Journal of Geophysical Research: Oceans*, *121*(1), 617–637. doi: 10.1002/2015JC011156

Oliver, H., Luo, H., Castelao, R. M., van Dijken, G. L., Mattingly, K. S., Rosen, J. J., ... Yager, P. L. (2018). Exploring the Potential Impact of Greenland Meltwater on Stratification, Photosynthetically Active Radiation, and Primary Production in the Labrador Sea. *Journal of Geophysical Research: Oceans*, *123*(4), 2570–2591. doi: 10.1002/2018JC013802

Østerhus, S., Woodgate, R., Valdimarsson, H., Turrell, B., de Steur, L., Quadfasel, D., ... Berx, B. (2019). Arctic Mediterranean exchanges: a consistent volume budget and trends in transports from two decades of observations. *Ocean*

Science, *15*(2), 379–399. doi: 10.5194/os-15-379-2019

Parkinson, C. L., & Comiso, J. C. (2013). On the 2012 record low Arctic sea ice cover: Combined impact of preconditioning and an August storm. *Geophysical Research Letters*, *40*(7), 1356–1361. doi: 10.1002/grl.50349

Peterson, B. J., McClelland, J., Curry, R., Holmes, R. M., Walsh, J. E., & Aagaard, K. (2006). Trajectory shifts in the Arctic and subarctic freshwater cycle. *Science*, *313*(5790), 1061–1066. doi: 10.1126/science.1122593

Piecuch, C. G., Ponte, R. M., Little, C. M., Buckley, M. W., & Fukumori, I. (2017). Mechanisms underlying recent decadal changes in subpolar North Atlantic Ocean heat content. *Journal of Geophysical Research: Oceans*, *122*(9), 7181–7197. doi: 10.1002/2017JC012845

Prandle, D. (1993). Year-long measurements of flow-through the Dover Strait by H.F. Radar and acoustic Doppler current profilers (ADCP). *Oceanologica Acta*, *16*(5-6), 457–468.

Proshutinsky, A., Dukhovskoy, D., Timmermans, M.-L., Krishfield, R., & Bamber, J. L. (2015). Arctic circulation regimes. *Philosophical Transactions of the Royal Society A: Mathematical, Physical and Engineering Sciences*, *373*(2052), 20140160. doi: 10.1098/rsta.2014.0160

Proshutinsky, A., Krishfield, R., Timmermans, M.-L., Toole, J., Carmack, E., McLaughlin, F., ... Shimada, K. (2009). Beaufort Gyre freshwater reservoir: State and variability from observations. *Journal of Geophysical Research: Oceans*, *114*(C1). doi: 10.1029/2008JC005104

Rabe, B., Karcher, M., Kauker, F., Schauer, U., Toole, J. M., Krishfield, R. A., ... Su, J. (2014). Arctic Ocean basin liquid freshwater storage trend 1992–2012. *Geophysical Research Letters*, *41*(3), 961–968. doi: 10.1002/2013GL058121

Redi, M. H. (1982). Oceanic Isopycnal Mixing by Coordinate Rotation. *Journal of Physical Oceanography*, *12*(10), 1154–1158. doi: 10.1175/1520-0485(1982)012⟨1154:OIMBCR⟩2.0.CO;2

Rennermalm, A. K., Wood, E. F., Weaver, A. J., Eby, M., & Déry, S. J. (2007). Relative sensitivity of the Atlantic meridional overturning circulation to river discharge into Hudson Bay and the Arctic Ocean. *Journal of Geophysical Research*, *112*(G04S48). doi: 10.1029/2006JG000330

Reverdin, G., Durand, F., Mortensen, J., Schott, F., Valdimarsson, H., & Zenk, W. (2002). Recent changes in the surface salinity of the North Atlantic subpolar gyre. *Journal of Geophysical Research: Oceans*, *107*(C12), 8010. doi: 10.1029/2001JC001010

Rhein, M., Kieke, D., Hüttl-Kabus, S., Roessler, A., Mertens, C., Meissner, R., ... Yashayaev, I. (2011). Deep water formation, the subpolar gyre, and the meridional overturning circulation in the subpolar North Atlantic. *Deep Sea Research Part II: Topical Studies in Oceanography*, *58*(17), 1819–1832. doi: 10.1016/j.dsr2.2010.10.061

Rhein, M., Steinfeldt, R., Huhn, O., Sültenfuß, J., & Breckenfelder, T. (2018). Greenland Submarine Melt Water Observed in the Labrador and Irminger Sea. *Geophysical Research Letters*, *45*(19), 10,570–10,578. doi: 10.1029/2018GL079110

Rignot, E., Box, J. E., Burgess, E., & Hanna, E. (2008). Mass balance of the Greenland ice sheet from 1958 to 2007. *Geophysical Research Letters*, *35*(20). doi: 10.1029/2008GL035417

Robson, J., Ortega, P., & Sutton, R. (2016). A reversal of climatic trends in the North Atlantic since 2005. *Nature Geoscience*, *9*, 513–517. doi: 10.1038/ngeo2727

Rossby, T., Flagg, C., Chafik, L., Harden, B., & Søiland, H. (2018). A Direct Estimate of Volume, Heat, and Freshwater Exchange Across the Greenland-Iceland-Faroe-Scotland Ridge. *Journal of Geophysical Research: Oceans*, *123*(10), 7139–7153. doi: 10.1029/2018JC014250

Sarafanov, A., Sokov, A., Demidov, A., & Falina, A. (2007). Warming and salinification of intermediate and deep waters in the Irminger Sea and Iceland Basin in 1997–2006. *Geophysical Research Letters*, *34*(23). doi: 10.1029/2007GL031074

Schauer, U., & Beszczynska-Möller, A. (2009). Problems with estimation and interpretation of oceanic heat transport – conceptual remarks for the case of Fram Strait in the Arctic Ocean. *Ocean Science*, *5*(4), 487–494. doi: 10.5194/os-5-487-2009

Schauer, U., & Losch, M. (2019). "Freshwater" in the Ocean is Not a Useful Parameter in Climate Research. *Journal of Physical Oceanography*, *49*(9), 2309–2321. doi: 10.1175/JPO-D-19-0102.1

Schauer, Ursula and Beszczynska-Möller, Agnieszka and Walczowski, Waldemar and Fahrbach, Eberhard and Piechura, Jan and Hansen, Edmond. (2008). Variation of Measured Heat Flow Through the Fram Strait Between 1997 and 2006. In R. R. Dickson, J. Meincke, & P. Rhines (Eds.), *Arctic–Subarctic Ocean Fluxes: Defining the Role of the Northern Seas in Climate* (pp. 65–85). Dordrecht: Springer Netherlands. doi: 10.1007/978-1-4020-6774-7_4

Smedsrud, L. H., Ingvaldsen, R., Nilsen, J. E. Ø., & Skagseth, Ø. (2010). Heat in the Barents Sea: transport, storage, and surface fluxes. *Ocean Science*, *6*(1), 219–234. doi: 10.5194/os-6-219-2010

Straneo, F., & Saucier, F. (2008). The outflow from Hudson Strait and its contribution to the Labrador Current. *Deep-Sea Research Part I-Oceanographic Research Papers*, *55*(8), 926–946. doi: 10.1016/j.dsr.2008.03.012

Tesdal, J.-E., Abernathey, R. P., Goes, J. I., Gordon, A. L., & Haine, T. W. N. (2018). Salinity Trends within the Upper Layers of the Subpolar North Atlantic. *Journal of Climate*, *31*(7), 2675–2698. doi: 10.1175/JCLI-D-17-0532.1

Thompson, P. R., Piecuch, C. G., Merrifield, M. A., McCreary, J. P., & Firing, E. (2016). Forcing of recent decadal variability in the Equatorial and North Indian Ocean. *Journal of Geophysical Research: Oceans*, *121*(9), 6762–6778. doi: 10.1002/2016JC012132

Thornalley, D. J. R., Oppo, D. W., Ortega, P., Robson, J. I., Brierley, C. M., Davis, R., … Keigwin, L. D. (2018). Anomalously weak Labrador Sea convection and Atlantic overturning during the past 150 years. *Nature*, *556*(7700), 227–230. doi: 10.1038/s41586-018-0007-4

Trusel, L. D., Das, S. B., Osman, M. B., Evans, M. J., Smith, B. E., Fettweis, X., … van den Broeke, M. R. (2018). Nonlinear rise in Greenland runoff in response to post-industrial Arctic warming. *Nature*, *564*(7734), 104–108. doi: 10.1038/s41586-018-0752-4

Tsubouchi, T., Bacon, S., Naveira Garabato, A. C., Aksenov, Y., Laxon, S. W., Fahrbach, E., … Ingvaldsen, R. B. (2012). The Arctic Ocean in summer: A quasi-synoptic inverse estimate of boundary fluxes and water mass transformation. *Journal of Geophysical Research: Oceans*, *117*(C1). doi: 10.1029/2011JC007174

Vellinga, M., Dickson, B., & Curry, R. (2008). The Changing View on How Freshwater Impacts the Atlantic Meridional Overturning Circulation. In R. R. Dickson, J. Meincke, & P. Rhines (Eds.), *Arctic–Subarctic Ocean Fluxes: Defining the Role of the Northern Seas in Climate* (pp. 289–313). Dordrecht: Springer Netherlands. doi: 10.1007/978-1-4020-6774-7_13

Vinogradova, N. T., & Ponte, R. M. (2017). In Search of Fingerprints of the Recent Intensification of the Ocean Water Cycle. *Journal of Climate*, *30*(14), 5513–5528. doi: 10.1175/JCLI-D-16-0626.1

Wadley, M. R., & Bigg, G. R. (2002). Impact of flow through the Canadian Archipelago and Bering Strait on the North Atlantic and Arctic circulation: An ocean modelling study. *Quarterly Journal of the Royal Meteorological Society*, *128*(585), 2187–2203. doi: 10.1256/qj.00.35

Yashayaev, I. (2007). Hydrographic changes in the Labrador Sea, 1960–2005. *Progress in Oceanography*, *73*(3), 242–276. doi: 10.1016/j.pocean.2007.04.015

Yashayaev, I., & Loder, J. W. (2016). Recurrent replenishment of Labrador Sea Water and associated decadal-scale variability. *Journal of Geophysical Research: Oceans*, *121*(11), 8095–8114. doi: 10.1002/2016JC012046

Yashayaev, I., & Loder, J. W. (2017). Further intensification of deep convection in the Labrador Sea in 2016. *Geophysical Research Letters*, *44*(3), 1429–1438. doi: 10.1002/2016GL071668

Zhang, J., Weijer, W., Steele, M., Cheng, W., & Verma, T. (2020). Labrador Sea freshening linked to Beaufort Gyre freshwater release. *Nature Communications*. (in revision)

Zhang, R., Sutton, R., Danabasoglu, G., Kwon, Y.-O., Marsh, R., Yeager, S. G., … Little, C. M. (2019). A Review of the Role of the Atlantic Meridional Overturning Circulation in Atlantic Multidecadal Variability and Associated Climate Impacts. *Reviews of Geophysics*, *57*(2), 316–375. doi: 10.1029/2019RG000644

Zhao, J., & Johns, W. (2014). Wind-forced interannual variability of the Atlantic Meridional Overturning Circulation at 26.5°N. *Journal of Geophysical Research: Oceans*, *119*(4), 2403–2419. doi: 10.1002/2013JC009407

Supporting Information for "Dominant terms in the freshwater and heat budgets of the subpolar North Atlantic Ocean and Nordic Seas from 1992 to 2015"

Jan-Erik Tesdal[1], Thomas W. N. Haine[2]

[1]Lamont-Doherty Earth Observatory, Columbia University, Palisades, New York, USA

[2]Earth and Planetary Sciences, The Johns Hopkins University, Baltimore, Maryland, USA

Contents of this file

Text S1.

The supplemental material includes additional results supporting the main findings of the article. In particular, Figures S2, S6, and S7 include budget results for salinity, which clarifies the consistency between liquid freshwater content and salinity in our results .

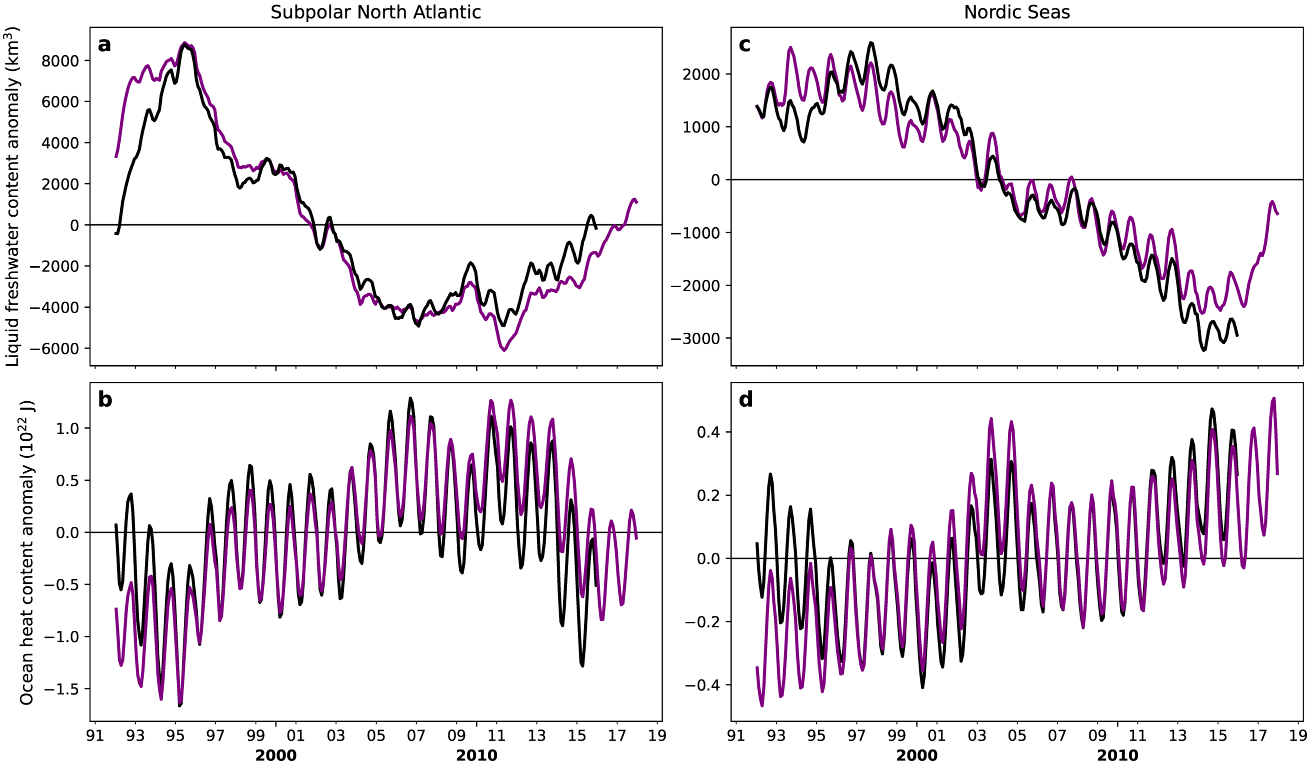

Figure S1. Liquid freshwater and heat content anomalies from ECCOv4 over the (a,b) subpolar North Atlantic and (c,d) Nordic Seas. For comparison, estimates are included for spatial definition as in Figure 1 using Release 3 (1992-2015, black line) and as defined in Figure 3a with Release 4 (1992-2017, purple line). Note the different y scales for the subpolar North Atlantic (a,b) and Nordic Seas (c,d).

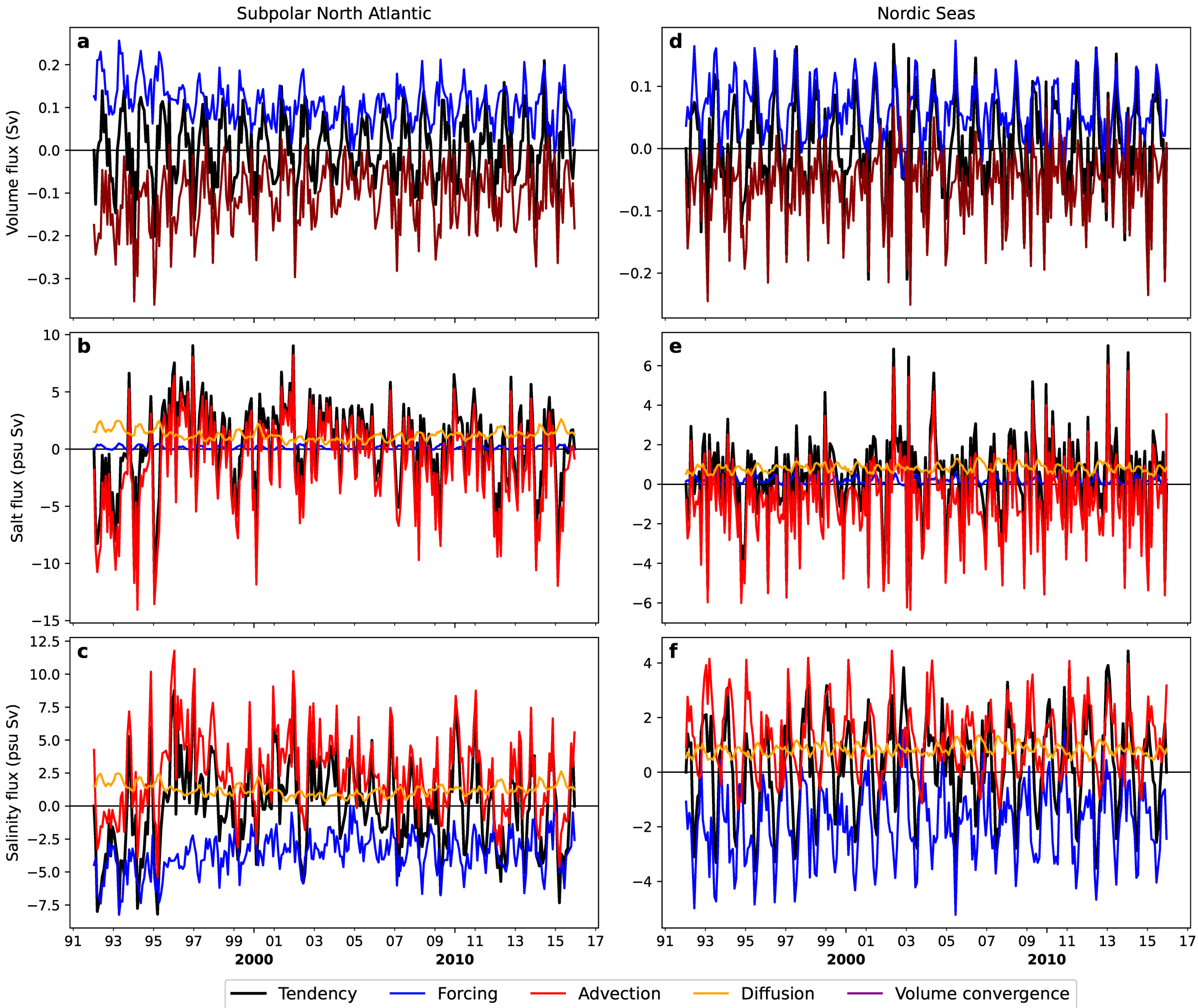

Figure S2. Monthly time series of volume, salt and salinity fluxes of the (a-c) subpolar North Atlantic and (d-f) Nordic Seas, including total tendency and individual components for surface forcing, advection, and diffusion. Note the different y scales for the subpolar North Atlantic (a,b) and Nordic Seas (c,d).

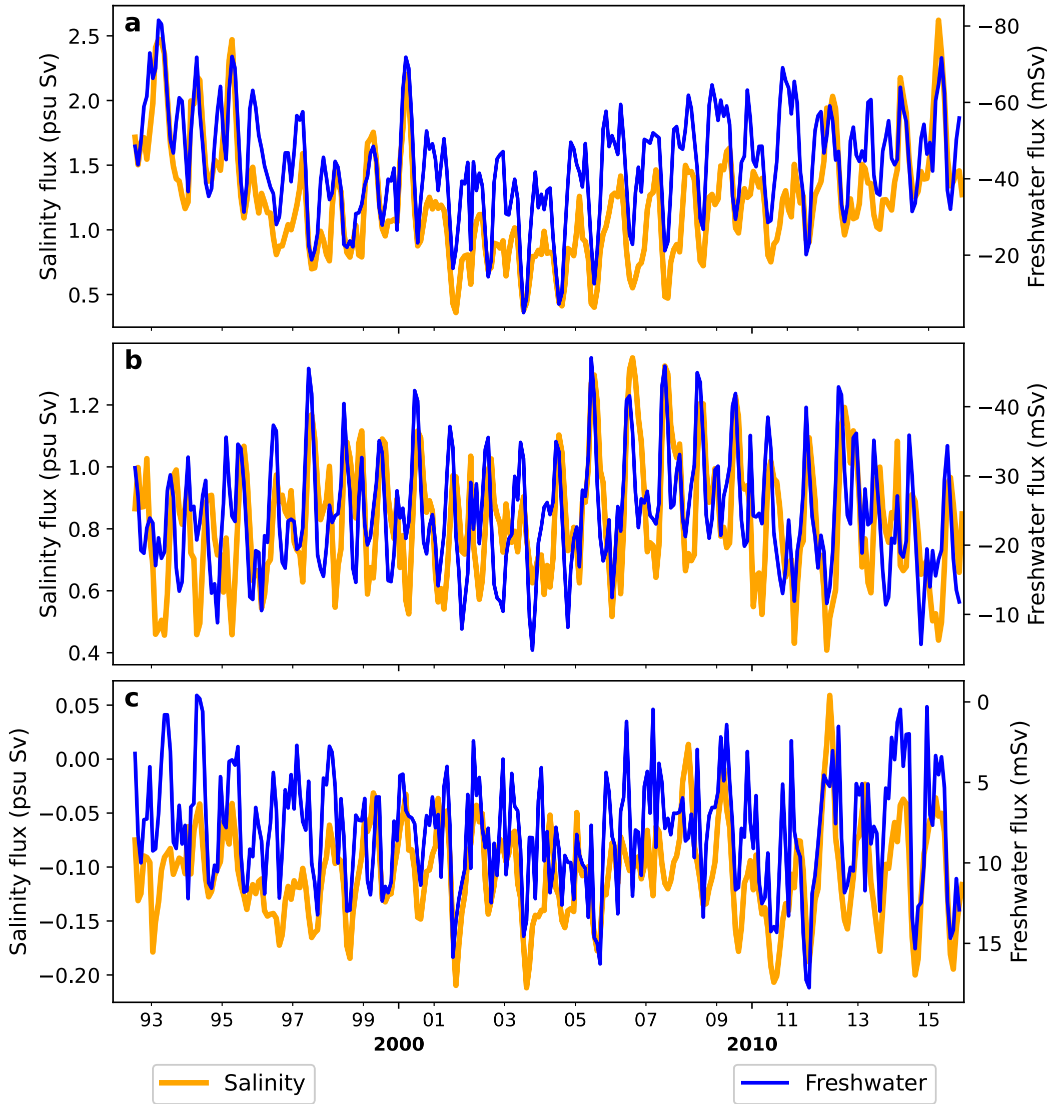

Figure S3. Comparison of diffusive flux convergence between salinity and freshwater for the (a) subpolar North Atlantic, (b) Nordic Seas and (c) Labrador Sea.

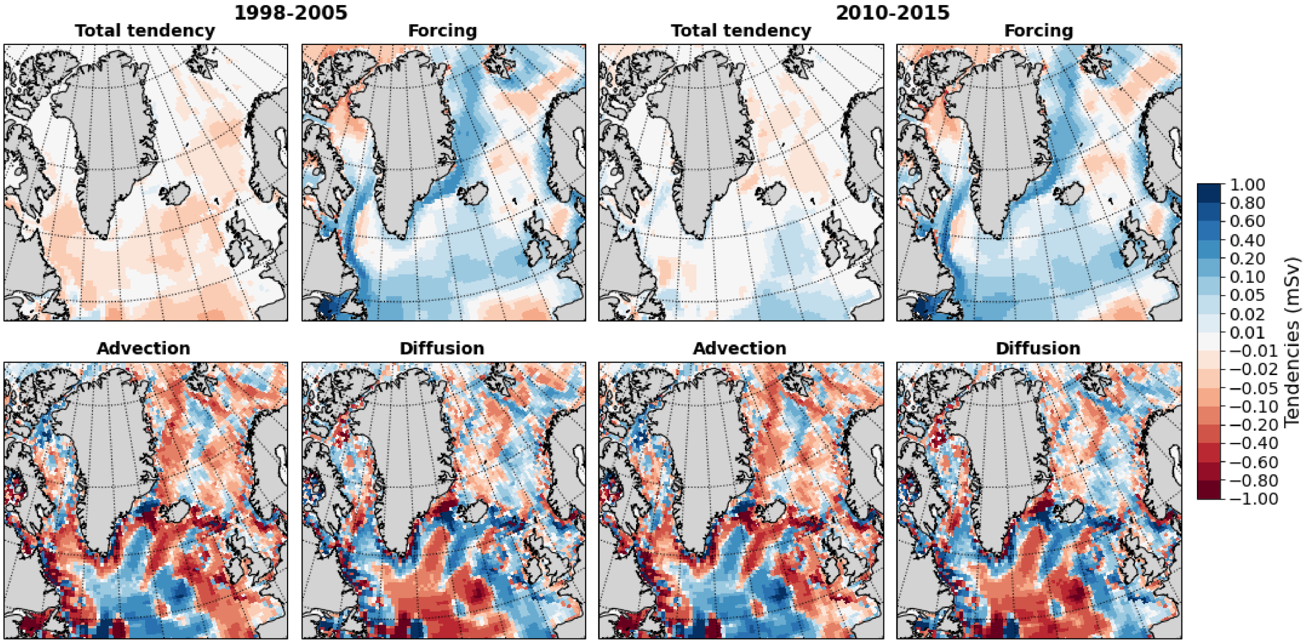

Figure S4. Spatial distributions of means for each major term in the ECCOv4 freshwater budget for the North Atlantic over 1998-2005 and 2010-2015.

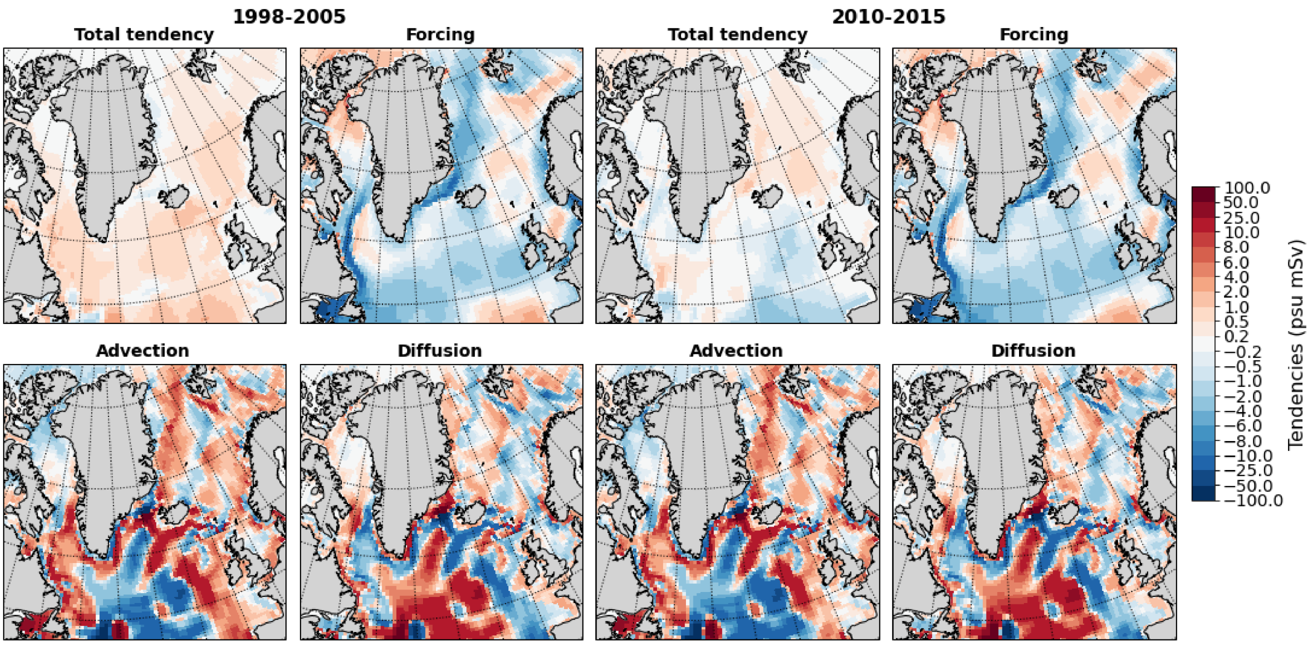

Figure S5. Spatial distributions of means for each major term in the ECCOv4 salinity budget for the North Atlantic over 1998-2005 and 2010-2015.

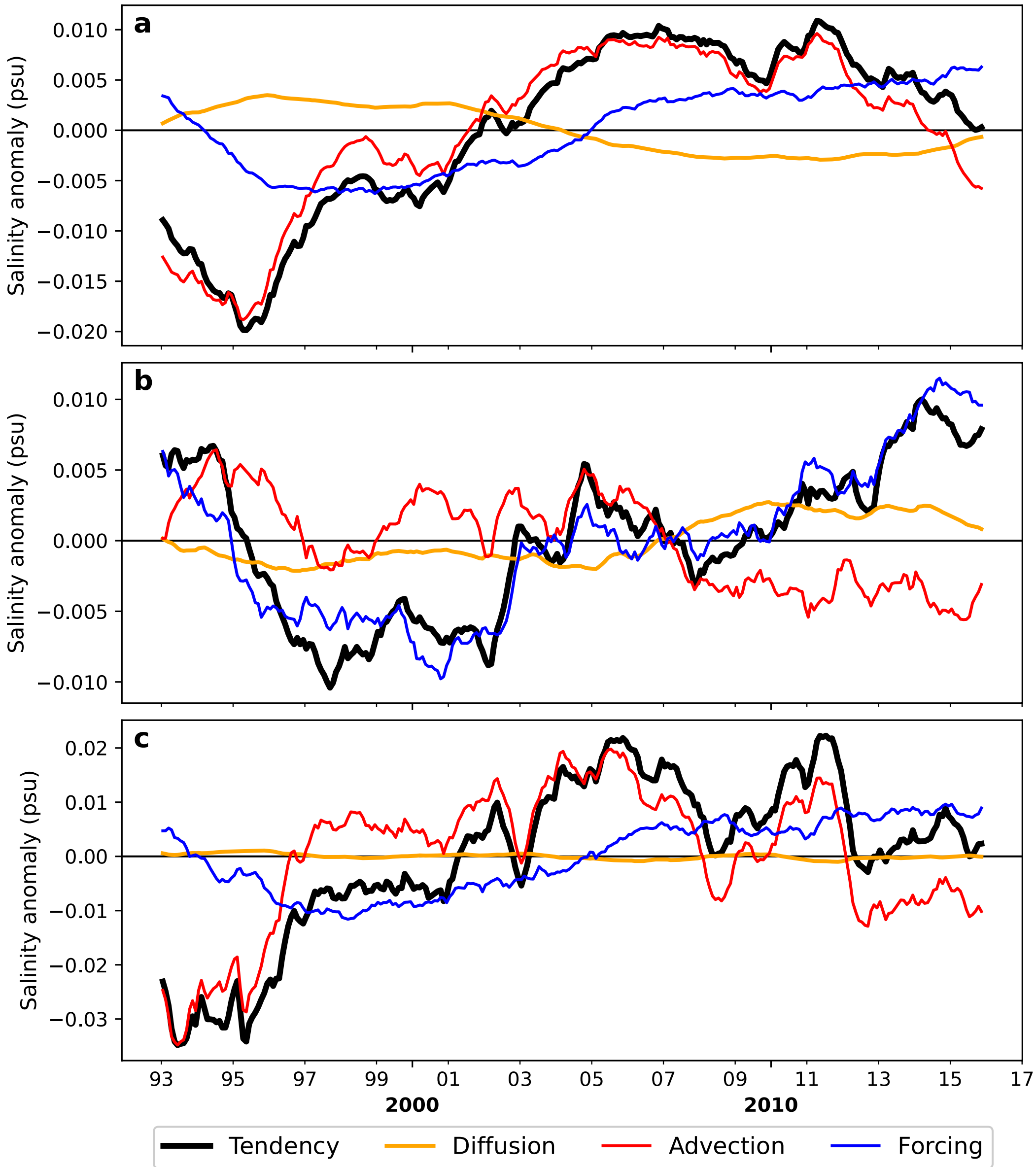

Figure S6. Integrated monthly time series of salinity anomaly for the (a) subpolar North Atlantic, (b) Nordic Seas and (c) Labrador Sea, including total tendency and individual components for surface forcing, advection, and diffusion.

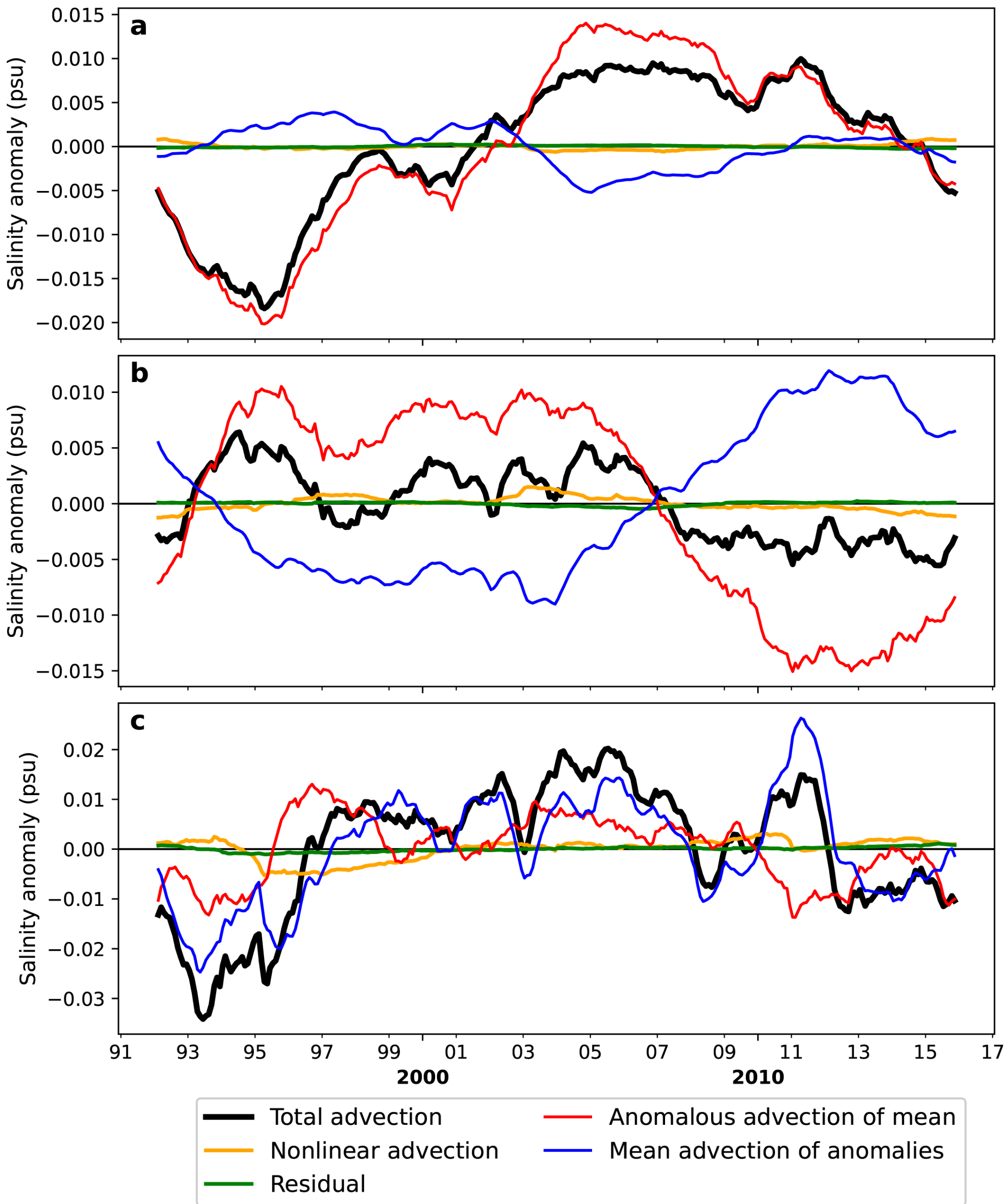

Figure S7. Decomposition of advective convergence of salinity anomaly into contributions from anomalous advection of mean, mean advection of anomalies, nonlinear advection and residual for the (a) subpolar North Atlantic, (b) Nordic Seas and (c) Labrador Sea. Note the different y scales for the subpolar North Atlantic (a,b) and Nordic Seas (c,d).

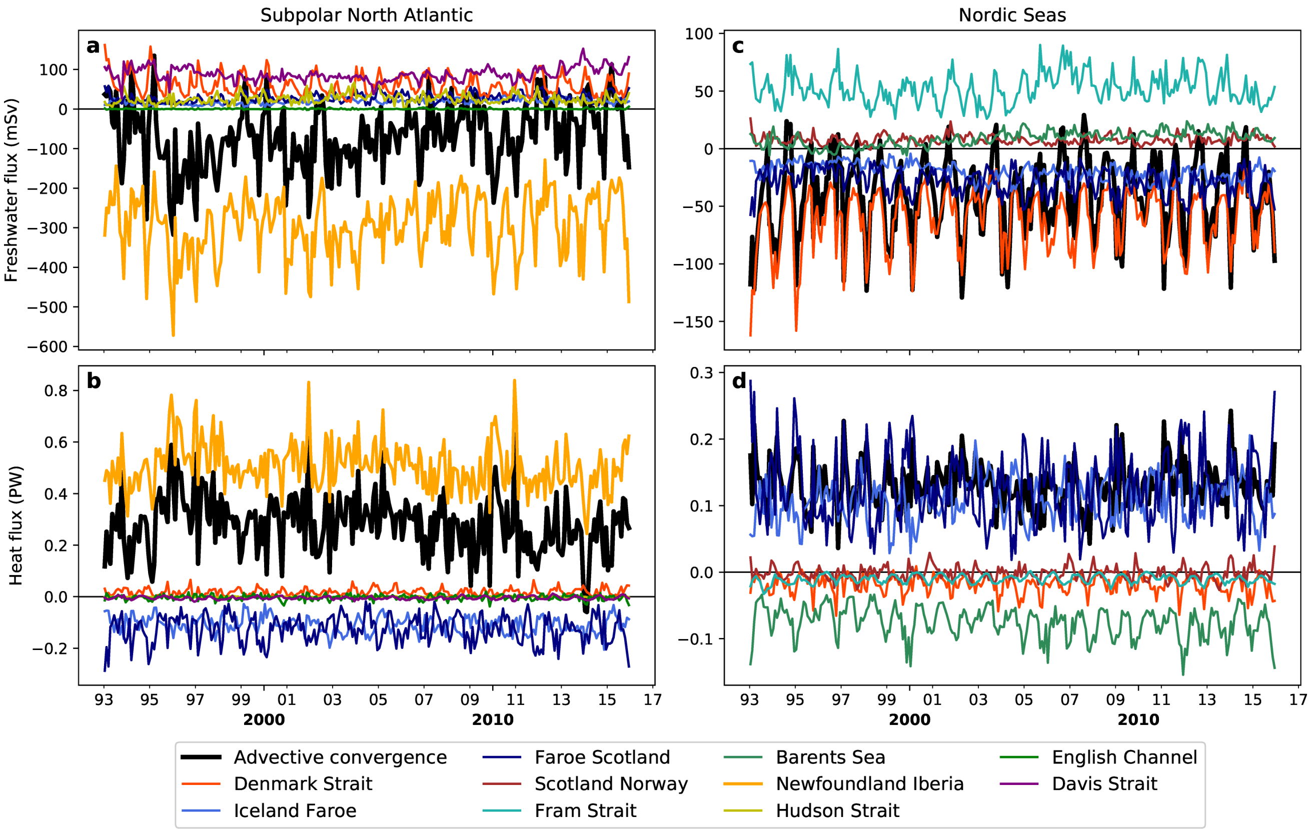

Figure S8. Total advective convergence and boundary fluxes into the (a,b) subpolar North Atlantic and (c,d) Nordic Seas for (a,c) freshwater and (b,d) heat content. Note the different y scales for the subpolar North Atlantic (a,b) and Nordic Seas (c,d).

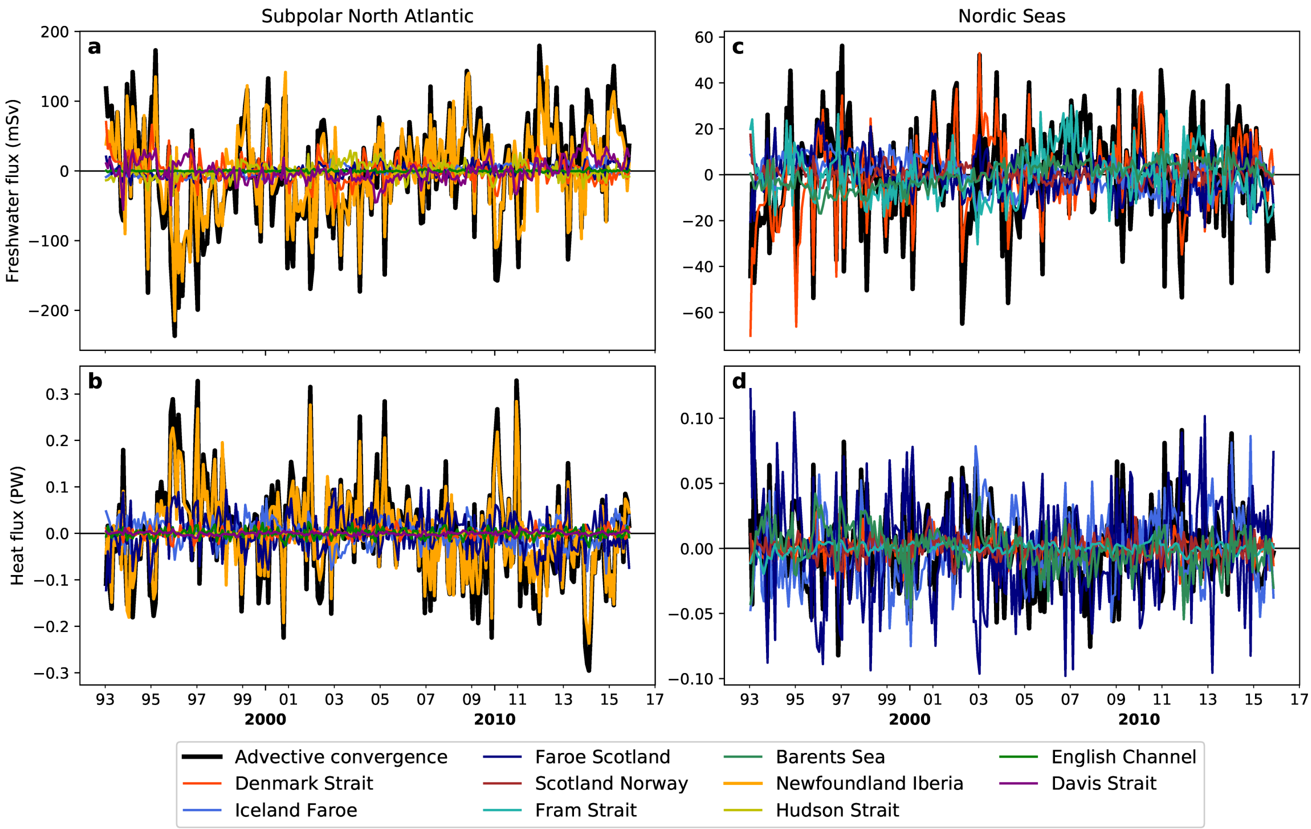

Figure S9. Seasonal anomalies of advective convergence and boundary fluxes into the (a,b) subpolar North Atlantic and (c,d) Nordic Seas for (a,c) freshwater and (b,d) heat content. Note the different y scales for the subpolar North Atlantic (a,b) and Nordic Seas (c,d).

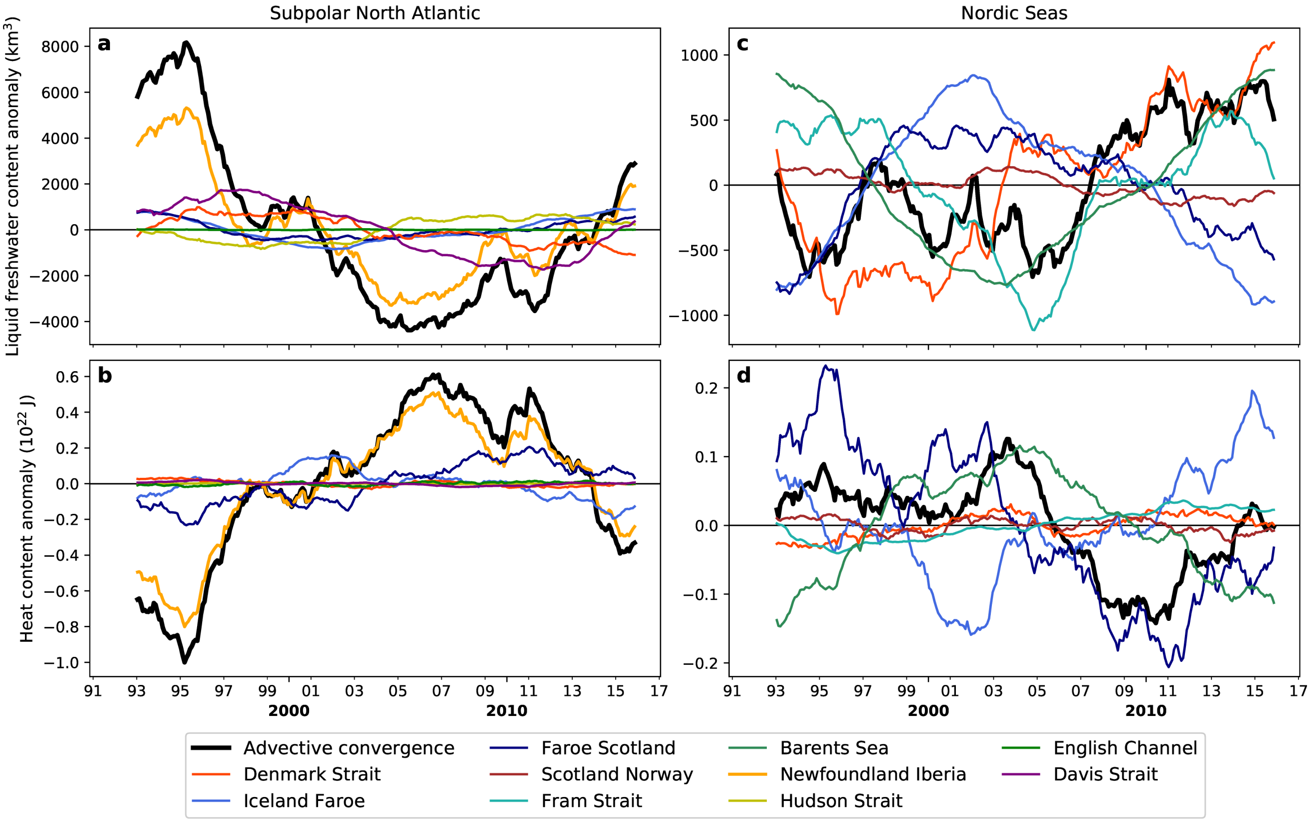

Figure S10. Integrated time series showing the total advective convergence and the contribution of each boundary flux into the (a,b) subpolar North Atlantic and (c,d) Nordic Seas for (a,c) freshwater and (b,d) heat content. Note the different y scales for the subpolar North Atlantic (a,b) and Nordic Seas (c,d).

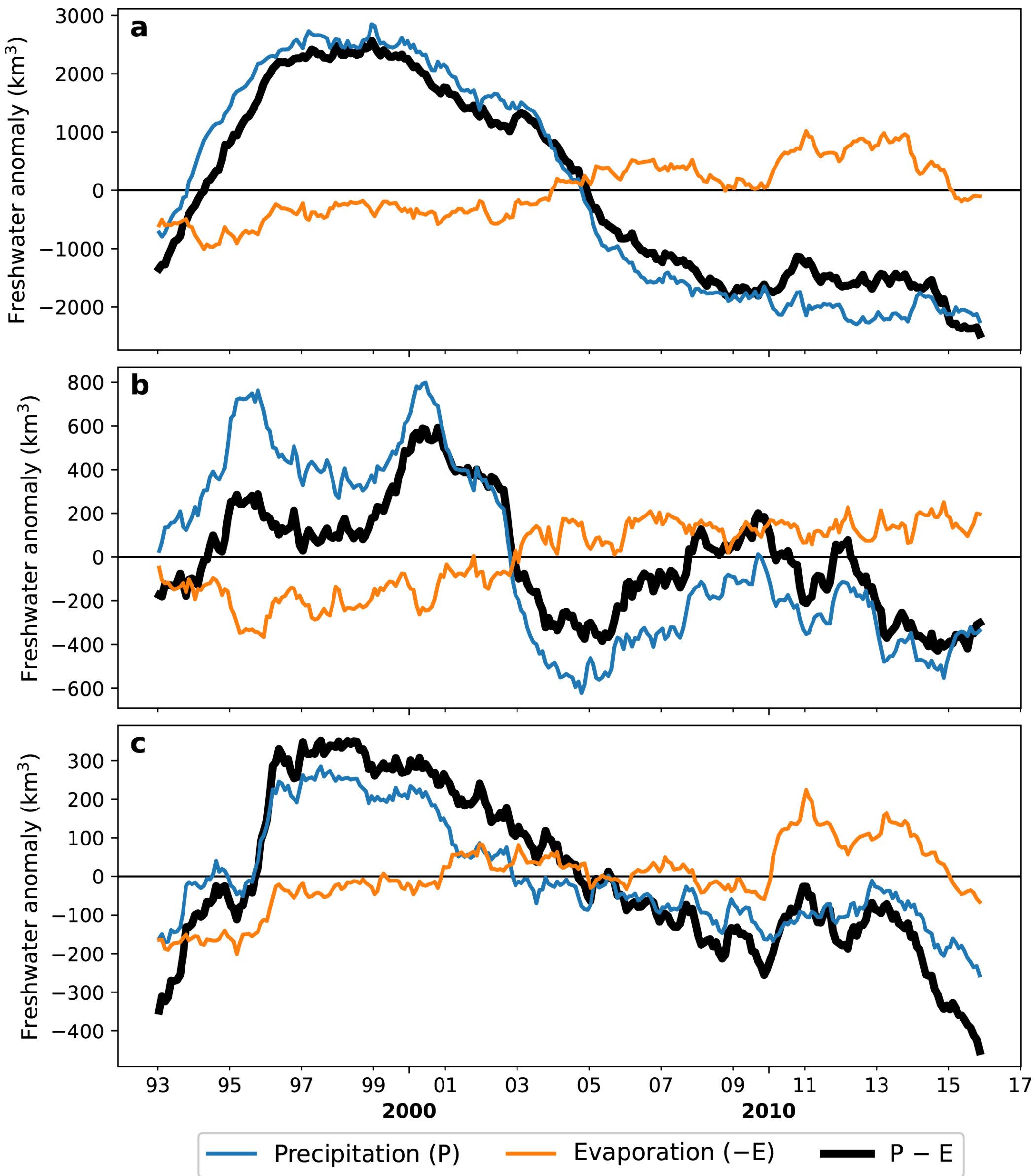

Figure S11. Decomposition of atmospheric freshwater flux into precipitation and evaporation for the (a) subpolar North Atlantic, (b) Nordic Seas and (c) Labrador Sea.

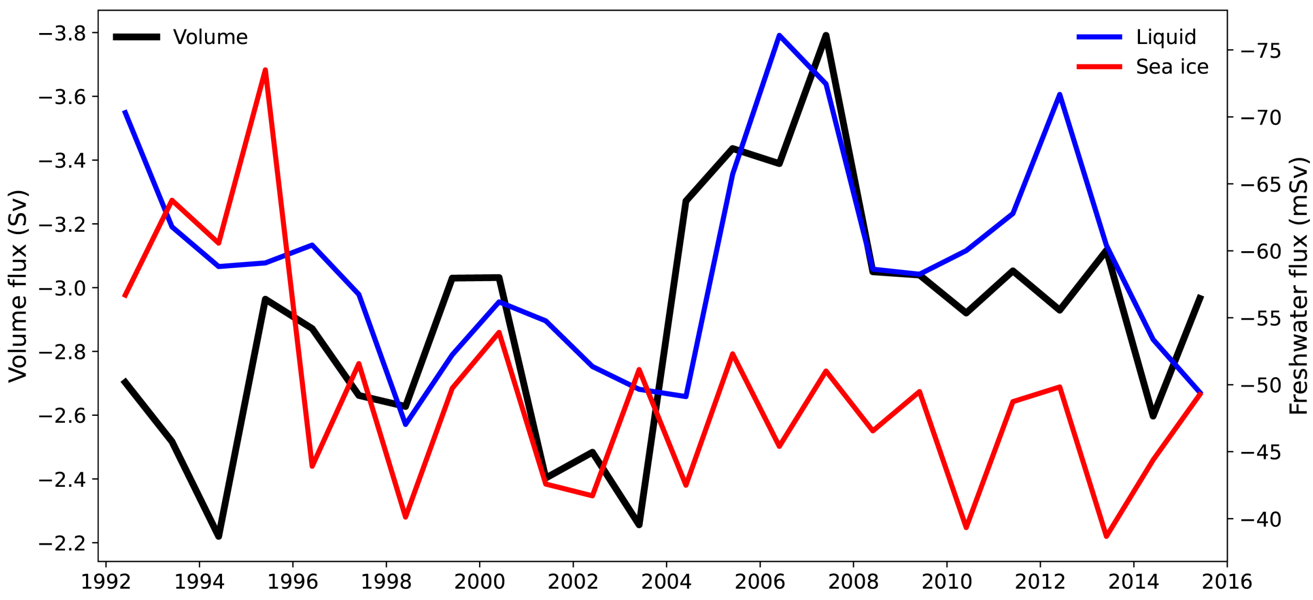

Figure S12. Annual means of volume and freshwater fluxes through the Fram Strait. Freshwater fluxes are shown for liquid freshwater and sea ice.

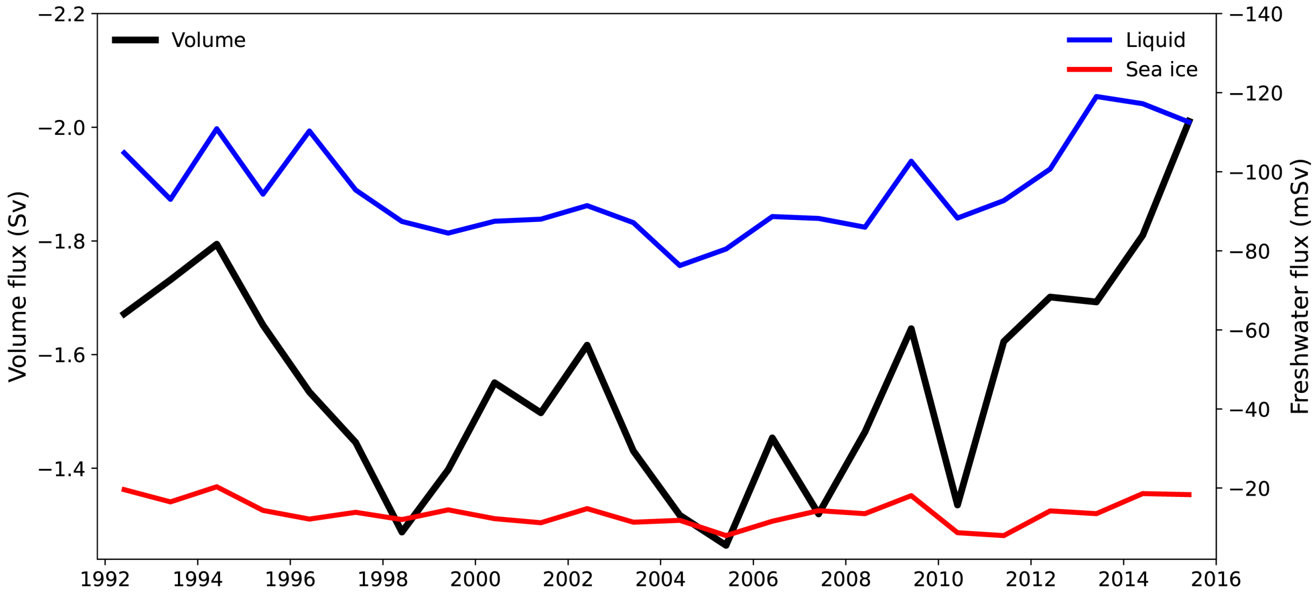

Figure S13. Annual means of volume and freshwater fluxes through the Davis Strait. Freshwater fluxes are shown for liquid freshwater and sea ice.

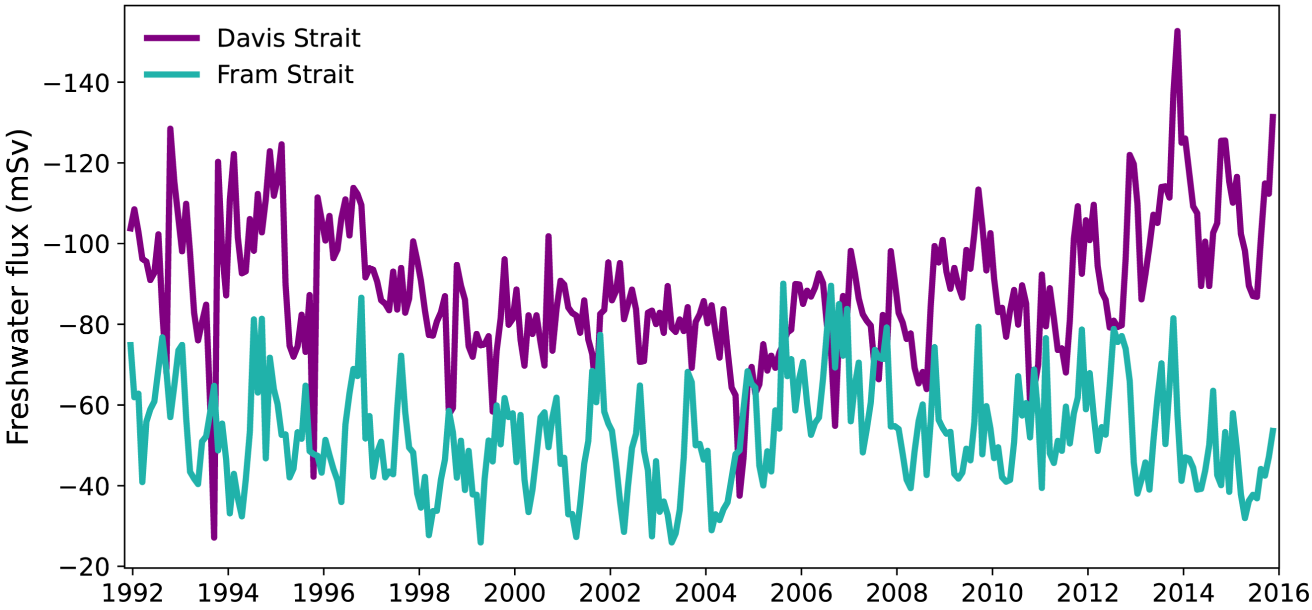

Figure S14. Comparison of monthly mean freshwater fluxes through the Davis Strait and Fram Strait. Freshwater fluxes are calculated using $S_{ref} = 35\,\mathrm{g\,kg^{-1}}$.

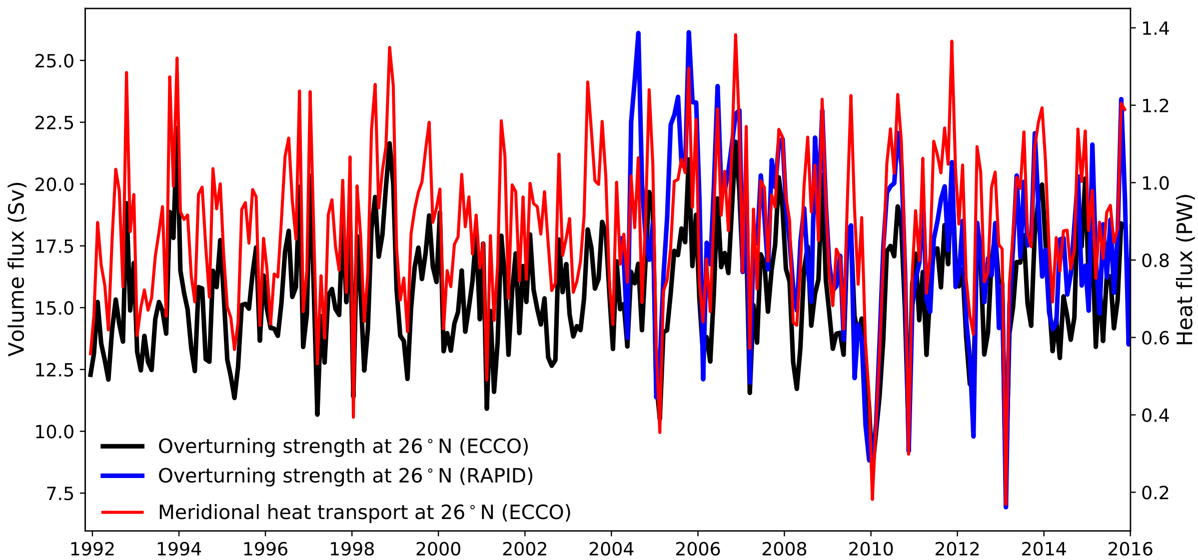

Figure S15. Comparison of AMOC strength (black) and meridional heat flux (red) estimate from ECCOv4 plotted with AMOC strength from RAPID (blue) at 26°N.

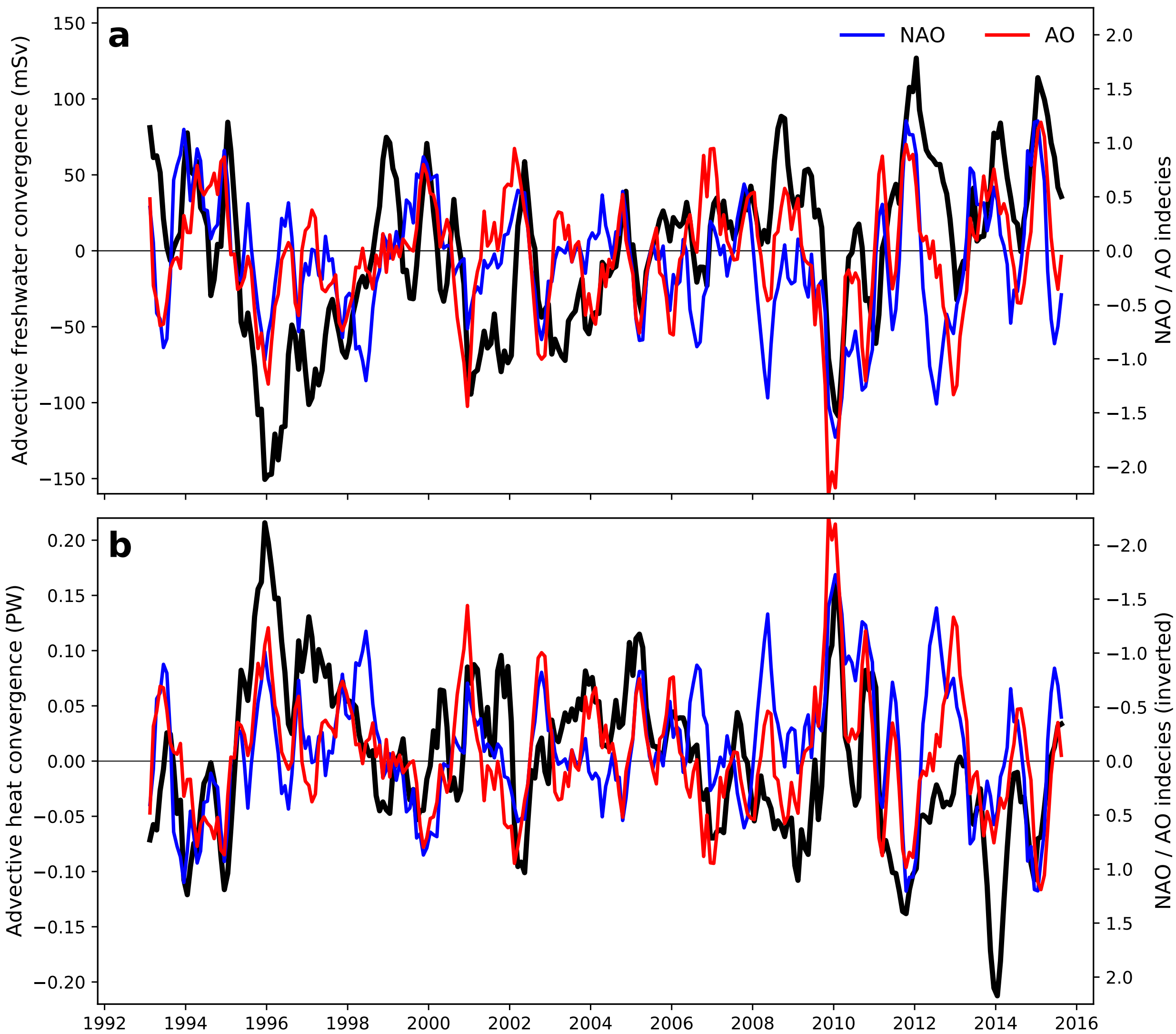

Figure S16. Anomalous advective (a) freshwater and (b) heat convergence in the SPNA (black) plotted with time series of NAO (blue) and AO climate index (red). Note that y axis for NAO/AO is inverted in panel b.

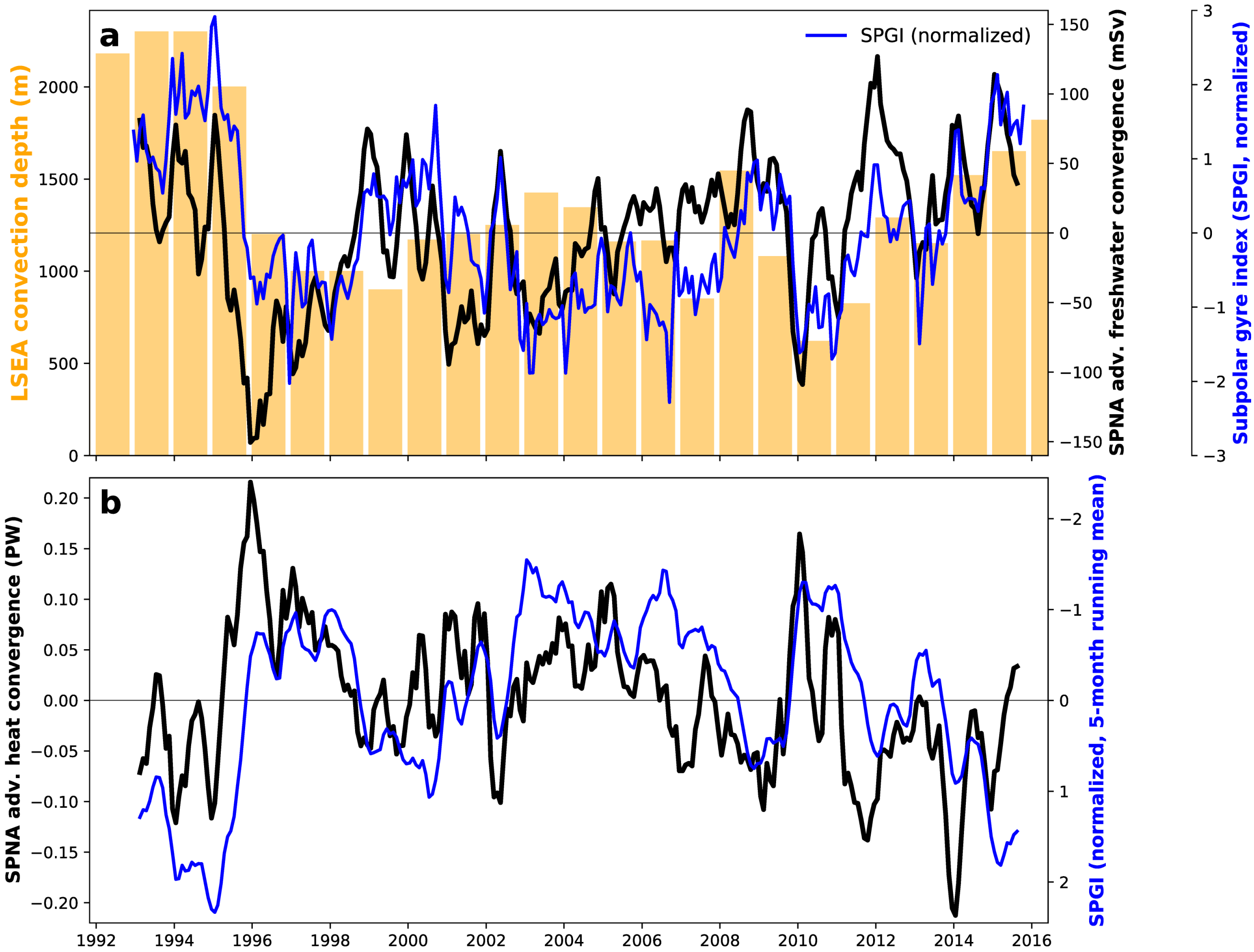

Figure S17. (a) Winter convective depth in the Labrador Sea (LSEA) plotted with anomalous advective freshwater convergence and monthly time series of SPGI (blue). (b) Anomalous heat convergence in the SPNA (black) plotted with 5-month running mean of SPGI (blue). SPGI has been normalized by subtracting its mean and dividing it by its standard deviation. Note that y axis for SPGI is inverted in panel b.